Modeling congenital heart disease with human iPS cell-derived cardiomyocytes in vitro and in vivo using a genomics approach

by

Renee Nicole Rivas

DISSERTATION

Submitted in partial satisfaction of the requirements for the degree of

DOCTOR OF PHILOSOPHY

in

Biochemistry and Molecular Biology

in the

GRADUATE DIVISION

of the

UNIVERSITY OF CALIFORNIA, SAN FRANCISCO

Modeling congenital heart disease with human iPS cell-derived cardiomyocytes in vitro and in vivo using a genomics approach

by

Renee Nicole Rivas

DISSERTATION

Submitted in partial satisfaction of the requirements for the degree of

DOCTOR OF PHILOSOPHY

in

Biochemistry and Molecular Biology

in the

GRADUATE DIVISION

of the

UNIVERSITY OF CALIFORNIA, SAN FRANCISCO

Approved:

Chair

.....

.....

.....

.....

Committee in Charge

Dedication

To my darling husband,

for making me laugh at the strangest of times. You are adored.

Acknowledgements

There are so many people that I would like to thank that I am afraid I will forget someone; in some ways I feel that the path of my PhD training has been a group endeavor. I have been in turns elated and so terribly frustrated by this training process but it is something that I am so glad I decided to do.

I have had a wonderful time at the Gladstone Institutes as everyone is so kind and interested in science. The cores are first rate and filled with amazing people, your expertise has been invaluable, especially that of Caroline Miller, Jinny Wong, and Ian Spencer. I have loved my time in lab and contribute a lot of that to the supporting and enriching environment of my lab. Everyone has been helpful at multiple points along the way, and I know I will miss you all. My time in 4C has been thrilling and I could not have asked for better bay mates. Emily Berry, Yen-Sin Ang, Karen Carver-Moore, David Hassel, and Janell Rivera you guys have been a welcome source of humor and support. Sometimes just the few seconds of charming interaction with you guys is just the little pick me up that I need. I am glad that through the course of my scientific meanderings I was able to meet Alex Ribeiro as he could probably inspire enthusiasm in science in a rock. I am always enlivened by our conversations. Yen-Sin Ang has been both my mentor and partner in crime. There were so many times when we served as sources of support and helpful criticism for each other. I'm not sure if we would have gotten through all this without a lot of stubbornness and optimism and the ability to share the burden. I know there were times when I would be

overwhelmed and you served to keep the ball going. I would like to think I helped you with the same. You are one of the most hardworking and fearless people that I have ever met, and I thank you for helping me to grow as a scientist and a person. Deepak is of course the center of the lab and it is from his influence and support that the lab stays such a warm and productive place to learn and work. I cannot thank you enough for giving me the opportunity to learn and grow in this environment. You have been truly inspiring as a mentor. These have been good years filled with a lot of hard work but also a lot of fun. I hope that you have enjoyed having me in your lab as much as I have enjoyed being a part of it.

I would also like to thank the Biomedical Sciences and Medical Science Training Program for the supervision of my training and deigning to pick me in the first place. I have had wonderful experiences with all of you. Jana Toutolmin and Catherine Norton and more recently Geri Ehle have been wonderful sources of support in navigating the multiple transitions of the MSTP.

My committee has been wonderful and supportive. Jay Debnath has always been available for discussions and is a great mentor. I can always count on him to surprise me with his depth of insight. Bob Nussbaum knows a lot about almost everything related to genetics and not and has provided some great suggestions. I know you both have contributed to my development and for that I thank you.

My friends that I have made on this journey are phenomenal. I treasure you all. Even though we do not all live close together anymore, we still maintain

our ties. You all have helped me get through a lot, laugh a lot, and eat a lot of really good food.

I, of course, would like to thank my family. To my mom and my dad, Jewel and Michael Swiateck, you have taught me so much both intentionally and perhaps unintentionally. You have always had every confidence in me and that has gotten me through so many tough times. Growing up, I felt like the foundation of my world was your unwavering love for me. It gave me the confidence to reach for the stars and know that however far I wandered, I always had a haven of love and support waiting for me at home. Considering that I remember a time when I wasn't even sure I would go to college, I feel like I have run quite far afield. However, I know that you are only a phone call away. My sister Daphne can always make me smile with her gift of laconic understatement. It has been a joy to be a part of your life and watch you grow up; I only wish I could have been closer.

Finally, I would like to thank my husband and baby girl. You two are the center of my little world. I met my husband in college and he has been my unwavering friend and companion ever since. Your quirky sense of humor and dramatic flair has lightened many a dark moment, although perhaps not always in the way you intended. I love you so much and can't even imagine what this journey would have been like without you. My baby girl Sidonie, although only a recent addition to the world, has been an innumerable source of happiness and

joy. I thank you all and probably many more that I have forgotten. I couldn’t have done it without you.

Genomic and Cellular Analysis of a GATA4 Mutation in Human iPS Cell-derived Cardiomyocytes

by

Renee Nicole Rivas

Abstract

GATA4 is a central transcriptional regulator during cardiac development and for postnatal function. Familial mutations in *GATA4* lead to autosomal dominant congenital heart disease and cardiomyopathy. We previously reported a *GATA4 G296S* mutation that resides near the second zinc finger of GATA4, involved in DNA-binding and protein-protein interactions thought to be dominant due to haploinsufficiency. However, the mechanisms by which this mutation affects the transcriptional and epigenetic landscape as well as the cellular physiology is unknown. Here, we have used genomic approaches as well as cell-based assays to delineate the consequences of the *GATA4 G296S* mutation in cardiomyocytes.

We generated iPS cells from human patients with or without the *GATA4 G296S* mutation and differentiated them to a purified population of cardiomyocytes. Using these cells, we conducted investigations into the role of a putative modifier gene identified by bioinformatics analyses for its potential involvement in the development of the GATA4 cardiomyopathy. However we were not able to uncover a disease causing relationship independent of GATA4.

We performed chromatin immunoprecipitation followed by DNA sequencing (ChIP-Seq) on endogenous GATA4 protein and revealed hundreds of previously unidentified GATA4-bound loci while confirming known GATA4 targets. We also performed ChIP-Seq on TBX5, a transcription factor associated

with congenital heart disease that physically interacts with GATA4 and whose interaction is specifically disrupted by the G296S mutation. Genome-wide we identified thousands of loci where GATA4 and TBX5 co-localized in wild-type cells, but surprisingly this co-occupancy was lost in cardiomyocytes heterozygous for the *GATA4 G296S* mutation, despite the presence of the wildtype allele. RNA-Seq revealed dysregulation of transcription at many of these loci, along with expected epigenetic changes, with clustered dysregulation of genes involved in cellular respiration, inflammation, and muscle contraction. To investigate the effect of these genes, we undertook a number of cell-based assays. In collaboration with Beth Pruitt's lab at Stanford, we developed a platform for performing individual cell-based force generation and contractility studies. These contractility and other cell-based studies confirmed defects in contractility and calcium handling in cardiomyocytes heterozygous for the *GATA4 G296S* mutation. We also verified that the heterozygous *Gata4 G295S* mouse has an increased susceptibility to pressure-overload induced hypertrophy and demonstrated its limited ability to validate targets dysregulated by RNA-seq.

The deep "-omic" interrogation of iPS-derived cardiomyocytes effectively revealed the transcriptional and cellular consequences of an important human mutation and may explain many of the disease features observed in individuals with *GATA4* mutations. Further study is still required to delineate the full consequences of this dysregulated transcriptome, but these observations help to confirm the role of GATA4 in the heart and set a strong foundation for future investigations.

Table of Contents

Chapter 2: Lamp2 as a Potential Modifier of GATA4 Cardiomyopathy

Chapter 3: Genomic and Cellular Analysis of a GATA4 Mutation in Human iPS Cell-derived Cardiomyocytes

List of Figures

Chapter 2

List of Tables

Chapter 3

List of Abbreviations

AA – aortic aneurysm

ARVD – arrythmogenic right ventricular dysplasia

ASD – atrial septal defect

AVSD – atrioventricular septal defect

BafA – Bafilomycin A1

BME – beta mercaptoethanol

CHD – congenital heart disease

ChIP-seq – chromatin immunoprecipitation followed by sequencing

ChIP-seq – chromatin immunoprecipitation followed by sequencing

CM - cardiomyocyte

cTnI – cardiac troponin I

cTnT – cardiac troponin T

DAPI - 4',6-diamidino-2-phenylindole

DMEM – Dulbecco's Modified Eagle Medium

DMP - dorsal mesenchymal protrusion

DMSO – dimethyl sulfoxide

EF – ejection fraction

EM – electron microscopy

ESC – embryonic stem cell

FBS – fetal calf serum

Fig – figure

FS – fractional shortening

GSEA – gene set enrichment analysis

H&E – hemotoxylin and eosin

HDF – human dermal fibroblast

HDR – homology directed repair

HF – heart failure

ICC – immunocytochemistry

IHC – immunohistochemistry

iPSC – induced pluripotent stem cell

KD - knockdown

KI – knock in

KO – knock out

KSR – knockout serum replacement

LAMP2 – lysosomal associated membrane protein 2

LVNC – left ventricular non-compaction

NEAA – non-essential amino acids

NHEJ – non-homologous end joining

P/S – penicillin/streptomycin

PBS – phosphate buffered saline

PS – pulmonary stenosis

pVAAST – pedigree – Variant Annotation Analysis and Search Tool

RNA-seq – mRNA sequencing

RNA-seq – RNA collection followed by sequencing

RPMI – Roswell Park Memorial Institute medium

RT – room temperature

TF – transcription factor

TUNEL - Terminal deoxynucleotidyl transferase dUTP nick end labeling

VIM – vimentin

VSD – ventricular septal defect

WT – wildtype, normal

Chapter 1

Introduction

Overview of the Development of the Heart

The heart is the first organ to develop in the embryo and its formation represents a complex biologic process that serves to coordinate the oxygenation and provision of vital nutrients to the rest of the body. The heart forms just as the embryo reaches the limit of what diffusion can accomplish for perfusion and will beat for the entire lifespan of the organism. Much is known about the development of the heart from studies in vertebrate and invertebrate model systems, but it is a more recent development to be able to define the genetic and environmental program that governs the formation of the heart (Srivastava and Olson 2000).

The formation of the heart begins from the activation of the cardiac gene program in the anterior lateral mesoderm by factors secreted from the endoderm. The transcription factor Nkx2.5 is activated at this step and it represents one of the earliest markers of the cardiac lineage and contributes to its specification. Other factors involved in this process include the GATA family of transcription factors and Mef2 (Srivastava and Olson 2000). At this point the tissue that will become the heart is in the shape of a flat crescent, but as the embryo folds, so

too does the crescent until the arms are brought together to form the primitive heart tube (Sylva *et al.* 2013). GATA transcription factors, in particular GATA4, are essential during this morphogenic event (Molkentin *et al.* 1997).

The heart tube continues to grow not by proliferation but by the addition of Islet1+ positive cells from the surrounding mesoderm (van den Berg, 2009). Most of these primitive heart cells exit the cell cycle and do not re-enter it until the chambers are specified. The cells that initially formed the cardiac crescent are referred to as the first heart field, while the second heart field is composed of the cells that are added later.

Next, the vertebrate heart tube undergoes looping in the rightward direction. This asymmetric morphogenetic event is due to early patterning in the embryo that establishes the left-right axis. Sonic hedgehog, Nodal, and Pitx2 are involved in this early patterning step. The growth of the cardiac chambers proceeds from selective growth of distinct regions of the looped tube, with the specific segments showing distinct gene expression and functional properties. For example, HAND1 and HAND2 are involved in patterning the left and right sides of the heart, respectively and absence of CoupTFII leads to a lack of atrial myocytes and Mef2c to hypoplastic ventricles (Srivastava 2006). Initially, the myocardium is spongy and heavily trabeculated. These trabecules grow by the addition of cells at their base, leading to the ballooning of the chambers. Finally, the compact layer forms under the influence of epicardially-derived cardiac

fibroblasts that induce proliferation and differentiation that ultimately results in the compacted ventricular layer (Ieda *et al.* 2009; Sylva *et al.* 2013).

The accurate formation of the cardiac valves is essential for the proper partitioning of the heart and is a significant source of malformation. The valves form from regional swellings of the extracellular matrix to form what is known as the cardiac cushions. Signaling by TGFβ family members and other factors between the endocardium and myocardium induces the transformation of the endocardial cells into mesenchymal cells. These mesenchymal cells then migrate into the cushions, fibrose to form the valves, and contribute to the septation of the atrioventricular canal (Srivastava 2006).

Septation of the heart occurs from the confluence of multiple different tissues. A muscular component from the ventricles, the endocardial cushions, outflow tract ridges, and the dorsal mesenchymal protrusion (DMP) all participate in the process of septation. The DMP is of particular interest because it is extra-cardiac tissue and more pronounced in humans than in mice. The ventricular septum is arguably less complicated. The muscular component is a remainder of the primitive heart tube that did not undergo the rapid growth to create the four cardiac chambers. The membranous part is a result of the endocardial and outflow tract cushions fusing together. A ventricular septal defect (VSD) is a result of improper fusion in this region (Sylva *et al.* 2013). Proper atrial septation is complicated by the need for the left side of the heart to receive bloodflow. Thus, a series of steps are followed to allow shunting of blood from the right to

left atrium *in utero* while still permitting a complete separation after birth. The solution to this quandary is to create a unidirectional valve such that in the low pressure environment of the left side of the heart *in utero*, blood flow passes from right to left, yet after birth the resultant increase in pressure on the left closes the valve and terminates shunting. This valve is formed in two steps. The primary septum grows caudally, but before it closes off the tract, another hole forms called the ostium secundum which maintains the shunt. Next, the septum secundum forms in the right atrium and contains its own non-overlapping ostium. Physically, this means that there is an open pathway for blood to flow from the higher pressures of the right to the left. At birth, the pressure gradient shifts, forcing the septa together and closing the communication. If this process is altered or misaligned, a communication may be left between the atria resulting in an atrial septal defect (ASD). Atrioventricular septal defects (AVSDs) are a result of a communication remaining open in both the atria and the ventricles.

Development of the outflow tract is another area that is highly susceptible to malformation. It is complicated by the exquisite specificity required for proper morphogenesis of the aorta and pulmonary artery and by the migration of neural crest cells that contribute to the formation of this structure. Essentially, neural crest cells must migrate from the neural folds into the pharyngeal arches and the heart to contribute to the ventricular septum, the aorta, ductus arteriosus, subclavian, carotid, and pulmonary arteries (Srivastava 2006). Defects in the migration or development of the neural crest can cause devastating malformations in these regions.

Thus, there are many complicated and incompletely understood steps involved in the correct morphogenesis of the heart. The development of the heart is of particular interest not just because of the fascinating biology involved, but also because defects in the formation of the heart lead to congenital heart disease, the most common birth defect in humans. Congenital heart defects affect nearly 1% (about 40,000) newborns each year in the United States and are the cause of substantial mortality and morbidity in children (Hoffman and Kaplan 2002; Reller et al 2008).

GATA4 in Heart Development and Congenital Heart Disease

As this abbreviated version of cardiac development makes clear, cardiac development is a complex and highly regulated process wherein many events may go awry and contribute to both morphologic and functional deficits. Genetics has played a critical role in making significant progress toward understanding CHD, with several families found to have mutations in transcription factors that are essential for cardiac development in mouse models of CHD (Hatcher *et al.* 2003). GATA4 is one such transcription factor (Garg *et al.* 2003) that is important for cardiac development and that has been found mutated in multiple families affected with congenital heart disease.

GATA4 controls the expression of many different cardiac genes involved in diverse processes such as compensation, maintenance (Bisping *et al.* 2006),

proliferation (Rojas *et al.* 2008), conduction (Munshi *et al.* 2009), and cardiomyocyte survival (Aries *et al.* 2004). GATA4 interacts with other cardiac transcription factors, like HAND2 (Dai *et al.* 2002), TBX5 (Garg *et al.* 2003) and NKX2.5 (Durocher *et al.* 1997), which are required for normal cardiac development to regulate the cardiac gene program (He *et al.* 2011; Schlesinger *et al.* 2011)

The role of GATA4 in the heart is essential, not only during development but throughout life. In the null *Gata4* mouse, there is a ventral morphogenesis and heart looping defect that results in lethality by E9.5 (Molkentin *et al.* 1997). Cre-specific deletion results in regional and time specific abnormalities that underlie the overall importance of GATA4 in the heart. Specifically, early embryonic cre drivers point to the importance of GATA4 in the right ventricle and for proliferation in the myocardium (Zeisberg *et al.* 2005). Postnatally, mice heterozygous for *Gata4* deletion have mild systolic and diastolic dysfunction at baseline, smaller hearts due to a reduction in cardiomyocytes number, and an impaired response to pressure overload (Bisping *et al.* 2006, Oka *et al.* 2006). Additionally, overexpression of GATA4 in the adult mouse heart induces cardiac hypertrophy (Liang *et al.* 2001). More recently, *GATA4* mutations have also been described in familial dilated cardiomyopathy (Li *et al.* 2013, Zhao *et al.* 2014).

There are also data that implicates GATA4 in the non-myocardial layers of the heart. A *Tie2*-Cre specific deletion of *Gata4* revealed hypocellular cushions and inadequate septation (Rivera-Feliciano *et al.* 2006). GATA4 likely also has a

role in the epicardium, as the *Gata4* null mice do not have proepicardium (Watt *et al.* 2004).

Congenital heart defects have also been associated with GATA4 missense mutations. Previous studies in the Srivastava lab have found that a mutation in *GATA4* can cause familial congenital heart defects – primarily atrial and ventricular septal defects (Garg *et al.* 2003). This family has a heterozygous G296S missense mutation in *GATA4* that disrupts the C-terminal zinc finger domain. The mutation is highly penetrant and causes an autosomal dominant heart defect, possibly due to haploinsufficiency. The exact same *GATA4 G296S* mutation has been reported in at least three other families with a similar phenotype (Moskowitz *et al.* 2011, Sarkozy *et al.* 2005). *In vitro* the mutation reduces DNA binding affinity, decreases activation of downstream genes, and disrupts an interaction between GATA4 and TBX5, another cardiac transcription factor (Garg *et al.* 2003). The importance of this interaction is evident in the double heterozygous mouse for deletions in *Gata4* and *Tbx5*, which demonstrates near 100% synthetic lethality (Maitra *et al.* 2009). The homozygous *Gata4 G295S* knock-in mouse has embryonic lethality by E11.5, two days after the full knock-out, and has no defect in ventral morphogenesis (Misra *et al.* 2012). Interestingly, many of the *Gata4 G295S*/+ mice have atrial septal defects and a subset show aortic and pulmonary stenosis as well (Misra *et al.* 2012). The *GATA4 G296S* mutation also affects the interaction of GATA4 with SMAD4. In the endocardium, double heterozygous knock-out mice for *Gata4* and *Smad4* display severe atrioventricular defects and die by E12.5 (Moskowitz *et al.* 2011)

reinforcing the importance of GATA4 in the septation of the heart . Moreover, when the heterozygous *Gata4* deletion mouse is crossed into different genetic backgrounds, it displays a variable phenotype from septal defects, endocardial cushion defects, right ventricular hypoplasia, and cardiomyopathy (Rajagopal *et al.* 2007) arguing that there are many potential modifiers *in vivo*. This information explains some of the variability found in human patients with idiopathic mutations in *GATA4*, as there has been a wide spectrum of phenotypes associated with *GATA4* mutations (Tomita-Mitchell *et al.* 2007; Zhang *et al*. 2008).

It should be added that although mutations in *GATA4* have been associated with both familial congenital heart disease (Chen *et al.* 2010, Yang *et al.* 2013) and idiopathic CHD (Tomita-Mitchell *et al.* 2007; Yang *et al.* 2012), mutations in *GATA4* are not considered to be major contributor to the burden of congenital heart disease. Even deep sequencing of hundreds of patients only reveals a few patients with *GATA4* mutations (Tomita-Mitchell *et al.* 2007; Yang *et al.* 2012). However, GATA4 is not solely expressed in the heart and has been shown to have important roles in other tissues, like the brain (Agnihotri *et al.* 2011), small intestine (Battle *et al.* 2008), gonads (Tevosian *et al.* 2002, Efimenko *et al.* 2013), and liver (Watt *et al.* 2007). A strong negative selection pressure in this case would be expected to make the frequency of *GATA4* mutation low in the population, especially as GATA4 is required for normal gonadal development (Tevosian *et al.* 2002, Efimenko *et al.* 2013). Yet, this information also argues for the importance of GATA4 in other tissues of the body, and highlights why further study of this transcription factor is warranted.

Transcription Factors in Cardiac Development and Function

Transcription factors have many roles in the heart, from specifying cell fate, maintenance of the cardiac gene program and responding dynamically to perturbations in environment. The transcriptional network has been extensively studied in the heart, not only during development, but also in adulthood and under conditions of stress. Highlighting the importance of transcription factors in the heart, there are many congenital defects associated with mutations in transcription factors such as Holt-Oram syndrome associated with *TBX5* mutations (Li *et al.* 1997) and DiGeorge syndrome linked to *TBX1* (Garg *et al.* 2001, Merscher *et al.* 2001). There are even more transcription factor mutations that have been reproducibly linked back to disease phenotypes in patients, like the previously discussed *GATA4 G296S* mutation and its association with septal defects (see Bruneau 2008 for a review).

Transcription factors work in concert with each other in dense, overlapping networks. These networks contribute to tissue specificity and functional output and are carefully regulated at multiple steps from direct post-translational modifications to recruitment at specific loci and inhibition at others. The GATA4 protein, for example, can be acetylated to increase its activity and methylated to decrease its activity at distinct sites (Zhou *et al.* 2012). Transcription factors often work together, co-occupying the same enhancer sites. Chromatin immunoprecipitation followed by sequencing (ChIP-seq) is a way to find where

transcription factors bind in the genome. In a ChIP-seq based analysis of the transcription factors GATA4 NKX2.5, TBX5, SRF, and MEF2A in the cardiomyocyte-like cell line HL-1, over 20% of the peaks co-occurred with the peak of at least one other transcription factor (He *et al.* 2011). These transcription factors represent some of the most well studied transcription factors in the heart, yet there were many more transcription factors not included in this analysis. Therefore, this analysis probably represents an underestimation of the actual level of co-occupancy of transcription factors in the genome. Consistent with this hypothesis, that same study found that motifs for other cardiac transcription factors were enriched in the ChIP-seq peaks. Moreover, many of these transcription factors are known to interact with each other. This co-occupancy likely is representative of their interactions, wherein they serve to recruit each other to genomic loci.

There is also much regulation of the transcriptional network with microRNAs, interaction with activating and repressive complexes, and epigenetic signals serving to modulate transcription factor activity and access to the genome. For example, the gene *GATA4* has a mir-208 targeting sequence and appears to be indirectly regulated by mir-1 (Zhou *et al.* 2012). When mir-208 is genetically deleted, a failure to respond to hypertrophy results, whereas overexpression of mir-1 yields thin myocardium, heart failure, and developmental arrest by E13.5 (Zhang 2008). These experiments point to the wide range of phenotypes possible through alterations of microRNA dosage. The effects of

these microRNAs are also significant, as these phenotypes are substantial and speak to the powerful role that microRNAs can have on a transcriptional network.

The epigenetic landscape is another factor that can significantly affect the transcriptome. Chromatin regulation is central to specifying cell fate, maintenance, and the responsiveness of the cell to environmental factors. The accessibility of chromatin is determined by many factors that may make genomic regions more or less available for transcription. However, this influence is not unidirectional. Transcription factors can also serve to alter the epigenome by binding chromatin and recruiting activating factors. Pioneer factors, like GATA4, specifically are dubbed 'pioneers' in that they can bind closed chromatin and assist in making that region more accessible to active transcription (Cirillo *et al.* 2002, Smale *et al.* 2010). GATA4 reflects this bivalent activating and repressive state. GATA4 interacts with both p300, which marks active chromatin with H3K27ac, as well as HDAC2, which serves to deacetylate chromatin. These epigenetic alterations can then reflect cell type specificity as in cardiac tissue GATA4 is known to be an activator of transcription due in part to the p300 interaction (He *et al.* 2014) whereas in the small intestine GATA4 serves to repress ileal identity in the duodenum and jejunum (Aronson *et al.* 2014).

There are many factors to take into account when considering the roles of transcription factors in the heart. Ever more comprehensive and sophisticated studies to delineate the perturbations in the transcriptome and their effects in the disease state are possible. These analyses allow for insights and points of

malleability to be ascertained in returning the disease state back to wildtype and represent an important avenue for future research.

Modeling Disease with iPS Cells

The finding that adult somatic cells could be reprogrammed into induced pluripotent stem cells (iPSCs) was a remarkable discovery for disease-centered research, regenerative medicine, and pharmacology studies (Takahashi *et al.* 2006). iPS cells can be generated from adult human fibroblasts, allowing for the efficient creation of patient-specific cells that can then theoretically be converted into any cell in the body. Several groups have made patient-derived iPS cell models of diseases such as Long QT syndrome (Moretti *et al.* 2010), spinal muscular atrophy (Ebert *et al.* 2009), LEOPARD syndrome (Carvajal-Vergara *et al.* 2010), and arrhythmogenic right ventricular dysplasia (Kim *et al.* 2013). Since the initial discovery of iPS cells, there have been many advances made in their production and use. One of these discoveries was that pluripotency could be reprogrammed using an episomal, integration-free method that avoids the complications of gene silencing introduced by viral integration (Okita *et al.* 2011). Gene silencing due to ectopic introduction of viral vectors is a valid concern when considering using these cells to do unbiased genomic profiling and thus integration-free iPS cells should be considered a higher standard. More recently genome engineering technology has sprung forward with the introduction of the CRISPR-Cas9 system, which allows for a more straightforward and efficient

targeting of genomic loci for Non-Homologous End Joining (NHEJ) or Homology Directed Repair (HDR) (Sander and Joung 2014). HDR can be used to introduce a donor section that contains the wildtype sequence and thereby allowing for the correction of the previously mutant iPS cell line. This approach allows the investigator to determine if the phenotype is therefore due solely to the mutation or to the particular genetic background of the cell line. These isogenic corrections have been used in a number of papers to study diverse areas such as aortic valve disease (Theodoris *et al.* 2015), Parkinson's disease (Ryan *et al.* 2013), and sickle cell disease (Huang *et al.* 2015). The major hurdle in generating these isogenic clones is a technical one. Human ES cells do not survive well as independent cells, making clonal selection a difficult and time consuming process. However, making the iPS cells is only the first part of the process of creating an *in vitro* model of human disease.

Generation of Cardiomyocytes from iPS Cells

For cardiac modeling there already exist many methods whereby cardiomyocytes may be efficiently generated in large enough batches to facilitate study. In general, differentiation protocols attempt to recapitulate the signals that occur during development in a directed fashion. One of the more reproducible and efficient methods that we use in the Srivastava lab is the Wnt modulation protocol. This protocol takes advantage of the fact that Wnt signaling appears to have a biphasic effect on cardiac development in multiple systems. Through

early inhibition of Wnt signaling followed by later enhancement, cardiomyocytes can be coaxed from human stem cells in a directed fashion (Lian *et al.* 2012). There are many technical hurdles in carrying out these differentiations as each line has its own preferred levels of the small molecules used in the differentiation process and cells in culture naturally tend to drift over time leading to inconsistencies in timing and growth requirements from batch to batch. Yet, with proper optimization and care, these hurdles can be surmounted and the process of cardiac differentiation can be scaled up to generate large single batches of CMs that can then be used for many downstream assays.

Unfortunately, we found that none of the published methods of generating cardiomyocytes could produce a very purified population of cardiomyocytes with great fidelity. Using this directed differentiation method, the purity does not usually reach greater levels of purity than 80% and is often lower than that. This level of purity is considered adequate for most applications, but additional optimization is possible. Cardiomyocytes have been difficult to isolate with cell sorting via flow cytometry for lack of a cell surface antigen to use for selection. There have been a few methods published using SIRPA (Dubois *et al.* 2011) and VCAM-1 (Uosaki *et al.* 2011) that describe such methods, but these methods are better for small scale enrichment. IPS cell lines may also be genetically engineered to have a cardiac specific selection marker. Yet, genetically modifying every iPS cell line that is under investigation can be time consuming. Thankfully, there is a nongenetic method that relies on the differential metabolic capabilities of cardiomyocytes. Most cells, including ES cells, neurons, skeletal

muscle cells, and mouse embryonic fibroblasts (MEFs), die in glucose-depleted media that has abundant lactate *in vitro* (Tohyama *et al.* 2013). Cardiomyocytes are preferentially retained in this state, perhaps because they are better able to use lactate as an alternative energy source (Tohyama *et al.* 2013). However, given a long enough exposure (usually greater than 4-5 days) cardiomyocytes will die as well. The exposure to this metabolically limiting media can be carefully titrated to get the maximal amount of death in non-cardiomyocytes with the cardiomyocytes being retained and thus facilitating the large scale purification of cardiomyocytes *in vitro*.

Maturation of Cardiomyocytes In Vitro *and* In Vivo

The heart is structurally complete at birth. Yet, on the cellular level there are important functional differences in neonatal and adult cardiomyocytes. Some of the more significant differences between the fetal and adult heart are in their ability to regenerate and their metabolic potential. However, there are many more points of difference not covered here.

One of the more intriguing differences found between fetal and adult hearts is the fetal heart's ability to regenerate (Porrello *et al.* 2011). There is a small window immediately after birth when the mammalian heart can regenerate. After this period, the heart loses this ability, as the adult heart does not have this regenerative potential (Porrello *et al.* 2011).

The metabolic profile is another difference between fetal and adult heart. Less developed CMs tend to have a more glycolytic metabolism and as they mature mitochondrial oxidation increases and fatty acid oxidation becomes a larger source of the energy utilized (Cedwick 2013; Breckenridge *et al.* 2013). The PPARα pathway has received the most attention in this switch as it is involved in many steps of fatty acid metabolism. The HIF-1α pathway is also thought to play a role in this switch (Lopaschuk and Jaswal 2010). HIF-1 is itself highly upregulated in fetal mouse hearts and declines in expression after birth (Madan *et al.* 2002). HIF-1α controls a glycolytic gene program and so remains an intriguing target. The low oxygen environment of the fetus would make dependence on mitochondrial oxidation problematic. Therefore, it is appropriate that the fetal CMs rely more on glycolysis. However, mitochondrial oxidation can provide a greater, more consistent level of energy and is the predominant source of energy in the adult heart.

The switch from more glycolytic to oxidative phosphorylation in metabolism is of interest to researchers using iPS cell models, as the cardiomyocytes derived from iPS cells have an immature phenotype (Kim *et al.* 2013). If one had more interest in developmentally immature hearts, then the immature status of iPS cell-derived CMs is not an issue, but this is obviously a problem for modeling disease found in mature myocardium. Some of the regenerative potential and plasticity found in neonatal heart cells is lost during maturation, which may influence the susceptibility to many genetic and environmental insults. Often when an iPS model of genetic disease is

investigated and a phenotype is not uncovered or is not as severe as would be expected, the explanation given is that the cells simply are not mature enough to evince the phenotype. The problem of functional immaturity is a persistent point of contention in many differentiated ES cell-derived tissues. A study on arrythmogenic right ventricular dysplasia (ARVD) encountered the problem of the phenotype being more subtle than expected. The experimenters then went on to develop a method of metabolically maturing their iPS cell-derived CMs and found that as the CMs exhibited a more mature metabolic profile, so too did their phenotype worsen (Kim *et al.* 2013).

The subject of whether ES-derived CMs can be functionally matured is another active area of research, not only because it would make the *in vitro* models of disease more accurate, but also because it represents a way to understand the signals underlying the normal developmental processes involved in maturation. The influence of the *in vivo* environment appears to have a large effect on the maturation of CMs. The differences between *in vitro* and *in vivo* reprogrammed CMs speak to the power of the native environment to induce maturation (Qian *et al.* 2012). Translating these observations to definitive mechanisms to promote maturation is a complicated process. Studies that increase the substrate stiffness yield greater levels of maturation *in vitro*. This method is used to recapitulate the changes in the native environment after birth where the cardiac tissue becomes stiffer (Young and Engler 2011). Intriguingly a recent study of *in vitro* maturation has pointed to the role that the let-7 family of microRNAs plays in the heart during maturation. The let-7 family is significantly

upregulated during the process of maturation and its overexpression resulted in larger sarcomere length, contractile force, and respiratory capacity (Kuppusamy *et al.* 2015). This study points to the importance of gene regulatory networks in the maturation process of cardiomyocytes, yet it remains unknown if this process occurs normally in the heart.

Summary

- Mammalian heart development is complex and dependent on many cellular and genetic morphogenic events
- GATA4 has many roles in the heart, both during development and postnatally. GATA4 interacts with many other transcription factors and epigenetic regulators and seems to play a dominant role in the heart at many steps.
- iPS cell technology can be leveraged to explore many genetic heart diseases, although a greater maturation of the derived cardiomyocytes is required.

REFERENCES

Agnihotri S., Wolf A., Munoz D.M., Smith C.J., Gajadhar A., Restrepo A., Clarke I.D., Fuller G.N., Kesari S., Dirks P.B., McGlade C.J., Stanford W.L., Aldape K., Mischel P.S., Hawkins C., Guha A. (2011). A GATA4-regulated tumor suppressor network represses formation of malignant human astrocytomas. J Exp Med. *208(4)*, 689-702.

Aries, A. Paradis P., Lefebvre C., Schwartz R.J., Nemer M. (2004). Essential role of GATA-4 in cell survival and drug-induced cardiotoxicity. PNAS *101*, 6975-80.

Aronson B.E., Aronson S.R., Berkhout R.P., Chavoushi S.F., He A., Pu W.T., Verzi M.P., Krasinski S.D. (2014). GATA4 represses an ileal program of gene expression in the proximal small intestine by inhibiting the acetylation of histone H3, lysine 27. Biochimica et Biophysica Acta *1839*, 1273–1282.

Battle M.A., Bondow B.J., Iverson M.A., Adams S.J., Jandacek R.J., Tso P., Duncan S.A. (2008). GATA4 is essential for jejunal function in mice. 135(5): 1676–1686.

Bisping E., Ikeda S., Kong S.W., Tarnavski O., Bodyak N., McMullen J.R., Rajagopal S., Son J.K., Ma Q., Springer Z., Kang P.M., Izumo S., Pu W.T. (2006). Gata4 is required for maintenance of postnatal cardiac function and protection from pressure overload-induced heart failure. PNAS *103*,14471-6.

Breckenridge R.A., Piotrowska I., Ng K.E., Ragan T.J., West J.A., Kotecha S., Towers N., Bennett M., Kienesberger P.C., Smolenski R.T., Siddall H.K., Offer J.L., Mocanu M.M., Yelon D.M., Dyck J.R.B., Griffin J.L., Abramov A.Y., Gould A.P., Mohun T.J. (2013). Hypoxic Regulation of *Hand1* Controls the Fetal-Neonatal Switch in Cardiac Metabolism. PLoS Biology *11(9)*, e1001666.

Bruneau, B. (2008). The developmental genetics of congenital heart disease. Nature *451(21)*, 943-8.

Carvajal-Vergara, X., Sevilla A., D'Souza S.L., Ang Y., Schaniel C., Lee D., Yang L., Kaplan A.D., Adler E.D., Rozov R., Ge Y., Cohen N., Edelmann L.J., Chang B., Waghray A., Su J., Pardo S., Lichtenbelt K.D., Tartaglia M., Gelb B.D., Lemischka I.R. (2010). Patient-specific induced pluripotent stem-cell-derived models of LEOPARD syndrome. Nature *465*, 808-12.

Cedwick C. (2013) Fine Tuning Metabolic Switches. PLoS Biology *11(9)*, e1001664.

Chen Y., Han Z.Q., Yan W.D., Tang C.Z., Xie J.Y., Chen H., Hu D.Y. (2010) A novel mutation in GATA4 gene associated with dominant inherited familial atrial septal defect. J Thorac Cardiovasc Surg *140*, 684-687.

Cirillo L.A., Lin F.R., Cuesta I., Friedman D., Jarnik M., Zaret K.S. (2002). Opening of Compacted Chromatin by Early Developmental Transcription Factors HNF3 (FoxA) and GATA-4. Molecular Cell *9*, 279–289.

Dai Y.S., Cserjesi P., Markham B.E., Molkentin J.D. (2002). The transcription factors GATA4 and dHAND physically interact to synergistically activate cardiac gene expression through a p300-dependent mechanism. J. Biol. Chem. *277(27)*, 24390–8.

Dubois, N.C., Craft A.M., Sharma P., Elliott D.A., Stanley E.G., Elefanty A.G., Gramolini A., Keller G. (2011). SIRPA is a specific cell-surface marker for isolating cardiomyocytes derived from human pluripotent stem cells. Nature Biotechnology *29(11)*, 1011-1019.

Durocher D., Charron F., Warren R., Schwartz R.J., Nemer M. (1997). The cardiac transcription factors Nkx2-5 and GATA-4 are mutual cofactors. EMBO Journal *16(18)*, 5687–5696.

Ebert, A.D., Yu J., Rose F.F., Jr, Mattis V.B., Lorson C.L., Thomson J.A., Svendsen C.N. (2009). Induced pluripotent stem cells from a spinal muscular atrophy patient. Nature *457*, 277-280.

Efimenko E., Padua M.B., Manuylov N.L., Fox S.C., Morse D.A., Tevosian S.G. (2013). The Transcription Factor GATA4 is required for Follicular Development and Normal Ovarian Function. Dev Biol. *381(1)*, 144–158.

Garg V., Kathiriya I.S., Barnes R., Schluterman M.K., King I.N., Butler C.A., Rothrock C.R., Eapen R.S., Hirayama-Yamadak K., Joo K., Matsuokak R., Cohen J.C. , Srivastava D. (2003). GATA4 mutations cause human congenital heart defects and reveal an interaction with TBX5. Nature *424*, 443-447.

Garg V.,Yamagishi C., Hu T., Kathiriya I.S., Hiroyuki Yamagishi, and Deepak Srivastava. (2001). Tbx1, a DiGeorge Syndrome Candidate Gene, Is Regulated by Sonic Hedgehog during Pharyngeal Arch Development. Developmental Biology 235, 62-73.

Hatcher C.J., Diman N.Y., McDermott D.A., Basson C.T. (2003). Transcription factor cascades in congenital heart malformation. Trends in Molecular Medicine *9*, 512-515.

He A., Gu F., Hu Y., Ma Q., Ye L.Y., Akiyama J.A., Visel A., Pennacchio L.A., Pu W.T. (2014). Dynamic GATA4 enhancers shape the chromatin landscape central to heart development and disease. Nat Comm *5*, 4907.

He A., Kong, S.W., Ma, Q., and Pu, W.T. (2011). Co-occupancy by multiple cardiac transcription factors identifies transcriptional enhancers active in heart. PNAS *108*, 5632–5637.

He A., Shen X., Qing M., Cao J., von Gise A., Zhou P., Wang G., Marquez V.E., Orkin S.H., Pu W.T. (2012). PRC2 directly methylates GATA4 and represses its transcriptional activity. Genes and Development *26*:37–42.

Hoffman J.L., Kaplan S. (2002). The incidence of congenital heart disease. J Am Coll Cardiol. *39(12)*, 1890-1900.

Huang X., Wang Y., Yan W., Smith C., Ye Z., Wang J., Gao Y., Mendelsohn L., Cheng L. (2015). Production of Gene-Corrected Adult Beta Globin Protein in Human Erythrocytes Differentiated from Patient iPSCs After Genome Editing of the Sickle Point Mutation. Stem Cells *33(5)*, 1470-9.

Ieda M., Tsuchihashi T., Ivey K.N., Ross R.S., Hong T., Shaw R.M., Srivastava D. (2009). Cardiac Fibroblasts Regulate Myocardial Proliferation through b1 Integrin Signaling. Developmental Cell *16*, 233–244.

Kim C., Wong J., Wen J., Wang S., Wang C., Spiering S., Kan N.G., Forcales S., Puri P.L., Leone T.C., Marine J.E., Calkins H., Kelly D.P., Judge D.P., Chen H.V. (2013). Studying arrhythmogenic right ventricular dysplasia with patient-specific iPSCs. Nature *494(7435)*:105–110.

Kuppusamy K.T., Jones D.C., Sperber H., Madan A., Fischer K.A., Rodriguez M.L., Pabon L., Zhu W., Tulloch N.L., Yang X., Sniadecki N.J., Laflamme M.A., Ruzzo W.L., Murry C.E., Ruohola-Baker H. (2015). Let-7 family of microRNA is required for maturation and adult-like metabolism in stem cell-derived cardiomyocytes. PNAS *112(21)*, E2785-94.

Li Q.Y., Newbury-Ecob R.A., Terrett J.A., Wilson D.I., Curtis A.R.J., Yi C.H., Gebuhr T., Bullen P.J., Robson S.C., Strachan T., Bonnet D., Lyonnet S., Young I.D., Raeburn J.A., Buckler A.J., Law D.J., Brook J.D. (1997). Holt-Oram syndrome is caused by mutations in TBX5, a member of the Brachyury (T) gene family. Nat Genetics *15(1)*, 21-9.

Li R.G., Li L., Qiu X.B., Yuan F., Xu L., Li X., Xu Y., Jiang W., Jiang J., Liu X., Fang W., Zhang M., Peng L., Qu X., Yang Y. (2013) GATA4 loss-of-function mutation underlies familial dilated cardiomyopathy. BiochemBiophys Res Commun *439*, 591–596.

Lian X., Hsiao C., Wilson G., Zhu K., Hazeltine L.B., Azarin S.M., Raval K.K., Zhang J., Kamp T.J., Palecek S.P. (2012). Robust cardiomyocyte differentiation from human pluripotent stem cells via temporal modulation of canonical Wnt signaling. PNAS *109(27)*, E1848-57.

Liang Q., De Windt L.J., Witt S.A., Kimball T.R., Markham B.E, Molkentin J.D. (2011). The Transcription Factors GATA4 and GATA6 Regulate Cardiomyocyte Hypertrophy *in Vitro* and *in Vivo* J. Biol. Chem*. 276,* 30245-30253.

Lopaschuk G.D., Jaswal J.S. (2010). Energy Metabolic Phenotype of the Cardiomyocyte During Development, Differentiation, and Postnatal Maturation. J Cardiovasc Pharmacol *56(2)*,130-140.

Maitra M., Schluterman M.K., Nichols H.A., Richardson J.A., Lo C.W., Srivastava D., Garg V. (2009). Interaction of Gata4 and Gata6 with Tbx5 is critical for normal cardiac development. Developmental Biology *326*, 368–377.

Misra, C., Sachan N., McNally C.R., Koenig S.N., Nichols H.A., Guggilam A., Lucchesi P.A., Pu W.T., Srivastava D., Garg V. (2012). Congenital Heart Disease–Causing Gata4 Mutation Displays Functional Deficits *In Vivo*. PLOS Genetics *8*, e1002690.

Molkentin, J.D., Lin Q., Duncan S.A., Olson E.N. (1997). Requirement of the transcription factor GATA4 for heart tube formation and ventral morphogenesis. Genes & Development *11*, 1061-72.

Moretti, A., Bellin M., Welling A., Jung C.B., Lam J.T., Bott-Flügel L., Dorn T., Goedel A., Höhnke C., Hofmann F., Seyfarth M., Sinnecker D., Schömig A., Laugwitz K. (2010). Patient-Specific Induced Pluripotent Stem-Cell Models for Long-QT Syndrome. NEJM *363(15)*, 1397-1409.

Moskowitz I. P, Wang J., Peterson M.A., Pu W.T., Mackinnon A.C., Oxburgh L., Chu G.C., Sarkar M., Berul C., Smoot L., Robertson E.J., Schwartz R., Seidman J.G., and Seidman C.E. (2011). Transcription factor genes *Smad4* and *Gata4* cooperatively regulate cardiac valve development. PNAS *108*, 4006-4011.

Munshi N.V., McAnally J., Bezprozvannaya S., Berry J.M., Richardson J.A., Hill J.A., Olson E.N. (2009). *Cx30.2* enhancer analysis identifies Gata4 as a novel regulator of atrioventricular delay. Development *136*, 2665-2674.

Oka T., Maillet M., Watt A.J., Schwartz R.J., Aronow B.J., Duncan S.A., Molkentin J.D. (2006). Cardiac-Specific Deletion of *Gata4* Reveals Its Requirement for Hypertrophy, Compensation, and Myocyte Viability. *Circ Res 9*, 837-845.

Okita, K., Matsumura Y., Sato Y., Okada A., Morizane A., Okamoto S., Hong H., Nakagawa M., Tanabe K., Tezuka K., Shibata T., Kunisada T., Takahashi M., Takahashi J., Saji H., Yamanaka S. (2011). A more efficient method to generate integration-free human iPS cells. Nature Methods *8*, 409–412.

Porrello E.R., Mahmoud A.I., Simpson E., Hill J.A., Richardson J.A., Olson E.N., Sadek H.A. (2011). Transient Regenerative Potential of the Neonatal Mouse Heart. Science 331, 1078-80.

Qian, L., Huang Y., Spencer C.I., Foley A., Vedantham V., Liu L., Conway S.J., Fu J., Srivastava D. (2012). *In vivo* reprogramming of murine cardiac fibroblasts into induced cardiomyocytes. Nature *485*, 593-8.

Rajagopal S.K., Ma Q., Obler D., Shen J., Manichaikul A., Tomita-Mitchell A., Boardman K., Briggs C., Garg V., Srivastava D., Goldmuntz E., Broman K.W, Benson D.W., Smoot L.B., Pu W.T. (2007). Spectrum of heart disease associated with murine and human GATA4 mutation. J Mol Cell Cardiology *43*, 677–685.

Reller M.D., Strickland M.J., Riehle-Colarusso T., Mahle W.T., Correa A. (2008). Prevalence of congenital heart defects in Atlanta, 1998-2005. J Pediatr. *153*, 807-13.

Rivera-Feliciano J., Lee K.H., Kong S.W., Rajagopal S., Ma Q., Springer Z., Izumo S., Tabin C.J., Pu W.T. (2006). Development of heart valves requires Gata4 expression in endothelial-derived cells. Development *133,* 3607–3618.

Rojas, A., Kong S.W., Agarwal P., Gilliss B., Pu W.T., Black B.L. (2008). GATA4 is a direct transcriptional activator of cyclin D2 and Cdk4 and is required for cardiomyocyte proliferation in anterior heart field-derived myocardium. Molecular and cellular biology *28(17)*, 5420-31.

Ryan S.D., Dolatabadi N., Chan S.F., Zhang X., Akhtar M.W., Parker J., Soldner F., Sunico C.R., Nagar S., Talantova M., Lee B., Lopez K., Nutter A., Shan B., Molokanova E., Zhang Y., Han X., Nakamura T., Masliah E., Yates J.R., Nakanishi N., Andreyev A.Y., Okamoto S., Jaenisch R., Ambasudhan R., Lipton S.A. (2013). Isogenic human iPSC Parkinson's model shows nitrosative stress-induced dysfunction in MEF2-PGC1α transcription. Cell 155(6), 1351-64.

Sander J.D. and Joung J.K. (2014). CRISPR-Cas systems for editing, regulating and targeting genomes. Nature Biotechnology *32(4)*, 347-55.

Sandra Merscher S., Funke B., Epstein J.A., Heyer J., Puech A., Lu M.M., Xavier R.J., Demay M.B., Russell R.G., Factor S., Tokooya K., St. Jore B., Lopez M., Pandita R.K., Lia M., Carrion D., Xu H., Schorle H., Kobler J.B., Scambler P., Wynshaw-Boris A., Skoultchi A.I., Morrow B.E., Kucherlapati R. (2001). *TBX1* Is Responsible for Cardiovascular Defects in Velo-Cardio-Facial/DiGeorge Syndrome. Cell *104*, 619–629.

Sarkozy A., Conti E., Neri C., D'Agostino R., Digilio M.C., Esposito G., Toscano A., Marino B., Pizzuti A., Dallapiccola B. (2005). Spectrum of atrial septal defects associated with mutations of NKX2.5 and GATA4 transcription factors. J Med Genet *42*, e16.

Schlesinger J., Schueler M., Grunert M., Fischer J.J., Zhang Q., Krueger T., Lange M., Tönjes M., Dunkel I., Sperling S.R. (2011). The cardiac transcription network modulated by Gata4, Mef2a, Nkx2.5, Srf, histone modifications, and microRNAs. PLoS genetics *7*, e1001313.

Smale S.T. (2010). Pioneer Factors in Embryonic Stem Cells and Differentiation. Curr Opin Genet Dev. *20(5)*, 519–526.

Srivastava D. (2006). Making or Breaking the Heart: From Lineage Determination to Morphogenesis. Cell *126*, 1037-48.

Srivastava, D., Olson E.N. (2000). A genetic blueprint for cardiac development. Nature *407(6801)*, 221–226.

Sylva M., van den Hoff M.J.B., Moorman A.F.M. (2013). Development of the Human Heart. Am J Med Genet Part A *164A*, 1347–1371.

Takahashi, K. & Yamanaka, S. (2006). Induction of pluripotent stem cells from mouse embryonic and adult fibroblast cultures by defined factors. Cell *126*, 663-76.

Tevosian S.G., Albrecht K.H., Crispino J.D., Fujiwara Y., Eicher E.M.' Orkin S.H. (2002). Gonadal differentiation, sex determination and normal Sry expression in mice require direct interaction between transcription partners GATA4 and FOG2. Development *129(19)*, 4627-34.

Theodoris C.V., Li M., White M.P., Liu L., He D., Pollard K.S., Bruneau B.G., Srivastava D. (2015). Human disease modeling reveals integrated transcriptional and epigenetic mechanisms of NOTCH1 haploinsufficiency. Cell *160(6)*, 1072-86.

Tohyama S., Hattori F., Sano M., Hishiki T., Nagahata Y., Matsuura T., Hashimoto H., Suzuki T., Yamashita H., Satoh Y., Egashira T., Seki T., Muraoka N., Yamakawa H., Ohgino Y., Tanaka T., Yoichi M., Yuasa S., Murata M., Suematsu M., Fukuda K. (2013). Distinct Metabolic Flow Enables Large-Scale Purification of Mouse and Human Pluripotent Stem Cell-Derived Cardiomyocytes. Cell Stem Cell *12*, 127–137.

Tomita-Mitchell A., Maslen C.L., Morris C.D., Garg V., Goldmuntz E. (2007) GATA4 sequence variants in patients with congenital heart disease. J Med Genet *44*, 779-783.

Uosaki H., Fukushima H., Takeuchi A., Matsuoka S., Nakatsuji N., Yamanaka S., Yamashita J.K. (2011). Efficient and Scalable Purification of Cardiomyocytes from Human Embryonic and Induced Pluripotent Stem Cells by VCAM1 Surface Expression. PLoS ONE *6(8)*, e23657.

van den Berg G., Abu-Issa R., de Boer B.A., Hutson R.A., de Boer P.A.J., Soufan A.T., Ruijter J.M., Kirby M.L., van den Hoff M.J.B., Moorman A.F.M. (2009). A Caudal Proliferating Growth Center Contributes to Both Poles of the Forming Heart Tube. Circ Res. *104*, 179-188.

Watt A.J., Battle M.A., Li J., Duncan S.A. (2004). GATA4 is essential for formation of the proepicardium and regulates cardiogenesis. PNAS *101(34)*, 12573-12578.

Watt A.J., Zhao R., Li J., Duncan S.A. (2007). Development of the mammalian liver and ventral pancreas is dependent on GATA4. BMC Dev Biol. *23*, 7-37.

Yang Y., Wang J., Liu X., Chen X., Zhang W., Wang X., Liu X., Fang W. (2012). Novel *GATA4* mutations in patients with congenital ventricular septal defects. Med Sci Monit. *18(6)*, CR344–CR350.

Yang Y.Q., Gharibeh L., Li R.G., Xin Y.F., Wang J., Liu Z.M., Qiu X.B., Xu Y.J., Xu L., Qu X.K., Liu X., Fang W.Y., Huang R.T., Xue S., Nemer G. (2014). GATA4 loss-of-function mutations underlie familial tetralogy of fallot. Hum Mutat. *34(12)*, 1662-71.

Young J.L., Engler A.J. (2011). Hydrogels with time-dependent material properties enhance cardiomyocyte differentiation *in vitro*. Biomaterials *32(4)*, 1002-9.

Zeisberg E.M., Ma Q., Juraszek A.L., Moses K., Schwartz R.J., Izumo S., Pu W.T. (2005). Morphogenesis of the right ventricle requires myocardial expression of *Gata4.* J. Clin Invest. *115(6)*, 1522-31.

Zhang C. (2008). MicroRNAs: role in cardiovascular biology and disease. Clinical Science *114*, 699–706.

Zhang W., Li X., Shen A., Jiao W., Guan X., Li Z. (2008). GATA4 mutations in 486 Chinese patients with congenital heart disease. Eur J Med Genet. *51(6)*, 527-35.

Zhao L., Xu J.H., Xu W.J., Yu H., Wang Q., Zheng H.Z., Jiang W.F., Jiang J.F., Yang Y.Q. (2014). A novel GATA4 loss-of-function mutation responsible for familial dilated cardiomyopathy. Int J Mol Med. *33(3)*, 654-60.

Zhou P., He A., Pu W.T. (2012). Regulation of GATA4 Transcriptional Activity in Cardiovascular Development and Disease. Current Topics in Developmental Biology *100*, 143-169.

Chapter 2

Lamp2 as a Potential Modifier of GATA4 Cardiomyopathy

ABSTRACT

The study of the contribution of genetic modifiers to disease is an area that needs further study. We identified a family with a known, well characterized genetically inherited congenital heart disease that is now presenting with new juvenile-onset cardiomyopathy in a branch of generation V. Complete genome sequencing of twenty-five members of the *GATA4 G296S* pedigree, including those with the cardiomyopathy, was performed and analyzed. From this analysis we identified a candidate list of genetic modifiers for the cardiomyopathy phenotype. *LAMP2 I252S* was the top hit by bioinformatics and interested us because *LAMP2* has been observed mutated in other patients with genetically defined cardiomyopathy and GATA4 has been shown to upregulate autphagy. We used dermal fibroblasts from eight affected or unaffected related controls to generate integration-free iPS cells and differentiated them to beating cardiomyocytes. We tested the hypothesis that mutation of a modifier gene in

family members with the *GATA4 G296S* mutation results in cardiomyopathy. We examined the cardiomyocytes for defects in autophagic flux with a particular focus on the fusion of the autophagosomes with the lysosome, the step that LAMP2 regulates, but did not observe a consistent defect. Therefore, we theorized that if there were a more subtle defect in autophagic clearance by the lysosomes, and GATA4 was upregulating autophagy, we might observe a synthetic lethality. We analyzed these CMs for a cell survival defect and did not see increased death in the double mutant CMs over the controls. Finally, upon examination of electron micrographs we saw evidence of an increased number of lipid droplets in the double mutants. This phenotype is interesting because fatty infiltrates in the heart can cause dysfunction and LAMP2 has a role in lipid transport. However, when quantified by confocal imaging of BODIPY-labeled lipid droplets, there was no observable defect in the amount of lipid accumulated or in the number or size of droplets per cell.

Some of these assays, like the autophagic flux experiment, were targeted specifically to LAMP2, but not all were so targeted. In particular, cell death and lipid accumulation, are not the sole province of LAMP2. Yet, it is still possible that this candidate is the real modifier or that it is a collection of modifiers that creates the cardiomyopathy phenotype. The failure to identify an *in vitro* phenotype associated with the cells from the affected individuals could be due to many factors like the difference of the *in vitro* versus *in vivo* environment, the difficulty in modeling an age-associated phenotype, or merely the difficulty in isolating a defect that is consistent across a number of different lines. However, our strategy

represents an interesting and potentially fruitful way to interrogate the significance of putative genetic modifiers in a model of disease.

INTRODUCTION

How one gene could modify the phenotype of another gene has been a question not just for genetically inherited diseases but for many different non-Mendelian inherited diseases. Many different modifiers for a common disease phenotype can be clustered together and said to have a strong effect en masse towards the development of disease, but it does not prove that those identified factors are actually causative. A way of getting around this problem is to use a Mendelian disease with high penetrance and limited expressivity and then screen for modifiers that might be affecting a discrete few in a pedigree. The advent of complete genome sequencing combined with powerful genetic bioinformatics tools has the power to reveal candidate susceptibility loci. Verifying if any of these candidate modifiers have the power to alter the phenotype *in vitro* can then be assayed through the use of Induced Pluripotent Stem Cell (iPSC) technology, which can then allow for the verification of these candidates in an *in vitro* system. We developed such a system to study a branch of the GATA4 G296S family previously published in (Garg *et al.* 2003).

The GATA4 G296S family is a large multi-generation family, in which many family members are affected by septal and valvular defects **(Fig 1)**. The

G296S mutation is completely penetrant and dominantly inherited. Most of the family members received surgical treatment of their heart defect and were described as healthy afterwards. Recently, however, despite surgical repair of septal defects, some family members in a specific branch of the GATA4 G296S family have developed a cardiomyopathy in their second decade of life **(Fig 2A, B)**. The two male patients are the most severely affected. In addition to their septal defects and pulmonary stenosis (PS), they now have also developed an enlargement of their right ventricles, hypertrabeculation of the right ventricle, and ascending aortic aneurysms (AAs). The younger of the two brothers also has heart failure; both were under the age of 18 at diagnosis **(Figure 2A, B)**. Cardiomyopathy has never been reported in a human patient carrying this *GATA4 G296S* mutation, despite other family members with the mutation having lived significantly longer in this family and other families with the same mutation (Moskowitz *et al.* 2011, Sarkozy *et al.* 2005). There are some data from mice that suggests that given the appropriate genetic background, a cardiomyopathy can develop in mice heterozygous for a *Gata4* gene knock out (KO) (Rajagopal *et al.* 2007). Additionally, there have been reports of families with other mutations in *GATA4* associated with dilated cardiomyopathy (Li *et al.* 2013, Zhao *et al.* 2014).

Mice heterozygous for a *Gata4* null deletion develop more severe systolic dysfunction upon pressure-overload stress and have other cardiac perturbations at baseline including mild systolic and diastolic dysfunction and decreased heart size (Bisping *et al.* 2006). It is remarkable that these phenotypes would be revealed in a heterozygous mouse, as heterozygous mice rarely have a

phenotype. Yet, the human patients have not previously demonstrated cardiac dysfunction. It is possible that the human GATA4 G296S patients have an increased susceptibility but the age of these cardiomyopathy patients compared to the ages of the other mutation carriers that are significantly older argues against this simple explanation. Therefore, while we suspected it was possible that the disease was due to *GATA4* in part, the novelty of this phenotype in only one branch of the family suggested another possibility; there could be genetic modifier maternally inherited that increased these patients' susceptibility to cardiomyopathy. Thus, we saw that this family's genetic disease could represent a unique opportunity to study the role of GATA4 in the development of cardiomyopathy and in the study of other genetic modifiers.

METHODS

Generation of iPS cells from patient-specific dermal fibroblasts

Skin biopsies were taken from eight family members both those affected and unaffected related controls. The biopsies were manually dissected to smaller fragments and plated on gelatin in high serum (DMEM, 20% FBS, Glutamax, NEAA, P/S). Once the fibroblasts and associated cells migrated out onto the plate, they were collected and frozen at p0 under standard sterile conditions.

We created iPS cells using a non-integrating episomal model described in (Okita *et al.* 2011). Episomal plasmids containing *OCT4*, *SOX2*, and *KLF4* were

transfected using the Neon Transfection Kit and Device (Invitrogen). Electroporation conditions were 1650 Volts, 10 mm width, and 3 pulses. Post-transfection cells were cultured in fibroblast conditions for 5 days before they were transferred to plates with growth-inactivated SNL feeders in ES cell media (KO DMEM, 20% KSR, NEAA, P/S, 100uM BME). Between days 20-30 post-transfection colonies with the appropriate stem cell morphology were picked by pipette and replated on hESC-qualified matrigel (BD Biosciences). iPS cells were maintained feeder-free with matrigel and mTeSR medium (Stem Cell Technologies) and passaged using Dispase in DMEM/F-12 (Stem Cell Technologies) to dissociate cells.

At least 10 clones of every line were isolated and passaged at least three times. The clone from each patient line that grew most robustly with minimal differentiation was selected for further downstream testing. This early clonal selection is reflected in the names of the clones used. For instance, “1.8” is one of the cell lines selected for further use and “1.8” simply means that it is the eighth clone obtained from patient 1 (IV-12). **Table 1** depicts the numbering scheme used throughout for discussions of the cell lines instead of the pedigree numbering system used with the patients. Genomic DNA was extracted from both the HDFs and the resultant iPS cells and verified by sequencing to have the same mutations (**Fig. 3A**). We also checked by STR profiling (Johns Hopkins Cell Line Authentication service) that these were the same from HDF to iPSC to CM.

iPS Cell Characterization

These cells were then tested for multiple markers of pluripotency and assayed for their ability to form all three germ layers. Immunohistochemistry was performed with antibodies against TRA-1-60 (Abcam), TRA-1-81 (Abcam), OCT4 (Cell Signaling), NANOG (Abcam), SSEA3 (eBioscience), and SSEA4 (Abcam) and the appropriate staining patterns were observed (**Fig. 3D**). Karyotypes were assessed by cytogenetic analysis on twenty G-banded metaphase cells by Cell Line Genetics (Madison, WI) and found to be normal (**Fig 3B**). The appropriate expression by quantitative RT-PCR of pluripotency genes (*POU5F1 (OCT4)*, *NANOG*, *SOX2*, *MYC*, *TERT1*, and *LIN28A)* as well as a lack of expression of genes seen in fibroblasts (*COL1A1* and *VIM)* was observed by quantitative RT-PCR, normalized to *GAPDH*. The original fibroblast lines as well as another ES cell line served as controls (**Fig. 3C**).

The ability of the cell lines to differentiate *in vitro* was assessed by embryoid bodies formation assay. Cells were aggregated in ultra-low attachment plates (Corning) in differentiation media (KO DMEM, 20% FBS, NEAA, Glutamax, 100 μM BME) for 14 days. Immunocytochemistry was performed using antibodies against GFAP (Dako) for ectoderm, SMA (Dako) for mesoderm, and AFP (R&D Systems) for endoderm (**Fig. 3D**).

In vivo differentiation ability was assessed with the teratoma formation assay. 8–14-week-old male CB17 SCID mice (Charles River) were injected with matrigel (BD Biosciences) plugs of iPS cells and collected 8-12 weeks later. Three injections were performed per line and then the teratomas were fixed overnight in 10% formalin. Fixed teratomas were sectioned and stained with Hematoxylin and Eosin (H&E) using standard methods to identify histologic structures for all three germ layers. **(Fig. 3D)**.

Directed Differentiation of CMs from iPSCs and Culturing Methods

Cardiomyocytes were made using the protocol in (Zhang *et al.* 2009) to generate beating sheets. Differentiation batches averaged from 50-80% purity of cardiomyocytes. The *in vitro* differentiated cardiomyocytes demonstrated appropriate staining of cardiomyocyte markers cTnT (Thermo Scientific), αActinin (Sigma), HCN4 (Alomone labs), GATA4 (Abcam), cTnI (Santa Cruz), VIM (Progen), MLC2a (MYL7 Abcam), and MLC2v (MLC2 Abcam) **(Figure 4)**. Cardiomyocytes were plated on fibronectin (Sigma F1141) diluted 1:80 in 0.02% gelatin (Sigma) in PBS. Cells were maintained in RPMI 1640 with B27 plus insulin (Life Technologies), with the media changed every 3 days.

Genomic Samples and Bioinformatics

Patient samples for sequencing were obtained for the publication (Hu *et al.* 2014) and analyzed according to that published protocol to verify the algorithm pVAAST. pVAAST is available at www.hufflab.org/software/pvaast for download. The human sequencing data has been submitted to the Genotypes and Phenotypes database (dbGaP), accession code: phs000758.v1.p1.

Immunocytochemistry

Cells were fixed in 4% paraformaldehyde (Electron Microscopy Sciences) for 20 minutes at room temperature (RT), washed with PBS, and permeabilized with PBS+ 1% bovine serum albumin + 0.1% Triton-100. Next, preparations were blocked with 1x Powerblock (Biogenex), and incubated on a rocker with primary antibody at 4 degrees overnight. The primary antibody was rinsed 3x, washed for 5 minutes 3x, blocked again for 30 mins at RT, and the AlexaFluor secondary antibody (Life Technologies) added 1:300 for 2 hours at RT. Coverslips were rinsed 3x, washed for 5 mins 3x, and stained with DAPI for 20 mins. After washing with PBS, slides were mounted with Prolong Gold Antifade Reagent (Life Technologies). Cells were imaged with a Zeiss Axiovert 200 M with a Zeiss Axiocam MRm or a Leica Microsystems DMI6000B with a Hamamatsu ORCA-R2 camera.

PCR, Cloning, Quantitative RT-PCR and siRNA Knockdown

Genomic DNA was isolated from fibroblasts, iPS cells, and CMS with the DNAeasy Blood and Tissue Kit (Qiagen). Genomic DNA was amplified with Platinum Taq DNA Polymerase High Fidelity (Invitrogen). Primer sequences used for the *GATA4 G296S* and *LAMP2 I252S* locus are in **Table 3**. RNA was extracted by the TRizol method (Invitrogen). RT–PCR was performed using the Superscript III first-strand synthesis system (Invitrogen). cDNA was amplified using Platinum Taq DNA Polymerase High Fidelity (Invitrogen) and the primers in **Table 3**. Then these PCR products were subcloned with the TOPO-TA Cloning Kit (Life Technologies), transfected using standard protocols, and sequenced. qPCR was performed using the ABI 7900HT (TaqMan, Applied Biosystems) per the manufacturer's protocols. Optimized primers from the Taqman Gene Expression Array were used. Gene Knockdown was performed using control siRNA or targeted using RNAiMAX Transfection Reagent (Life Technologies). Cells were harvested 48 hours later and assayed or used for RNA isolation with RNAeasy Micro Kit (Qiagen). Knockdown was done with several different siRNAs to test effectiveness for LAMP2 (Santa Cruz sc-92390) and GATA4 (Sigma SAS1_Hs01_00212513).

Autophagic Flux Assay

Beating cardiomyocytes were washed three times with PBS and either put back in normal media or serum starvation media for 24 hours. Serum starvation media was RPMI 1640 (without supplement) and 1x penicillin-streptomycin. For the last 2 hours of the of the 24 hours time point, the cells were washed again and given back the same media with DMSO or Bafilomycin A1 (BafA) 50nM. Finally, cells were rinsed 2x with ice cold PBS, aspirated, then 50uL per 12 well of RIPA plus additives (PMSF, NaVO4, PIC, NaF, BGP, Pepstatin A, E64d, and Calyculin A) were added. Cells were pipetted off the well with a 100uL pipette into chilled 1.5mL Eppendorf tubes on ice. They were then immediately transferred to the -80° freezer. Lysates were used in Western Blots and stained for LC3 and tubulin and quantified by densitometry. Assays were repeated twice and done blinded to genotype.

Electron Microscopy

For electron microscopy, cells were fixed in 2% glutaraldehyde, 1% paraformaldehyde in 0.1M sodium cacodylate buffer pH 7.4, post fixed in 2% osmium tetroxide in the same buffer, en block stained with 2% aqueous uranyl acetate, dehydrated in acetone, infiltrated, and embedded in LX-112 resin (Ladd Research Industries, Burlington, VT). Samples were ultrathin sectioned on a Reichert Ultracut S ultramicrotome and counter stained with 0.8% lead citrate. Grids were examined on a JEOL JEM-1230 transmission electron microscope

(JEOL USA, Inc., Peabody, MA) and photographed with the Gatan Ultrascan 1000 digital camera (Gatan Inc., Warrendale, PA).

Cell Death, Lipid Labeling Assays, and Flow Cytometry

Apoptosis (TUNEL) assays were performed using the In Situ Cell Death Detection Kit, Fluorescein (Roche) according to manufacturer instructions. Annexin V staining was done according to manufacturer's protocol with the Annexin V AlexaFluor conjugate 594 antibody (Life Technologies) and then assayed with flow cytometry. Lipids were labeled with BODIPY (Life Technologies) dye diluted 1:1000 in media. Cells were dissociated with Accutase (StemPro), quenched, and washed with PBS twice. Cells were resuspended in cold FACS buffer and placed on ice. Cells were immediately assessed on a BD Biosciences LSRII and analyzed with FlowJo software.

Statistical analyses

Differences between groups were examined for statistical significance using unpaired Student's t-test or ANOVA. A P-value of 0.05 was regarded as significant. Error bars indicate standard deviation, unless otherwise noted.

RESULTS

Screen for Genetic Modifiers

The utility of genomics has been expanding rapidly since its inception. Through collaboration with the Institute of Systems Biology in Seattle and Katherine Pollard at Gladstone, we have launched a search for a potential modifier of GATA4. The complete genomes of twenty-five members of the GATA4 pedigree have been sequenced **(Figure 1)**. This sequencing information was initially used to successfully validate an algorithm that can take into account the relatedness of individuals in a pedigree to find causative mutations for genetic disease (Hu *et al.* 2014). This same algorithm, called pVAAST, was then applied to the branch of the family with new onset cardiomyopathy and a list of candidate genes was identified **(see Table 2)**. *LAMP2* was found to have the greatest statistical significance of the possible mutations. The mutation is an I252S point mutation **(depicted in Fig 2D)**. This mutation was only found in the mother and her affected children and not in the rest of the GATA4 family or 400 unrelated controls. The allele frequency was found to be 0.05% in the 1000 Genomes Project (The 1000 Genomes Project Consortium 2012) and 0.1038% in the ExAC database (http://exac.broadinstitute.org/gene/ENSG00000005893), including once in the homozygous state in a female, indicating that it is rare. Interestingly, *LAMP2* is located on the X-chromosome and, of the three children, the two males are the most severely affected **(Figure 2A,B)**. As one might expect from the location of *LAMP2*, the cardiomyopathy with which it is

associated primarily affects males (Nishino *et al.* 2000). Taken together, these data make the *LAMP2 I252S* mutation a viable candidate as a modifier allele. Once I had this information, I sought to confirm that the mutation was the same in the mother and her children and to identify if there were any males in her family with the mutation and potentially with any form of heart disease. I was able to confirm the inheritance of the allele and trace it back to the maternal grandfather who did not report any heart disease **(Figure 2A,C)**. This means that, in this family, the *LAMP2 I252S* allele by itself does not lead to disease. This matched our expectations. If the grandfather had had heart disease, then this could have been a case of two independent diseases co-occurring together instead of this being a mutation that only causes disease when in the appropriate susceptible background as would be expected for a modifier. Interestingly, in the patients with bone fide *LAMP2* mutation-causing cardiomyopathy, the age of onset roughly matches the age of onset of these patients (Maron *et al.* 2009). Additionally, I confirmed that there was not a difference in the protein levels for LAMP2 in the cardiomyocytes of the different cell lines **(Fig 5A)**. Through labeling of the patient specific human dermal fibroblasts, I also did not observe a difference in cellular localization **(Fig 5B)**.

Consideration of LAMP2 as a potential genetic modifier of GATA4

LAMP2 stands for lysosomal associated membrane protein 2 **(Fig 2D)**. It is a heavily glycosylated protein that, along with LAMP1, makes up over 50% of

the proteins on the lysosomal membrane. LAMP2 has been found to have many different roles in protein turnover from macroautophagy to chaperone mediated autophagy (Eskelinen 2006). *LAMP2* is also associated with a cardiomyopathy called Danon disease (Nishino *et al.* 2000). Danon disease can be found sporadically (Nishino *et al.* 2000) as well as in small families (Arad *et al.* 2005) with mutations in *LAMP2*. There are a broad range of mutations associated with Danon disease, most with early truncations but some with point and splice junction mutations (Nishino *et al.* 2000). The *I252S LAMP2* mutation has thus far not been associated with Danon disease. Males are primarily affected as they are hemizygous at the locus. If heterozygous females are affected, it tends to be decades later than in the affected males of the family (Lobrinus *et al.* 2005). Ultrastructurally, these patients show an accumulation of autophagic vacuoles (Nishino *et al.* 2000), consistent with a block in the later stages of autophagy. The accumulation of autophagic vacuoles has also been shown in the *Lamp2*$^{-/-}$ mouse (Tanaka *et al.* 2000) and in cell culture models of *Lamp2* depletion (González-Polo *et al.* 2005). The accumulation of autophagic vacuoles represents a failure at the later stages of autophagy for autophagosomes to fuse with lysosomes and leads to an increase in cell death (Tanaka *et al.* 2000; González-Polo *et al.* 2005). The *Lamp2* KO mouse also demonstrates reduced cardiac function, consistent with the idea that LAMP2 loss is responsible for the cardiac phenotype (Tanaka *et al.* 2000; Stypmann *et al.* 2006).

LAMP2 and GATA4 have been shown to have effects on autophagy. GATA4 transcribes *Bcl-2* in a dosage-dependent manner in cardiomyocytes

(Aries *et al.* 2004, Kobayashi *et al.* 2006). BCL2, an anti-apoptotic protein, binds and inhibits the pro-autophagic protein Beclin1 (Kang *et al.* 2011). Lowered levels of GATA4 have been found in association with higher levels of Beclin1 and increased levels of autophagy (Kobayashi *et al.* 2010). This increase in autophagy leads to an increase in cell death, and an increase in cell death has been shown to cause contractile dysfunction in mice (Wencker *et al.* 2003), a phenotype seen in many cardiomyopathies. *LAMP2* knockout or depletion causes a block in later stages of autophagy and sensitizes the cell to apoptosis that can be rescued by BCL2 expression (Tanaka *et al.* 2000, González-Polo *et al.* 2005). An increase in the induction and a block in the later phase of autophagy may create a sensitized state in the cell leading to dysfunction. As both genes have a role in the common process of autophagy, a genetic interaction between *LAMP2* and *GATA4* could be revealed due to an overlap in a biologic pathway they both regulate **(See Figure 6 for a schematic)**.

Evaluation for Autophagic Defect

We sought to evaluate whether the *LAMP2 I252S* mutation had an effect on autophagy by testing autophagic flux. LC3 is a protein that has different localization patterns depending on its isoform. LC3 is transiently present in the cell before being converted to LC3-I, the major form in the cytosol. When autophagy is induced, LC3-I gets converted to LC3-II and is incorporated into the autophagosomal membrane. Thus, LC3-II levels are a way to assess autophagic

induction by western blot. Bafilomycin A1 (BafA) is an inhibitor of the fusion of the autophagosome with the lysosome and works at the same step that LAMP2 has been shown to have functional consequences (Tanaka *et al.* 2000, Eskelinen *et al.* 2006). When autophagy is induced in the presence of BafA, there is an increase in LC3-II accumulation under normal conditions (Barth *et al.* 2010) **(Figure 7A)**. However, if there were a fusion defect, there would not be an accumulation of LC3-II with BafA treatment, because the inhibitor would have minimal ability to further hinder a defective process (Mizushima *et al.* 2010). When we applied this assay to the cardiomyocytes, they demonstrated a normal level of flux that was inconsistent with there being a significant defect in this process **(Fig 5C)**. This result was true for both male lines with both mutations, as well as a female line that was a *GATA4 G296S* heterozygote and expressed primarily the mutant form of *LAMP2* (94% mutant allele) **(Figure 5B)**. Consistent with this finding, electron micrographs (EMs) failed to demonstrate a difference in accumulation of autophagic vacuoles, as has been described for *LAMP2* mutations previously **(Fig 5D)** (Tanaka *et al.* 2000). Thus, by these metrics it does not appear that the cardiomyocytes from these patients demonstrate a consistent autophagic flux defect.

Cell Death Is Not Increased in Double Mutants

Next, I wanted to evaluate if there was an effect on cell viability due to the combined effects of GATA4 and LAMP2 regulating a common pathway involved

in cell survival. To do this, I assayed multiple lines for apoptosis and DNA fragmentation by terminal deoxynucleotidyl transferase dUTP nick end labeling (TUNEL) **(image in Fig 8A)** followed by flow cytometry quantification. There were no consistent differences between lines by TUNEL on multiple lines or on different days **(Fig 8B)**. This result indicates that for these lines, there does not appear to be a survival disadvantage under baseline conditions. To determine if this lack of difference was due insufficient sensitivity of this assay, wildtype cardiomyocytes were transfected with siRNAs for GATA4 and LAMP2 for 48 hours in order to see if a more severe reduction of the protein levels would reveal a survival defect. Likewise, these cells did not reveal a survival difference by TUNEL (*data not shown*) or by the similar assay using an Annexin V conjugate antibody **(Fig 8C)** despite significant knockdown of the siRNA targets **(Fig 8D)**. This is a little surprising because GATA4 itself has many published roles in maintaining cell viability (Aries *et al.* 2004). Perhaps the knockdown was not for a sufficiently long enough time or the cells merely detached from the plate too readily once cell death became imminent. It could also be because the G296S mutation does not have a large effect on the downstream targets important for regulating CM viability and maintenance. Regardless, these results are consistent with there not being an autophagic defect. Moreover, the double mutant cells are not more difficult to maintain in culture as compared to control lines. These are terminally differentiated cells with minimal proliferative ability. Therefore for these cells to be maintained in culture over the months long time frame that they are observed argues against there being a higher baseline

phenotype for cell survival. Cell death is also not a LAMP2 specific phenotype. Although an abnormal phenotype observed here could contribute to a LAMP2-related modifier effect, it could also merely indicate that there is a difference in the patient lines that have cardiomyopathy. It is arguably more significant that 2.6 does not have a cell survival defect than that 3.2 does not, because the 2.6 cell line is from one of the patients with cardiomyopathy, unlike 3.2, which is from a patient with both mutations but without cardiomyopathy.

Cellular Lipid Stores

On EM, it appeared that there might be an increase in lipid droplets in the double mutant CMs **(Fig 9A)**. In the mouse, there is evidence that GATA4 is involved in regulating genes involved in dietary lipid uptake in the intestine (Patankar *et al.* 2011), but not in regulating lipid storage within cells. LAMP2, however, has been implicated in cholesterol storage and esterification (Schneede *et al.* 2011). It was shown that the luminal domain of LAMP2 near the hinge region (where the I252S mutation is located) is important for cholesterol trafficking **(see Fig 2D)**. It is also an observation made before we realized that there was a lipid-associated phenotype with LAMP2. But again, this assay is not as rigorously LAMP2-specific and, therefore, could represent a defect in lipid handling in general that could then be evaluated for rescue by LAMP2 or one of the other candidates. Therefore, I sought to see if there was a lipid accumulation defect in in these CMs using the nonpolar lipophilic dye BODIPY. BOPIDY was also reported to have revealed a lipid accumulation defect in LAMP -/- cells

(Schneede *et al.* 2011). BODIPY has been used by many studies to label intracellular lipid droplets and measure their shape and localization patterns (Cohen *et al.* 2004, Singh *et al.* 2009).

Here, the dye was applied to the CMs imaged via confocal microscopy and quantified with normalization for total area of BODIPY staining relative to area of cTnT **(Fig 9B)**. This analysis did not reveal a significant difference across the cell lines. When the total area of lipid was normalized to the number of nuclei, this was also not significantly different **(Fig 9C)** and also confirmed the trends of the prior normalization. To determine if there were perhaps more subtle defects associated with lipid droplet storage and transport, the average droplet size was quantified and no significant differences were found **(Fig 9D)**. We also quantified the total number of lipid droplets by nuclei to get a closer approximation for how many lipid droplets there were per cell. This measure was also negative for a significant difference across genotypes **(Fig 9E)**. Both of these pieces of data argue that the droplets themselves were not individually larger or more numerous. Taken together, this analysis revealed that there was not a significant difference across genotypes for total amount of BODIPY stained lipid accumulation, number of droplets, or size of droplets. In general, there was perhaps a trend towards the mutant lines having smaller and fewer droplets, but again this was not significant across genotypes. There was a significant difference when comparing with the 5.6 wildtype line, but not with the 6.1 wildtype line. Indeed, 5.6 was significantly different from 6.1 when comparing the area of BODIPY normalized to cTnT, although not when normalized to nuclei. It

is possible that this difference can again be attributed to line to line variation, although, there are many reports in the literature of iPS cells behaving consistently among different patient lines (Moretti *et al.* 2010, Carvajal-Vergara *et al.* 2010). Intriguingly, another iPS cell-derived cardiomyocytes paper on arrythmogenic right ventricular dysplasia (ARVD) points out that there are few lipid droplets in these iPSC or ES-derived CMs (Kim *et al.* 2013). The data here confirms this result, as there is on average only about one lipid droplet per nucleus in every cell line. The authors of this paper knew that the pathology of patients was fatty infiltration and CM apoptosis, predominantly of the right ventricle. When they saw that their cell model was not demonstrating this pathology, they sought to mature their CMs with a cocktail of factors designed to affect metabolism and skew differentiation toward the right ventricular fate. At the time the experiments in this chapter were done, this ARVD study was not yet published. It might be interesting to repeat these measurements in the presence of these factors.

To summarize, these data show that there were no consistent differences observed across genotypes for total cellular lipid accumulation, droplet size, or droplet number per nuclei. This finding does not rule out the possibility of there being a defect in lipid handling in the double mutants, but the conclusion now appears less likely.

DISCUSSION

These investigations into areas where LAMP2 and GATA4 might intersect to create a modifiable phenotype have not been successful. There was not a consistent, measureable phenotype observed by autophagic flux, cell death, or lipid accumulation. There are many possible reasons why these results could have been negative.

One of the more obvious possibilities is that *LAMP2* is not the modifier. It was only one of many possible candidates, albeit the most significant as indicated by the bioinformatics analysis and the most compelling candidate genetically, considering that the males of this family branch are most severely affected. However, this was a small branch with few meioses from which to draw conclusions. Additionally, our search was for a modifier, not a disease gene. This approach represented an important distinction when searching for a modifier as many of the programs designed to data mine from these large pedigrees are not actually designed for finding a modifier *per se*.

Another possibility is that perhaps there is more than one modifier. There may instead be many different modifiers contributing to the disease phenotype. Many of the diseases that are significant burdens on our society have a genetic component, and yet, despite genetic contribution, genetics is not destiny, merely predisposition. The young age of onset of this GATA4-related cardiomyopathy argues against this many factored model, as one might imagine there is more room for disease variance as more genes would have had to segregate appropriately in the siblings. However, the few meioses separating the affected

siblings involved does not preclude this possibility. Then again, this approach is one rarely conducted in genetic disease modeling. Arguably, it might be easier to identify a modifier of genetic disease using an opposite approach, wherein one tries to identify a modifier or small group of modifiers that protects against the genetic disease. Then, at least the disease phenotype would be known and an iPSC disease model could already be established, thus making the identification of a modifier more straightforward because the phenotype would be a return to wildtype.

However, these assays are not necessarily specific to LAMP2. Defects in cell survival have been tied to cardiomyopathy (Wencker *et al.* 2003, James 1994), and cell survival also represents a common area where many different genes could converge to modify the biology of GATA4. Yet, this assay and the lipid droplet assay were both negative. Therefore, on at least these two parameters, there was not a phenotype observed between the controls and double mutant lines. One could also conclude that it may just be difficult to elicit a phenotype for this cardiomyopathy.

Additionally, I would be remiss if I did not mention the technical hurdles in modeling disease phenotypes with ES-derived cardiomyocytes. The cardiomyocytes that are made are not mature, making modeling of an age-dependent disease difficult. Moreover, the phenotype must be more cell autonomous as the extracellular environment and components *in vitro* are vastly different from how it is *in situ* in the patient. A way of partially circumventing this

problem is to model this *in vivo* with a mouse model. There is a G*ata4 G295S* knock-in mouse with the orthologous mutation that recapitulates the human disease even in the heterozygous state (Misra *et al.* 2012). A mouse *Lamp2* KO demonstrates a cardiomyopathy phenotype that is also observed in human patients (Tanaka *et al.* 2000). Combining these two mutations in the mouse might be informative. Perhaps if perturbations were found in the mouse model, these observations could then be applied to iPSC-CMs and verified in the patient cells. Additionally, the technology has improved for genome engineering so that a more controlled set of experiments might be possible with relative ease.

ACKNOWLEDGEMENTS

Renee Rivas designed, performed experiments, analyzed and interpreted results, and wrote this chapter. Yen Sin Ang assisted with design and implementation of experiments. Lyndsay Murrow made Western blots and analyzed results. Scott Metzler took confocal images and analyzed BODIPY stained CMs. Jinny Wong from the Gladstone EM core performed EM. Amy Foley assisted with CM differentiations. Jared Roach and Chad Huff designed and performed bioinformatics analysis. Lee Hood, Alisha Holloway, Katherine Pollard, and David Galas designed and supervised the bioinformatics analysis. Jay Debnath designed and supervised autophagic flux experiments. Deepak Srivastava designed, provided funding, and supervised work.

REFERENCES

Arad M., Maron B.J., Gorham J.M., Johnson, Jr. W.H., Saul, J.P. Perez-Atayde A.R., Spirito P., Wright G.B., Kanter R.J., Seidman C.E., Seidman J.G. (2005). Glycogen Storage Diseases Presenting as Hypertrophic Cardiomyopathy. NEJM 352(4):362-72.

Aries, A. Paradis P., Lefebvre C., Schwartz R.J., Nemer M. (2004). Essential role of GATA-4 in cell survival and drug-induced cardiotoxicity. PNAS *101*, 6975-80.

Barth S., Glick D., Macleod K.F. (2010). Autophagy: assays and artifacts. J. Pathol. *221(2)*: 117–124.

Bisping E., Ikeda S., Kong S.W., Tarnavski O., Bodyak N., McMullen J.R., Rajagopal S., Son J.K., Ma Q., Springer Z., Kang P.M., Izumo S., Pu W.T. (2006). Gata4 is required for maintenance of postnatal cardiac function and protection from pressure overload-induced heart failure. PNAS *103*,14471-6.

Carvajal-Vergara, X., Sevilla A., D'Souza S.L., Ang Y., Schaniel C., Lee D., Yang L., Kaplan A.D., Adler E.D., Rozov R., Ge Y., Cohen N., Edelmann L.J., Chang B., Waghray A., Su J., Pardo S., Lichtenbelt K.D., Tartaglia M., Gelb B.D., Lemischka I.R. (2010). Patient-specific induced pluripotent stem-cell-derived models of LEOPARD syndrome. Nature *465*, 808-12.

Cohen A.W., Hnasko R., Schubert W., Lisanti M.P. (2004). Role of Caveolae and Caveolins in Health and Disease. Physiological Reviews *84(4)*, 1341-1379.

Eskelinen, E. (2006). Roles of LAMP-1 and LAMP-2 in lysosome biogenesis and autophagy. Molecular Aspects of Medicine *27*, 495–502.

Exome Aggregation Consortium (ExAC), Cambridge, MA (URL: http://exac.broadinstitute.org) [2015, June 10].

Garg V., Kathiriya I.S., Barnes R., Schluterman M.K., King I.N., Butler C.A., Rothrock C.R., Eapen R.S., Hirayama-Yamadak K., Joo K., Matsuokak R., Cohen J.C. , Srivastava D. (2003). GATA4 mutations cause human congenital heart defects and reveal an interaction with TBX5. Nature *424*, 443-447.

González-Polo, R-A., Boya P., Pauleau A., Jalil A., Larochette N., Souquère S., Eskelinen E., Pierron G., Saftig P., Kroemer G. (2005). The apoptosis/autophagy paradox: autophagic vacuolization before apoptotic death. *J.* Cell Science *118*, 3091-102.

Hu H., Roach J.C., Coon H., Guthery S. L., Voelkerding K.V., Rebecca L Margraf R.L., Durtschi J.D., Tavtigian S.V., Shankaracharya, Wu W., Scheet P., Wang S., Xing J., Glusman G., Hubley R., Li H., Garg V., Moore B., Hood L., Galas D.J., Srivastava D., Reese M.G., Jorde L.B., Yandell M., Huff C.D. (2014). A unified test of linkage analysis and rare-variant association for analysis of pedigree sequence data. Nature Biotechnology *32(7)*, 663-9.

James T.N. (1994). Normal and abnormal consequences of apoptosis in the human heart: from postnatal morphogenesis to paroxysmal arrhythmias. Trans Am Clin Climatol Assoc. *105*, 145–178.

Kang, R., Zeh H.J., Lotze M.T., Tang D. (2011). The Beclin 1 network regulates autophagy and apoptosis. Cell death and differentiation *18*, 571-80.

Kobayashi, S., Lackey T., Huang Y., Bisping E., Pu W.T., Boxer L.M., Liang Q. (2006). Transcription factor GATA4 regulates cardiac BCL2 gene expression *in vitro* and *in vivo*. FASEB Jo urnal *20*, 800-802.

Kobayashi, S., Volden P., Timm D., Mao K., Xu X., Liang Q. (2010). Transcription Factor GATA4 Inhibits Doxorubicin-induced Autophagy and Cardiomyocyte Death. J. Biological Chemistry *285*, 793-804.

Li R.G., Li L., Qiu X.B., Yuan F., Xu L., Li X., Xu Y., Jiang W., Jiang J., Liu X., Fang W., Zhang M., Peng L., Qu X., Yang Y. (2013) GATA4 loss-of-function mutation underlies familial dilated cardiomyopathy. BiochemBiophys Res Commun *439*, 591–596.

Lobrinus J.A., Schorderet D.F., Payot M., Jeanrenaud X., Bottani A., Superti-Furga A., Schlaepfer J., Fromer M., Jeannet P.-Y. (2005). Morphological, clinical and genetic aspects in a family with a novel LAMP-2 gene mutation (Danon disease). Neuromuscular Disorders *15*, 293–298.

Maron B.J., Roberts W.C., Arad M., Haas T.S., Spirito P., Wright G.B., Almquist A.K., Baffa J.M., Saul J.P., Ho C.Y., Seidman J., Seidman C.E. (2009). Clinical Outcome and Phenotypic Expression in *LAMP2* Cardiomyopathy. *301(12)*, 1253-1259.

Misra, C., Sachan N., McNally C.R., Koenig S.N., Nichols H.A., Guggilam A., Lucchesi P.A., Pu W.T., Srivastava D., Garg V. (2012). Congenital Heart Disease–Causing Gata4 Mutation Displays Functional Deficits *In Vivo*. PLOS Genetics *8*, e1002690.

Mizushima N., Yoshimori T., Levine B. (2010). Methods in Mammalian Autophagy Research. *Cell* **140**, 313-326.

Moretti, A., Bellin M., Welling A., Jung C.B., Lam J.T., Bott-Flügel L., Dorn T., Goedel A., Höhnke C., Hofmann F., Seyfarth M., Sinnecker D., Schömig A., Laugwitz K. (2010). Patient-Specific Induced Pluripotent Stem-Cell Models for Long-QT Syndrome. NEJM *363(15)*, 1397-1409.

Moskowitz I. P, Wang J., Peterson M.A., Pu W.T., Mackinnon A.C., Oxburgh L., Chu G.C., Sarkar M., Berul C., Smoot L., Robertson E.J., Schwartz R., Seidman J.G., and Seidman C.E. (2011). Transcription factor genes *Smad4* and *Gata4* cooperatively regulate cardiac valve development. PNAS *108*, 4006-4011.

Nishino, I., Fu J., Tanji K., Yamada T., Shimojok S., Koori T., Mora M., Riggs J.E.,Oh S.J., Koga [Y.], Sue C.M., Yamamoto A., Murakami N., Shanske S., Byrne E., Bonilla E., Nonaka [I.], DiMauro S., Hirano M. (2000). Primary LAMP-2 deficiency causes X-linked vacuolar cardiomyopathy and myopathy (Danon disease). Nature *406*, 906-910.

Okita, K., Matsumura Y., Sato Y., Okada A., Morizane A., Okamoto S., Hong H., Nakagawa M., Tanabe K., Tezuka K., Shibata T., Kunisada T., Takahashi M., Takahashi J., Saji H., Yamanaka S. (2011). A more efficient method to generate integration-free human iPS cells. Nature Methods *8*, 409–412.

Patankar J.V., Chandak P.G., Obrowsky S., Pfeifer T., Diwoky C., Uellen A., Sattler W., Stollberger R., Hoefler G., Heinemann A., Battle M., Duncan S, Kratky D., Levak-Frank S. (2011). Loss of intestinal GATA4 prevents diet-induced obesity and promotes insulin sensitivity in mice. Am J Physiol Endocrinol Metab *300*: E478–E488.

Rajagopal S.K., Ma Q., Obler D., Shen J., Manichaikul A., Tomita-Mitchell A., Boardman K., Briggs C., Garg V., Srivastava D., Goldmuntz E., Broman K.W, Benson D.W., Smoot L.B., Pu W.T. (2007). Spectrum of heart disease associated with murine and human GATA4 mutation. J Mol Cell Cardiology *43*, 677–685.

Sarkozy A., Conti E., Neri C., D'Agostino R., Digilio M.C., Esposito G., Toscano A., Marino B., Pizzuti A., Dallapiccola B. (2005). Spectrum of atrial septal defects associated with mutations of NKX2.5 and GATA4 transcription factors. J Med Genet *42*, e16.

Schneede A., Schmidt C.K., Hölttä-Vuori M., Heeren J., Willenborg M., Blanz J., Domanskyy M., Breiden B., Brodesser S., Landgrebe J., Sandhoff K., Ikonen E., Saftig P., Eskelinen E. (2011). Role for LAMP-2 in endosomal cholesterol transport. J. Cell. Mol. Med. *15(2)*, 280-295.

Singh R., Susmita Kaushik S., Wang Y., Xiang Y., Novak I., Komatsu M., Tanaka K., Cuervo A.M., Czaja M.J. (2009). Autophagy regulates lipid metabolism. Nature *458(7242)*: 1131–1135.

Stypmann, J., Janssen P.M.L., Prestle J., Engelen M.A., Kogler H., Lullmann-Rauch R., Eckardt L., von Figura K., Landgrebe J., Mleczko A., Saftig P. (2006). LAMP-2 deficient mice show depressed cardiac contractile function without significant changes in calcium handling. Basic Res Cardiol 101: 281–291.

Tanaka Y., Guhde G., Suter A., Eskelinen E., Hartmann D., Lüllmann-Rauch R., Janssen P.M.L., Blanz J., von Figura K., Saftig P. (2000). Accumulation of autophagic vacuoles and cardiomyopathy in LAMP-2-deficient mice. Nature *406*, 902-906.

The 1000 Genomes Project Consortium. (2012). An integrated map of genetic variation from 1,092 human genomes. Nature *491*, 56-65.

Wencker, D., Chandra M., Nguyen K., Miao W., Garantziotis S., Factor S.M., Shirani J., Armstrong R.C., Kitsis R.N. (2003). A mechanistic role for cardiac myocyte apoptosis in heart failure. Journal of Clinical Investigation *111*, 1497-1504.

Zhang, J., Wilson G.F., Soerens A.G., Koonce C.H., Yu J., Palecek S.P., Thomson J.A., Kamp T.J. (2009). Functional Cardiomyocytes Derived From Human Induced Pluripotent Stem Cells. Circulation Research *104*, e30-e41.

Zhao L., Xu J.H., Xu W.J., Yu H., Wang Q., Zheng H.Z., Jiang W.F., Jiang J.F., Yang Y.Q. (2014). A novel GATA4 loss-of-function mutation responsible for familial dilated cardiomyopathy. Int J Mol Med. *33(3)*, 654-60.

FIGURES

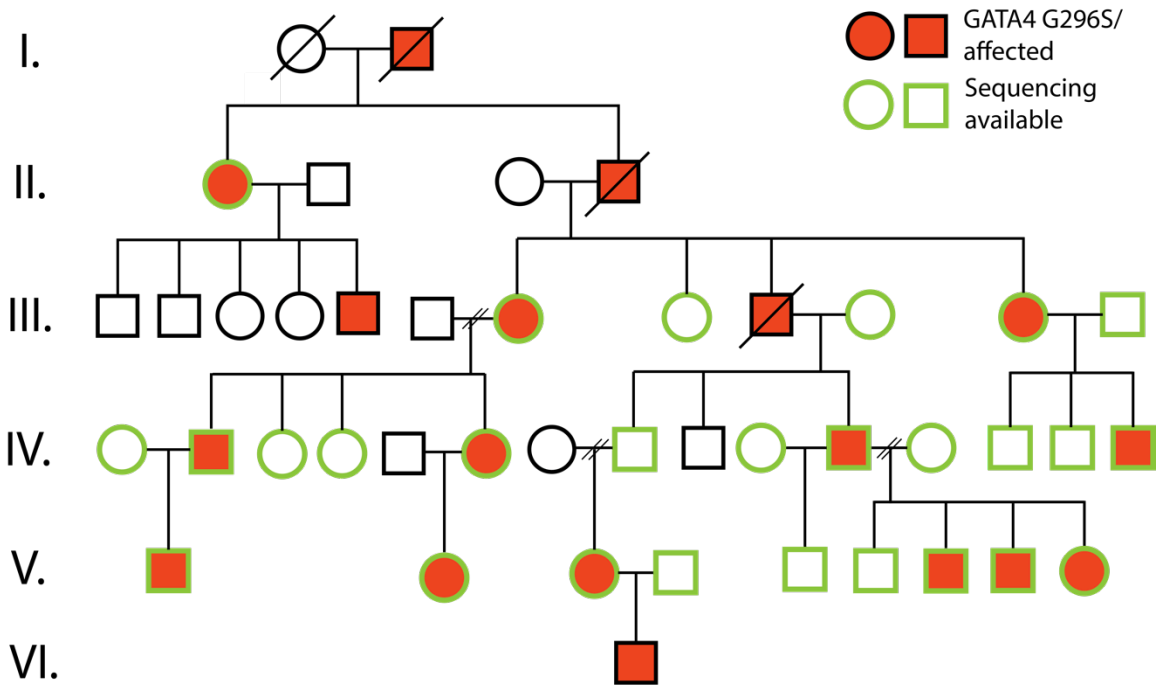

Fig. 1. *GATA4 G296S* family pedigree spans six generations. The red filling in the squares and circles signifies the presence of the mutation and the green outline indicates that the complete genome is sequenced for that individual.

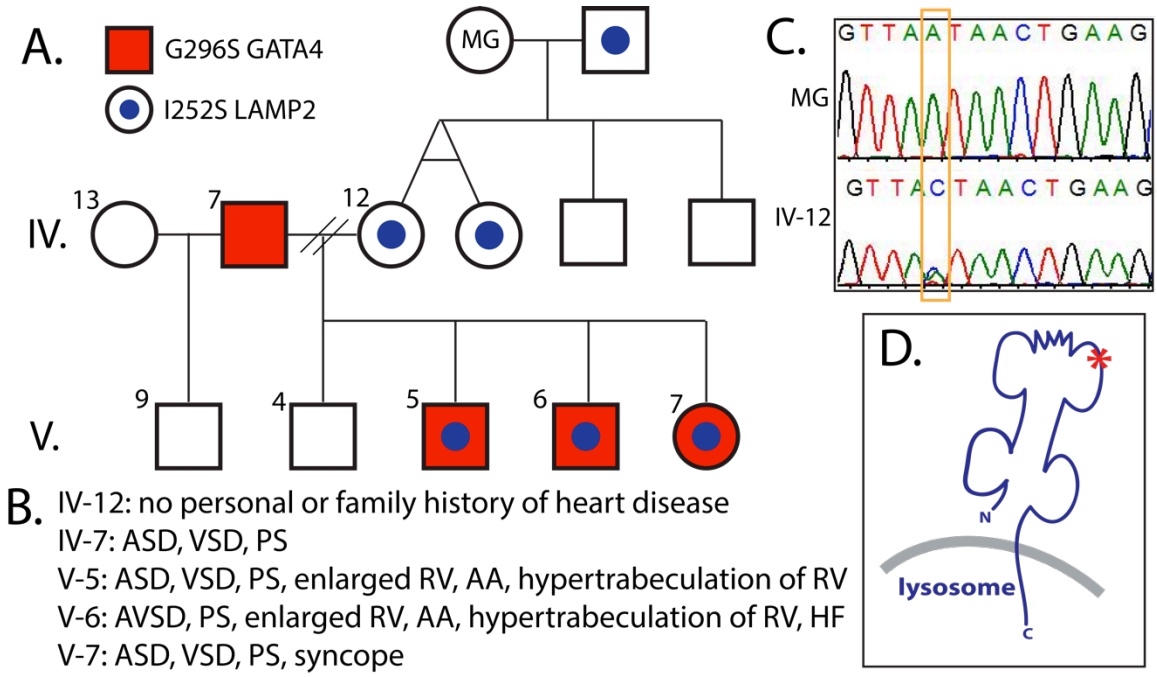

Fig. 2. Extended family of IV-12 depicting the transmission of *LAMP2 I252S*.

A. All eight family members from the clade under study for cardiomyopathy as well as the family of IV-12 depicting who carries the *LAMP2 I252S* mutation. **B.** The details of the cardiomyopathy phenotype from each patient. **C.** The sequencing of IV-12 and the maternal grandmother (MG) showing the wildtype sequence. **D.** A schematic of the LAMP2 protein on the lysosomal membrane with an asterisk depicting the location of the mutation near the hinge region in the luminal domain.

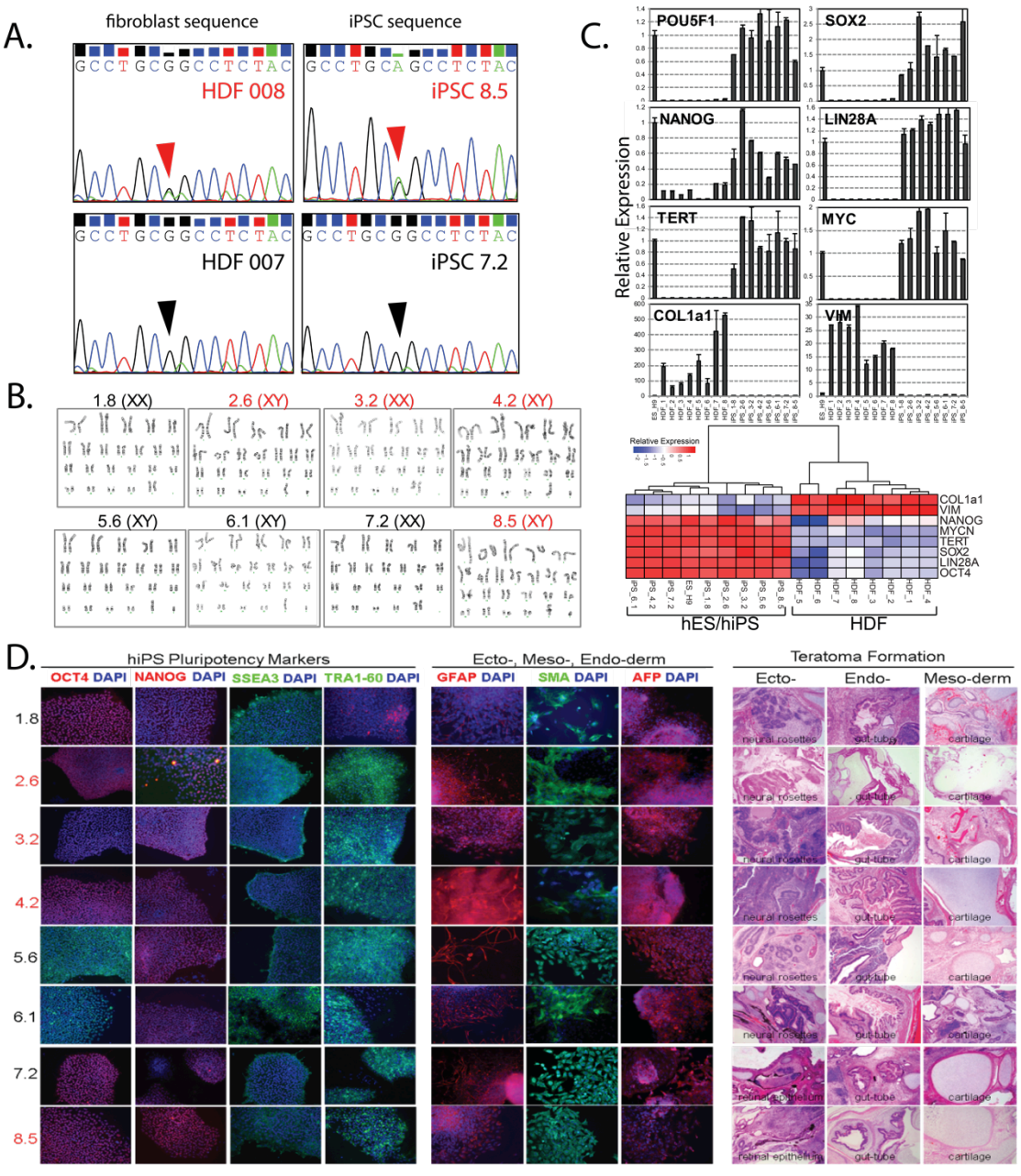

Fig. 3. iPS cell lines demonstrate pluripotency by multiple measures. A. Sequencing traces for the fibroblasts and iPS cell lines. Top boxes are from HDF 008 (left) and iPSC 8.5 (right). Bottom boxes are from HDF 007 and iPSC 7.2. The arrows point out the mutation site with the red arrows pointing to a heterozygous double peak for A and G. Black arrows show only the wildtype G.

B. Karyotypes for the iPS cell lines. **C.** (top) Relative expression of pluripotency markers *POU5F1 (OCT4), SOX2, NANOG, LIN28A, TERT*, and *MYC* and fibroblast markers *Col1a1* and *VIM*. (bottom) Clustering of aforementioned markers showing that the HDFs and ES/iPSCs segregate by gene expression. **D.** (left) Immunocytochemistry for (left) pluripotency markers in iPS cells across all 8 lines. Staining is for OCT4, NANOG, SSEA3, and TRA-1-60. (middle) *In vitro* differentiation of iPS cell lines reveals antibody labeling of all three germ layers: GFAP (ectoderm), SMA (mesoderm), and AFP (endoderm). (right) Teratoma formation assay reveals potential for iPS cell lines to *in vivo* differentiate into all three germ layers. Mutant lines are labeled in red, wildtype in black.

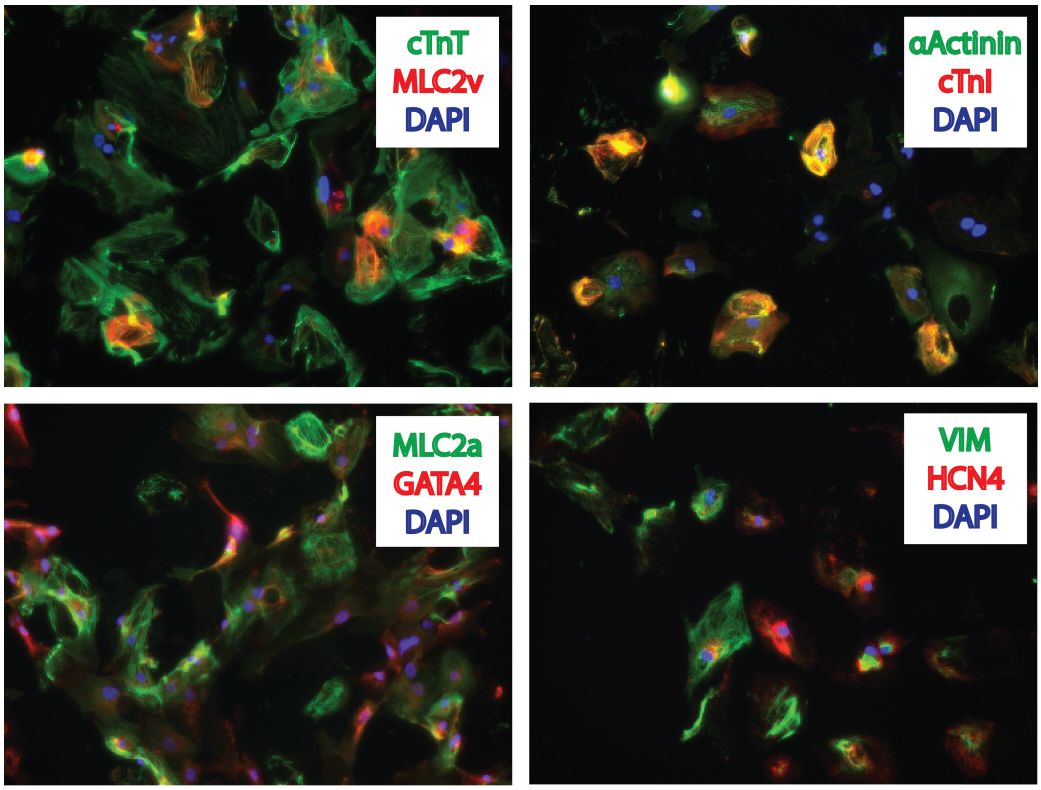

Fig. 4. Differentiated cells demonstrate antibody staining patterns characteristic of cardiomyocytes. Cells show the appropriate staining patterns of cTnT, MLC2v, aActinin, cTnI, MLC2a, GATA4, VIM, and HCN4 expected for CMs.

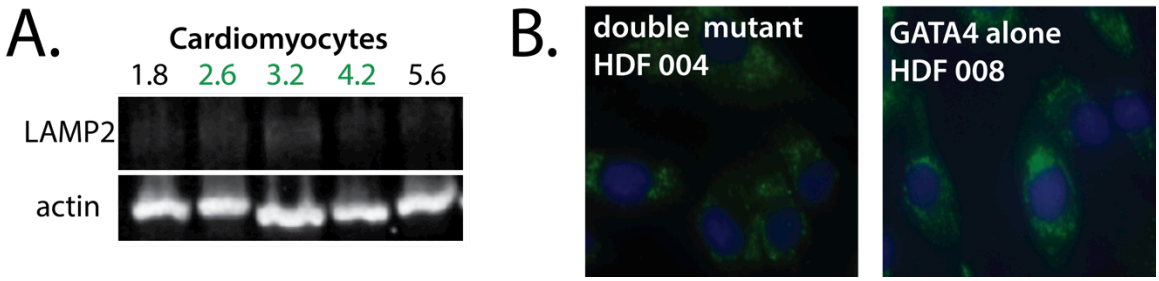

Fig. 5. Evaluation of protein levels of LAMP2 and localization pattern. A. Western blot of cardiomyocyte lysates (black are WTs, green are double mutant lines). **B.** Images of patient fibroblasts with LAMP2 in green and nuclei stained blue with DAPI.

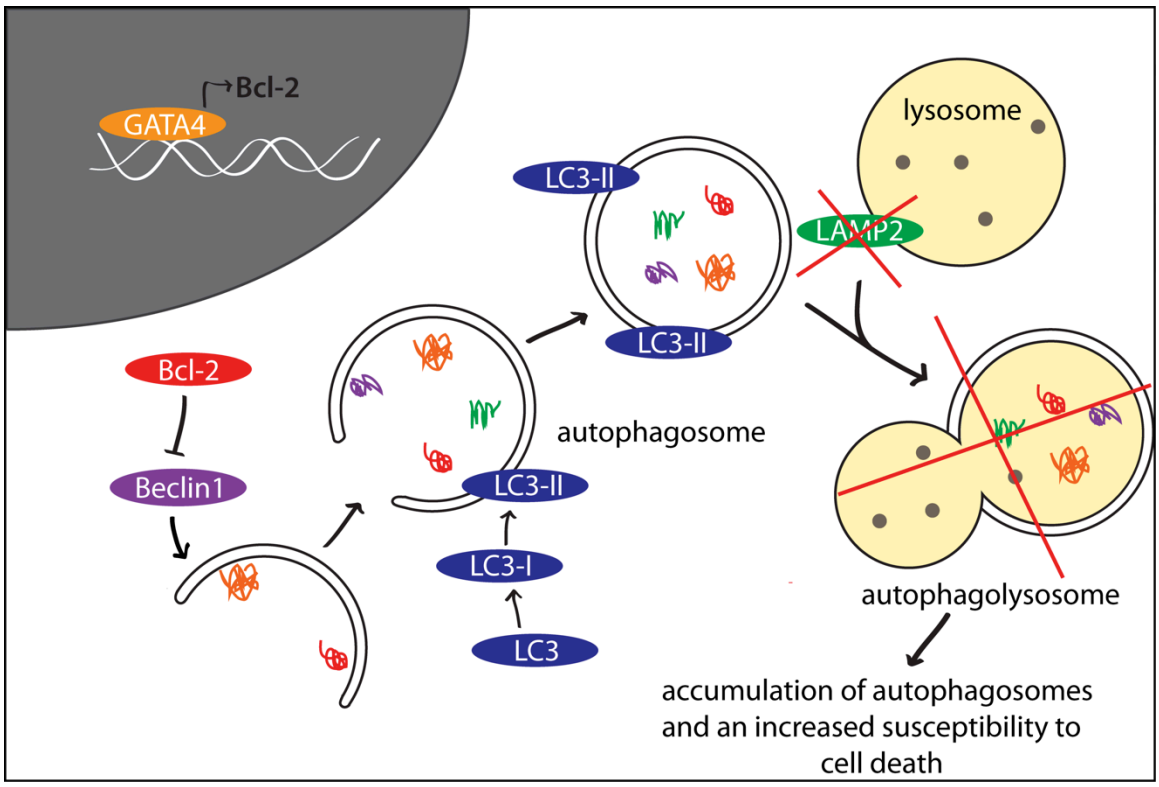

Fig. 6. A proposed model for how LAMP2 I252S could serve as a modifier of GATA4 G296S due to an overlap in autophagy, a pathway that both genes regulate.

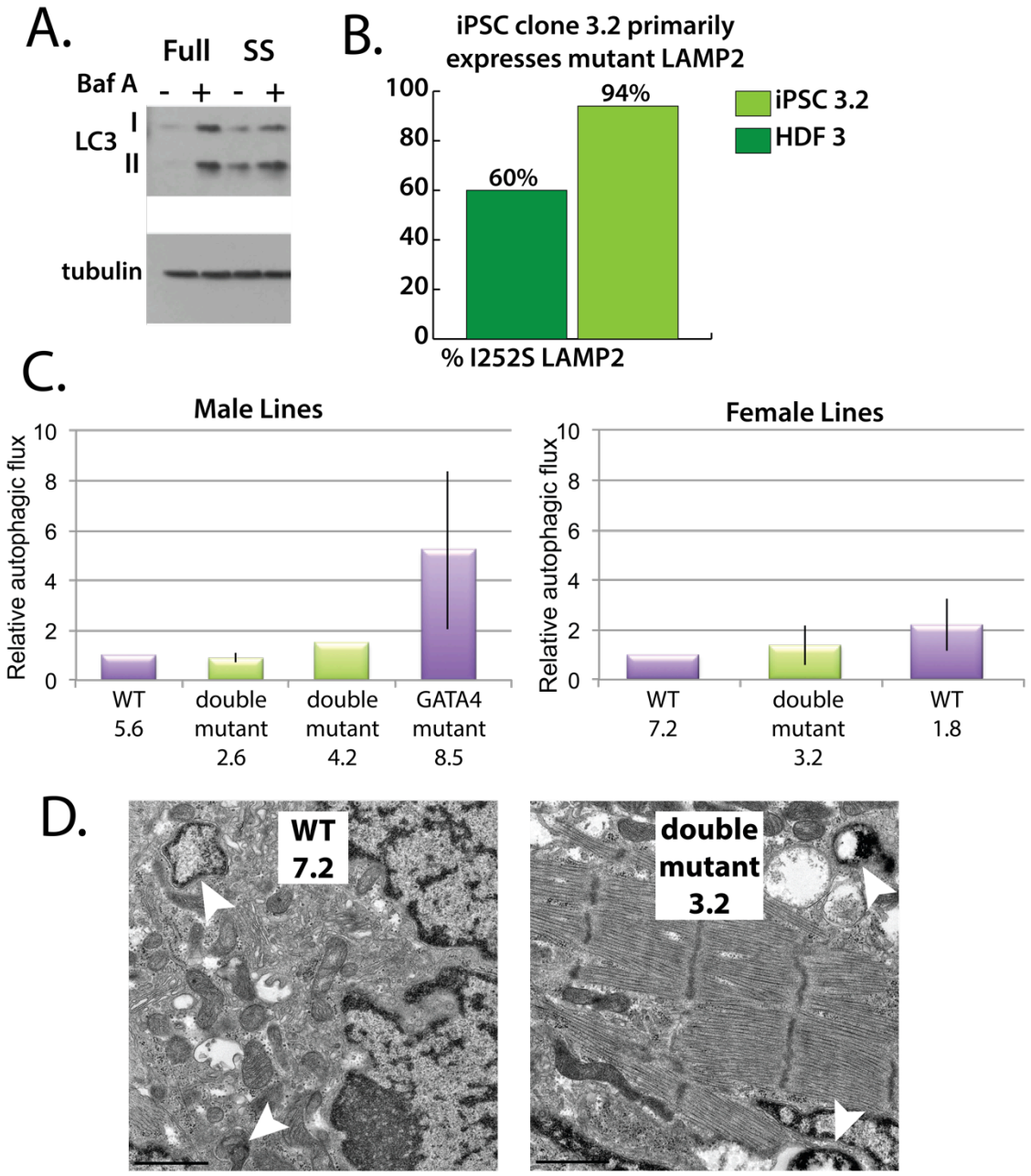

Fig. 7. No consistent difference in autophagy measurements. A. Example of normal autophagic flux from 1.8 CM line **B.** *LAMP2* cDNAs quantified by TOPO subcloning and sequencing from the HDF and iPS cells of the same patient. **C**. Relative autophagic flux across multiple lines (purple are controls, green are double mutant lines) in males and females. **D.** Electron micrographs of CMs from

WT 7.2 and double mutant 3.2 lines. Scale bar represents 1 micrometer. White arrows are pointing to rare double membrane autophagic structures.

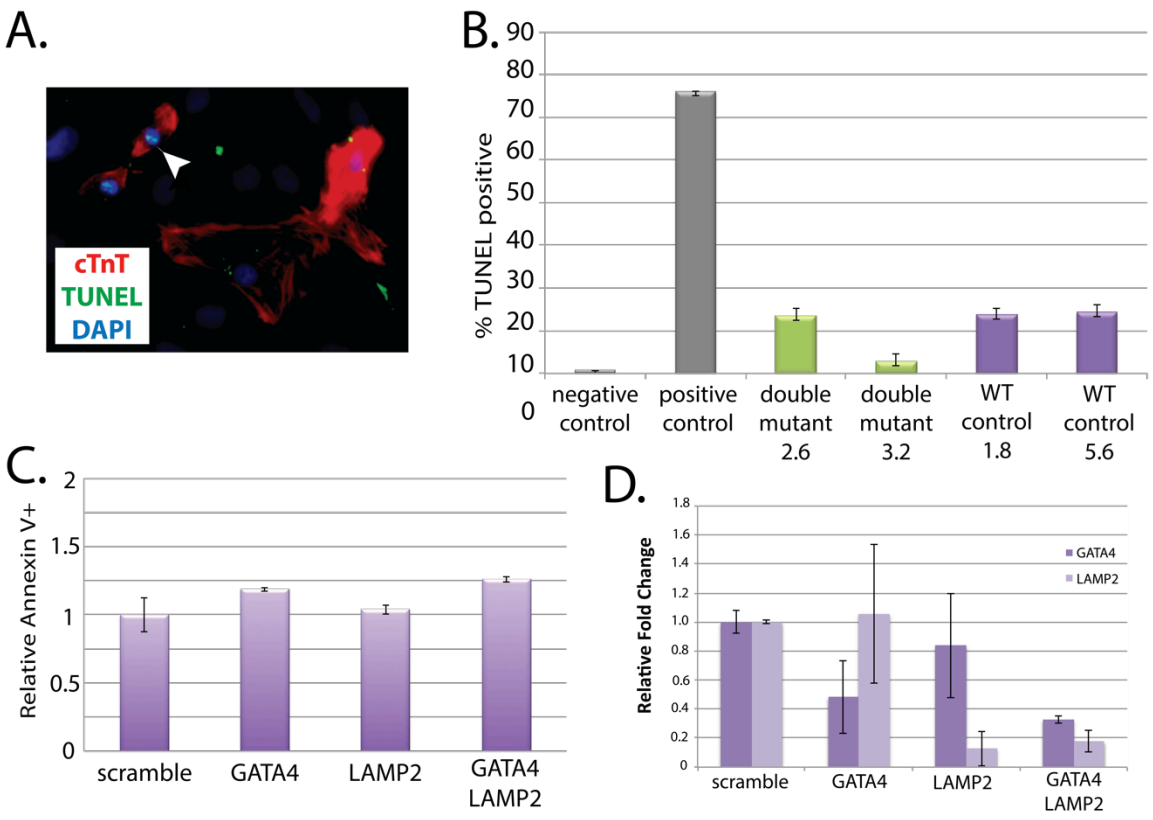

Fig 8. No greater susceptibility to cell death revealed with GATA4 and LAMP2 A. Image of CM with positive TUNEL staining (white arrow). **B.** Quantification by FACS of TUNEL staining in positive and negative controls and in double mutants (green) and controls (purple). Experiment used three biologic replicates. **C.** Annexin V staining of siRNA knockdown of *GATA4, LAMP2*, and both in WT CMs. **D.** Relative fold change in mRNA of *GATA4* and *LAMP2* with siRNA knockdown in WT CMs

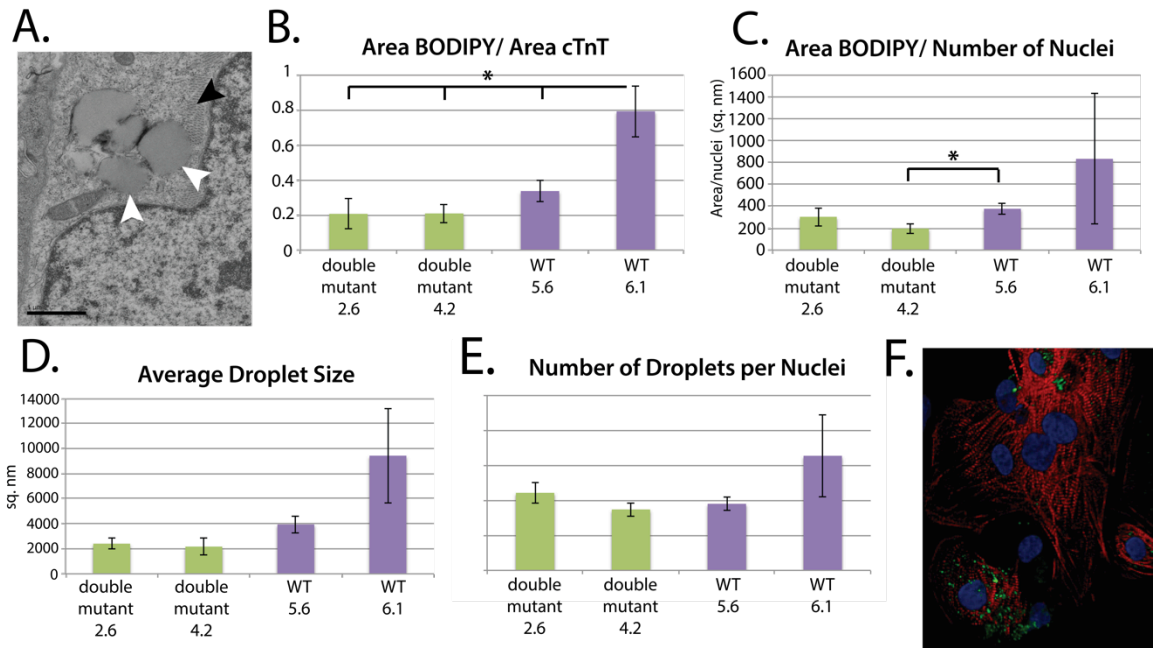

Fig.9. No consistent differences in lipid droplets between double mutant and wildtype lines. A. Electron micrograph of cluster of lipid droplets in a double mutant line (2.6). Scale bar represents 1micrometer. White arrows point to cluster of lipid droplets, and the black arrow points to a sarcomere cut in cross-section. **B.** Graph depicting BODIPY area normalized to area of cardiac troponin T showing significance for 2.6, 4.2, and 5.6 compared to 6.1 ($p<0.05$). **C.** Area of BODIPY also normalized to the number of nuclei in the sample. Significance shown for 4.2 and 5.6, the rest are not significant ($p<0.05$). **D.** Average droplet size (n.s) and **E.** number of droplets per nuclei (n.s.) also in CMs. **F.** Image of a cluster of CMs from WT 5.6 used to quantify graphs with cTnT staining in red, BODIPY labeled lipid droplets in green, and DAPI labeling nuclei in blue. Student's T-test used and standard error bars depicted.

TABLES

Pedigree chart number	Cell line identifier		
	HDF	iPSC	CM
IV-7	008	8.5	8.5
IV-12	001	1.8	1.8
IV-13	007	7.2	7.2
V-4	005	5.6	5.6
V-5	002	2.6	2.6
V-6	004	4.2	4.2
V-7	003	3.2	3.2
V-9	006	6.1	6.1

Table 1. Table depicting the patient's designation on pedigree chart and their corresponding cell line name.

Rank	Gene Name
1	*LAMP2*
2	*RASSF9*
3	*NCOA3*
4	*NBAS*
5	*FOXRED1*
6	*ZSCAN22*
7	*TMEM136*
8	*MYLK*
9	*KIAA0562*
10	*ADCY10*

Table 2. List of top ten modifier candidates with individual composite log likelihood score.

Primer Name	**Sequence: 5' to 3'**
GATA4 G296S 5'	GGT GAA TGA TGG TTA GGA CTG
GATA4 G296S 3'	GGC ATC AGA AGG CAA GGA TGC
LAMP2 I252S 5'	TGA AGA CAC CAT GAA TTT TAA
LAMP2 I252S 3'	TGT TTC TAA GAG AAT GAA CCT
LAMP2 cDNA cloning 5'	GAT GTT GTC CAA CAC TAC TGG G
LAMP2 cDNA cloning 3'	AGC CAT TAA CCA AAT ACA TGC TG

Table 3. List of primers used for genotyping verification and cloning

Chapter 3

Genomic and Cellular Analysis of a GATA4 Mutation in Human iPS Cell-derived Cardiomyocytes

ABSTRACT

GATA4 is a central transcriptional regulator during cardiac development and postnatal function. Familial mutations in *GATA4* lead to autosomal dominant congenital heart disease and cardiomyopathy. Our lab previously reported a heterozygous *GATA4 G296S/+* mutation that resided near the second zinc finger of GATA4, involved in DNA-binding and protein-protein interactions. However, the mechanisms by which this mutation affects the transcriptional and epigenetic landscape resulting in altered cellular physiology are unknown.

Here, we have used genomic approaches as well as cell-based assays to delineate the consequences of the *GATA4 G296S* mutation in cardiomyocytes. We generated human iPS cells from patients with or without the *GATA4 G296S* mutation and differentiated them to a purified population of cardiomyocytes. Using these cells, we performed chromatin immunoprecipitation followed by DNA

sequencing (ChIP-Seq) on endogenous GATA4 protein and revealed hundreds of previously unidentified GATA4-bound loci and confirmed known GATA4 targets.

We also performed ChIP-Seq for TBX5, a disease-causing transcription factor that physically interacts with GATA4 and whose interaction is specifically disrupted by the G296S mutation. Genome-wide we identified thousands of loci where GATA4 and TBX5 co-localized in wild-type cells, but where this co-localization was lost in cardiomyocytes containing the *GATA4 G296S* mutation. RNA-Seq revealed dysregulation of transcription at many of these loci, along with expected epigenetic changes, with clustered dysregulation of genes involved in cellular respiration, inflammation, and muscle contraction. Consistent with this observation, cell based assays demonstrated defects in contractility and calcium handling in cardiomyocytes heterozygous for the *GATA4 G296S* mutation. We confirmed that the *Gata4 G295S* knock-in mouse is unable to respond appropriately to pressure-overload induced hypertrophy and demonstrated a limited ability of this mouse model to validate GATA4 targets from RNA-seq.

The deep “-omic” approach of iPSC-derived cardiomyocytes has effectively revealed the transcriptional and cellular consequences of an important human mutation and may explain many of the disease features observed in individuals with *GATA4* mutations.

INTRODUCTION

Transcription factors (TFs) have a central role in development and the maintenance of cell state. These are crucial functions not only for the proper morphogenesis of the adult animal but also for its continued function and ability to respond to external stimuli. Understanding the network regulation and the key players involved in the process is important to gain a better understanding of TF biology and how this network can be leveraged to modulate the effects of disease processes.

GATA4 is one of the central transcription factors in the heart. It is a zinc-finger transcription factor that is essential for cardiac morphogenesis (Molkentin *et al.* 1997) and adult heart function (Bisping *et al.* 2006; Oka *et al.* 2006). GATA4 is known to interact and coordinately regulate the cardiac gene program with a number of other known cardiac transcription factors (Schlesinger *et al.* 2011, He *et al.* 2011). Previously, our lab published that *GATA4* was found mutated in a family with congenital heart disease, specifically with ASDs and valvular defects (Garg *et al.* 2003). It is described as a G296S mutation located near the C-terminal zinc finger with near 100% penetrance that functions in an autosomal dominant manner. The *GATA G296S* mutation has reduced DNA binding affinity and a selective loss of its interaction with TBX5, another cardiac transcription factor that also causes congenital heart disease when mutated (Li *et al.* 1997). GATA4 and TBX5 both have essential roles in the heart, as demonstrated by both being required with only one other factor for reprogramming in the heart (Ieda *et al.* 2010). GATA4 and TBX5 have also been

shown to interact *in vivo* (Maitra *et al.* 2009). The impact that the loss of this interaction has on the heart needs to be clarified with further investigations.

The precise mechanisms of how this transcription factor functions in the heart have previously been investigated using mouse models and experimental approaches that look at the wildtype state but not the diseased state. Here, we examine an iPS cell model for congenital heart disease by profiling the transcriptome and using cell-based assays and *in vivo* modeling to investigate the downstream consequences of the *GATA4 G296S* mutation.

METHODS

Differentiation to cardiomyocytes

iPS cells were differentiated to cardiomyocytes according to (Lian *et al.* 2012) with some small modifications. On day five after addition of CHIR99021, cells are split onto fibronectin (Sigma) diluted 1:80 in 0.02% gelatin (Sigma) coated plates at ratios of 1:2 to 1:4. Cells usually commence spontaneous beating by day 12.

CM purification

Cardiomyocytes are allowed to beat for two weeks in normal culturing conditions (RPMI 1640 plus B27 supplement with insulin (Sigma)). Cells are then washed twice and the media replaced with lactate media as in (Tohyama *et al.* 2013). Lactate media consists of DMEM without glucose or pyruvate (Life Technologies), 4mM lactate (Wako Pure Chemical), and 1x Na-HEPES (Life Technologies). Media is changed every other day whereupon it is also washed with PBS to dislodge dead cells for 4-6 days. Significant non-cardiomyocyte cell death should be observed within the first day. Caution should be used with the timing as eventually all cells will die, usually at about 7-8 days after induction. If significant death is not achieved, cells should be split so that they are more thinly plated. Cells are then washed again and put in high serum recovery media (DMEM with sodium pyruvate and Glutamax, 15% FBS, NEAA, P/S) for two days. Cells are washed and cultured in normal media conditions again afterwards.

mRNA-Seq (RNA-seq) and Analysis Pipeline

RNA-seq was performed with some modifications as described in (Theodoris *et al.* 2015). In brief, total RNA was isolated with the Allprep DNA/RNA Micro Kit (Qiagen). cDNA was prepared with the NuGen Ovation RNA-seq System V2 Kit using RT-PCR followed by RNase treatment. The dsDNA was then amplified using single primer isothermal amplification (SPIA). Finally, libraries from the SPIA-amplified cDNA were made using the NuGen Ovation Ultralow DR Kit. The mRNA-seq libraries were analyzed by Agilent Bioanalyzer

and quantified using an Illumina Library Quantification Kit (KAPA Biosystems) and sequenced on an Illumina HiSeq 2500 instrument.

Sequencing quality was assessed with FASTQC (http://www.bioinformatics.babraham.ac.uk/projects/fastqc/). Reads were trimmed using Fastq-mcf (http://code.google.com/p/ea-utils) and aligned to the hg19 (Homo sapiens assembly February 2009) genome using Tophat (Kim *et al.* 2013). To quantify mRNA arising from the WT versus mutant allele, reads were aligned to a custom index containing the WT or mutant sequence. Unmapped (-F 4) and low-quality reads with MAPQ score below 30 (-q 30) were removed using Samtools (Li *et al.* 2009), and duplicate reads were removed using Picard MarkDuplicates (http://broadinstitute.github.io/picard). USeq (Nix *et al.* 2008) was used to normalize raw read counts, calculate FPKM (fragment per kb per million reads mapped), and analyze differential expression using the negative binomial test with FDR correction. HOPACH was used for clustering with the correlation metric (van der Laan and Pollard 2001). GO analyses were completed using GO-Elite and ToppGene (Chen *et al.* 2009 and Zambon *et al.* 2012). Heatmap, bar graph, and network map representations of log2 fold changes between WT and mutant mRNA expression were Bayesian-corrected.

Chromatin immunoprecipitation followed by sequencing (ChIP-seq) and Analysis Pipeline

ChIP-seq was performed with some modifications as described in (Theodoris *et al.* 2015). Genome occupancy was determined by ChIP against GATA4 (Bethyl), TBX5 (gift of Bruneau lab), and MED1 (Bethyl) using the Millipore ChIP Assay Kit on 200 million iPSC-CMs. Histone marks were also determined by ChIP using antibodies against H3K4me3 (Abcam), H3K36me3 (Abcam), H3K27me3 (Abcam), and H3K27ac (Abcam) on 1-2 million cells each. Cells were cross-linked with 1% formaldehyde in culture medium at 37°C for 10 min. Cells were then washed, pelleted, and snap-frozen. Chromatin was sonicated on ice to 200–1000 bps as determined by gel electrophoresis. An aliquot was removed for Input DNA sequencing. Chromatin was pre-cleared with Protein A Agarose/Salmon Sperm DNA for 30 min on ice before adding antibody. 20 µg of antibody was added per 200 million cells, and samples were incubated overnight at 4°C. Antibody-bound chromatin was then collected using Life Technologies Protein G Dynabeads, washed, and precipitated. Precipitated chromatin was then eluted twice for 15 min each at room temperature. ChIP and Input DNA crosslinks were reversed and treated with RNase, then proteinase K. DNA was recovered with Agencourt AMPure XP Beads and quantified using the Life Technologies Qubit Fluorometer.

Barcoded ChIP-seq libraries were made from ChIP DNA using the NuGen Ovation Ultralow DR Kit, checked for adaptor artifacts by Agilent Bioanalyzer using DNA high-sensitivity reagents and chips, quantified by QPCR using an Illumina Library Quantification kit (KAPA Biosystems), and sequenced on an Illumina HiSeq 2500 instrument. Sequencing quality was assessed as with RNA-

seq, but aligned using Bowtie (Langmead and Salzberg 2012). ChIP peaks for the transcription factors were called using SPP, and individual peak significance was defined by SPP ChIP score (Kharchenko *et al.* 2008). Histone modification peaks were called using SICER (Zang *et al.* 2009).

PCR, Cloning, Quantitative RT-PCR and siRNA Knockdown

Genomic DNA was isolated from fibroblasts, iPS cells, and CMS with the DNAeasy Blood and Tissue Kit (Qiagen). Genomic DNA was amplified with Platinum Taq DNA Polymerase High Fidelity (Invitrogen). Primer sequences used for the *GATA4 G296S* locus are in **Table 1**. RNA was extracted by the TRizol method (Invitrogen). RT–PCR was performed using the Superscript III first-strand synthesis system (Invitrogen). qPCR was performed using the ABI 7900HT (TaqMan, Applied Biosystems) per the manufacturer's protocols. Optimized primers from the Taqman Gene Expression Array were used (Applied Biosystems). Gene Knockdown was performed using control scramble siRNA or targeted using RNAiMAX Transfection Reagent (Life Technologies). Cells were harvested 48 hours later and assayed or use for RNA isolation with RNAeasy Micro Kit (Qiagen). Knockdown was done with several different siRNAs to test effectiveness in order to choose one to use against *GATA4* (Sigma SAS1_Hs01_00212513).

Immunocytochemistry

Cells were fixed in 4% paraformaldehyde (Electron Microscopy Sciences) for 20 minutes at room temperature (RT), washed with PBS, and permeabilized with PBS+ 1% bovine serum albumin + 0.1% Triton-100. Next preparations were blocked with 1x Powerblock (Biogenex), and incubated on a rocker with primary antibody at 4 degrees overnight. The primary antibody was rinsed 3x, washed for 5 minutes 3x, blocked again for 30 mins at RT, and the AlexaFluor secondary antibody (Life Technologies) added 1:300 for 2 hours at RT. Coverslips were rinsed 3x, washed for 5 mins 3x, and stained with DAPI for 20 mins. After washing with PBS, slides were mounted with Prolong Gold Antifade Reagent (Life Technologies). Other antibodies used were VIM (Santa Cruz), cTnT (Thermo Scientific), GATA4 (Abcam), cTnI (Santa Cruz), MLC2v (MLC2 Abcam), and MLC2a (MYL7 Abcam). Cells were imaged with a Zeiss Axiovert 200 M with a Zeiss Axiocam MRm.

Calcium Flux

Isolated myocytes were loaded with Fluo-4 AM (Invitrogen) for 30 min at room temperature before being transferred to the superfusion chamber. The loading solution contained a 1:10 mixture of 5 mM Fluo-4 AM in dry DMSO and PowerloadTM concentrate (Invitrogen) which was diluted 100-fold into extracellular Tyrode's solution containing suspended myocytes. An additional 20 min was allowed for de-esterification before commencing recordings.

Contractions and calcium transients were evoked by applying voltage pulses at 0.33 Hz between platinum wires placed on either side of the cell of interest and connected to a field stimulator (IonOptix, Myopacer). The pulses were of 2 ms duration and set at 150% of the threshold required to elicit twitches. Fluo-4 fluorescence transients were recorded via a standard filter set (#49011 ET, Chroma Technology) in batches of ten to enable signal averaging. The fluorescence excitation light was blocked by an electromechanical shutter between stimuli (CS35; Vincent Associates). Resting fluorescence was recorded after cessation of pacing, and background light was obtained after picking up and removing the cell from the field of view with a patch electrode at the end of the experiment. The calcium transients were calibrated using the pseudo-ratio method, assuming an in situ dissociation constant of 1.1 mM for Fluo-4. The time course of $[Ca^{2+}]_i$-dependent fluorescence transients was quan- tified as the duration at 10% amplitude (10%–90% time). Contractions were optically recorded simultaneously with calcium transients by illuminating the cell of interest in red light (665 nm) subsequently directed to a CCD camera (IonOptix Myocam). To avoid movement artifacts in fluorescence recordings, cells and microclusters were framed by a cell-free border and bright-field images were recorded. In some experiments, cell motion was quantified from video- micrographs using an edge-detector algorithm written in LabView (National Instruments), calibrated using a stage micrometer.

Contractility Studies

Contractility studies were done in collaboration with Alex Ribeiro, a postdoc in Beth Pruitt's lab at Stanford. In order to do these experiments, iPS-CMs were seeded onto devices of micropatterned hydrogels of defined stiffness and shape and assessed via microscopy. The micropatterns were defined as being 2000-μm^2 rectangular patterns of Matrigel (BD Matrigel hESC-qualified Matrix, BD Biosciences) in aspect ratios of 7:1. Matrigel micropatterns were initially stamped on glass coverslips with microcontact printing using microstamps inked with Matrigel and then transferred from the micropatterned glass coverslips onto the surface of polyacrylamide hydrogels that had a stiffness of 10 kPa. To manufacture elastomeric microstamps of polydimethylsiloxane (PDMS; PDMS-182, Sylgard) for microcontact printing, standard soft lithography and microfabrication techniques were used (Azioune *et al.* 2010). To assess mechanical output in single hPSC-CMs by traction force microscopy, fluorescent microbeads (diameter, 0.5 μm) (Life Technologies) were added to the prepolymer solution (Kraning-Rush *et al.* 2012). Stock microbead solution (30 mL) was sonicated for 15 min and mixed with 90 μL of Milli-Q water; 86 μL of this solution was added to each milliliter of gel prepolymer solution to yield a final concentration of 6.25×10^9 microbeads/mL.

Traction stresses generated during the contraction of single iPSC-CMs were estimated by traction force microscopy (Kraning-Rush *et al.* 2012). Cells were maintained in culture on deformable hydrogels with dispersed fluorescent

microbeads (described above), and 10-s videos of moving microbeads were acquired at a minimum speed of 26 frames/s. To estimate forces from substrate displacements (Tseng *et al.* 2012), images of moving microbeads were processed with ImageJ 1.48 (National Institutes of Health) plugins. In brief, displacements were measured by particle image velocimetry (PIV) (Tseng *et al.* 2012) from an image of microbeads under a relaxed cell and another image of microbeads under that cell at its maximal contraction. Force fields were reconstructed from PIV displacements by a Fourier transform traction cytometry method (Tseng *et al.* 2012) and regularization scheme on the grid obtained from PIV. The regularization parameter was set at 9×10^{-10} for traction- force reconstructions. The absolute values of all stress vectors were summed, and the result was multiplied by cell area to estimate the total maximal force generated during single-cell contraction.

Maximal work was estimated by multiplying the maximal force and the sum of the absolute displacement values from PIV. The duration of contraction was calculated as the time difference between images taken at full contraction and at full relaxation. Contraction velocity was calculated by dividing the sum of absolute displacements by the duration of contraction. The power output of single cells was calculated by multiplying maximal force by velocity. Dimensions in acquired images were converted from pixels to μm with Zeiss software (ZEN 2011 blue edition) and verified with calibration slides (Electron Microscopy Sciences). Cell shortening velocity was calculating by subtracting the cell length in full contraction from the cell length in full relaxation and dividing the result by

the time between full contraction and full relaxation.

Mouse genotyping and colony maintenance

All transgenic lines for immunohistochemistry and functional studies were maintained by crossing with C57BL6 mice (Jackson Labs). The GATA G295S mouse is from (Misra *et al.* 2012) and was genotyped as according to their protocols. Mice were additionally backcrossed three times to C57BL/6 mice. For genotyping, allelic discrimination assay was used with the TaqMan Sample-to-SNP Kit (Applied Biosystems) with the primers and probes listed in **Tables 1 and 2,** respectively. Controls were always used, and sequencing was done on a sporadic basis to confirm genotype, as this assay has to discriminate on the basis of a single point mutation.

PRDM16 deletion mice were a gift of Bruce Spiegelman's lab. Generation of PRDM16 loxP/loxP mice was published in (Cohen *et al.* 2014). The deletion mice were generated by crossing male PRDM16 loxP/loxP mice to Zp3-cre mice, which deleted PRDM16 in fertilized eggs. Primers used for genotyping are included in **Table 1**.

Mouse echocardiography

Echocardiography was performed by the Vevo 770 High-Resolution Micro-Imaging System (VisualSonics) with a 15-MHz linear array ultrasound

transducer. The left ventricle was assessed in both parasternal long-axis and short-axis views at a frame rate of 120 Hz. End-systole or end-diastole was defined as the phase in which the smallest or largest area of the left ventricle, respectively, was obtained and used for ejection fraction measurement. Left ventricular end-systolic diameter and left ventricular end-diastolic diameter were measured from the left ventricular M-mode tracing with a sweep speed of 50 mms at the papillary muscle level for calculating the shortening fraction. B-mode was used for two-dimensional measurements of end-systolic and end-diastolic dimensions. Mice were analyzed by echocardiography at 2 and 6 months old. TAC was performed after the 6 month measurement, whereupon they were reanalyzed at 1 week and 4 weeks after TAC.

Trans-Aortic Constriction (TAC)

The animal protocol for surgery was approved by institutional guidelines (UCSF Institutional Animal Care and Use Committee). All surgeries and measurements were performed blinded for genotype and intervention. Mice were anaesthetized with isoflurane and placed in a supine position on a heating pad. Animals were intubated and ventilated with room air using a MiniVent Type 845 mouse ventilator (Hugo Sachs Elektronik-Harvard Apparatus; stroke volume, 250 ml; respiratory rate, 120 breaths per minute). TAC was performed through a 5 mm incision over the left thorax. A silk suture was tied around a 27-gauge needle positioned adjacent to the aorta. Successful TAC was confirmed by Doppler

measurement of pressure gradient 10 days after surgery. Pressure gradients were calculated according to the modified Bernoulli's equation as $4v^2$, where v is the blood velocity as determined by continuous wave Doppler. After ligation, the chest was closed with sutures and the mouse was allowed to recover on the mouse ventilator and heating pad. All surgical procedures were performed under aseptic conditions. At 4 weeks after ligation, the hearts were removed for sectioning and immunohistochemistry. Parameters were averaged for each genotype, and comparisons were made with Student's T-test.

Statistical Analyses

Differences between groups were examined for statistical significance using unpaired Student's t-test or one-way ANOVA with Bonferroni's correction for multiple hypothesis testing. A P-value less than 0.05 was regarded as significant. Error bars indicate standard error of the mean (s.e.m.).

RESULTS

Generation and Purification of Cardiomyocytes

The generation of the patient-specific iPS cell lines was discussed previously in Chapter 2. This study continues to use those lines to perform a deeper analysis of effects of the *GATA4 G296S* mutation. (See **Figure 1A** for the

family pedigree and their corresponding cell line names.) In order to do this analysis, we needed a large number of cells from single batches, which required switching differentiation protocols to one utilizing the Wnt pathway (Lian *et al.* 2012). We found that consistent results required we have more highly purified cardiomyocytes, more pure than the approximately 70% pure cardiomyocytes obtainied with the standard Wnt differentiation protocol. Purification to over 90% purity was achieved by employing a technique similar to that described in (Tohyama *et al.* 2013), in which cells are subjected to media without glucose after differentiation and with lactate as the primary carbon source. Imaging after immunocytochemistry of cardiomyocyte markers cTnT, cTnI, MLC2v, and αActinin and quantification of the staining show that these lactate-purified cardiomyocytes express all four markers at rates consistent with over 90% purity (**Fig 1B,C**). We also did additional experiments to verify the cardiomyocytes function appropriately by patch clamping measurements of action potentials (**Fig 1D**) and by calcium flux assay with pharmacologic stimulation (**Fig 1E**). Additionally, using EM, these cardiomyocytes show well-formed sarcomeres surrounded by abundant mitochondria (**Fig 1F**).

Genome-wide localization profiling of GATA4 and modified histones in iPS-cardiomyocytes

Purified human cardiomyocytes were then analyzed for endogenous GATA4 genome occupancy by ChIP-Seq. Over 70% of the peaks from the ChIP-

Seq show the GATA4 consensus motif (**Fig 2A**), which matches that which has been previously published in mice (He *et al.* 2011). In order to get a more complete picture of the impact of the *GATA4 G296S* mutation, we needed additional information from other transcription factors and histone marks. As GATA4 G296S has been shown to selectively lose its interaction with TBX5 (Garg *et al.* 2003) and GATA4 is known to promote (He at al 2014) and suppress (Aronson *et al.* 2014) the deposition of H3K27ac activating marks via its interaction with p300, we were interested in how these marks would be affected and correlate with expression analysis. An example of the tracks for GATA4, TBX5, and the activating marks H3K4me3 and H3K27ac in the wildtype in provided in (**Fig 2B**) for the *NPPA* and *NPPB* loci, both known targets of GATA4. We also chose to examine the activating histone marks H3K4me3 and H3K36me3, as these mark active/poised promoters and actively transcribed regions, respectively, and would confirm the active enhancer mark H3K27ac and the RNA-seq data. We also chose a repressive mark H3K27me3 for comparison. Finally, we decided to include the transcription factor MED1, which is known to interact with GATA4 (Crawford *et al.* 2002). MED1 has also been shown to regulate the activation of related transcription factors GATA1 (Stumpf *et al.* 2006) and GATA6 (Nakamura *et al.* 2009).

Gene Ontological (GO) analysis was used to profile all genes found within 10kb from the GATA4 binding sites, demonstrating the overwhelming bias of GATA4 for cardiac genes in CMs (**Fig 2C**). Genome-wide, binding sites for GATA4 show a strong correlation with TBX5 and H3K27ac sites, confirming the

strong association these two have with GATA4 (**Fig 2D**). A Pearson correlation matrix for the binding sites of all transcription factors and histone marks confirmed that these are associated appropriately (**Fig 2E**). The transcription factors bind in closely aligned sites as do the activating histone marks. H3K27ac and H3K4me3 are more closely associated with each other than with H3K36me3. However, this is expected as the H3K36me3 mark is found along gene bodies that are actively transcribed and H3K27ac and H3K4me3 mark discrete regulatory regions, enhancers and transcriptional start sites, respectively. Heatmap profiling of the GATA4 and TBX5 bound regions in WT and mutant CMs also suggests reduced TBX5 binding and increased H3K27ac binding at gene promoters (**Fig 2F**). This result is intriguing, because while it is not surprising that TBX5 would have reduced occupancy due to a decrease in recruitment of TBX5 to loci by GATA4, it is surprising that GATA4 G296S would lead to increased deposition of H3K27ac. Previously GATA4 has been shown to help recruit p300 and promote acetylation (He *et al.* 2011), as GATA4 G296S is reported to have reduced DNA binding affinity (Garg *et al.* 2003), the mechanism for how GATA4 could be creating increased levels of acetylation is unclear.

Transcriptional perturbations in GATA4 G296S/+ cardiomyocytes

To determine the consequences of GATA4 G296S on transcription, we performed RNA sequencing (RNA-Seq) on the wildtype and mutant cardiomyocytes and compared their clustered expression patterns to determine

the differential expression pattern between wildtypes and mutants (**Fig 3A**). We found that 156 genes were differentially expressed. 53% of these were upregulated (**Fig 3B**) and 37% were downregulated (**Fig 3C**) in the mutant lines as compared to wildtype.

As GATA4 G296S has previously been classified as haploinsufficient due to a loss of its interaction with TBX5 and reduced DNA-binding affinity (Garg *et al.* 2003), we were surprised at the number of genes that were comparably upregulated. Many of these upregulated genes include ion channel genes and genes involved in contraction like *RYR3* (ryanodine receptor), *SCN9A*, *CACNA1G*, *CFTR*, *DES* (desmin), and *GJA5* (connexin 40). Interestingly, it has previously been demonstrated that TBX5 serves to repress the GATA4/NKX2.5 dependent activation of the promoter of *Connexin40* (Linhares *et al.* 2004). This finding could suggest that TBX5 is serving as a transcriptional repressor at the *Connexin40* locus and is recruited to the site by GATA4. However, in the G296S/+ mutant cells, the recruitment is lost and thus so is the repressive activity of TBX5 at this site. Downregulated pathways in the mutant cells were less cardiac specific, but included the genes *FN1* (fibronectin), *STAT4*, *LPL* (lipoprotein lipase), *LAMA1* (laminin), and *MYH6*. *MYH6*, or α-myosin heavy chain (MHC), has previously been shown to be specifically downregulated *in vivo* in *Gata4-/+; Tbx5-/+* mice (Maitra *et al.* 2009), consistent with our results and highlighting the importance of the interaction of these two factors for maintaining expression of one of the dominant sarcomeric genes expressed in the adult heart. We also performed Gene Set Enrichment Analysis (GSEA) on genes

bound by GATA4 and dysregulated across the mutant and wildtype and found a significant correlation (**Fig 3D**), suggesting that the expression changes are due to differential binding patterns of GATA G296S/+.

Increased calcium transients present in G296S/+ mutant CMs.

Calcium imaging was performed to assess the impact of the dysregulated genes in the mutant cell lines. In brief, cells were plated onto coverslips with patterned lines of ECM to facilitate attachment into ordered lines, thereby creating functionally syncytial microtissues (**Fig 4A**). We used two cell lines each for WT and mutant. We then used Fluo-4 fluorescence levels to record and calculate the calcium fluorescent transients (FTs), which reflect the flux of calcium with each action potential (Spencer *et al.* 2014). Only the amplitude of calcium transients was found to be significantly different between the WT and mutant and lines (**Fig 4B**). Other parameters analyzed include the contraction frequency, the fluorescent transient duration, decay, and rise over the interval comprising 10-90% of the FT (**Fig 4C, D**). The increased amplitude of the calcium transient suggests that a larger release of calcium is required to propagate the action potential, which would have implications for the calcium sensitivity of the cardiomyocyte. GATA4 has not previously been shown to have a major role in calcium handling, so the effect that an increased amplitude of calcium transient might have is unclear. There have been other studies that link GATA4 to having a role in transcribing a particular connexin, like Connexin 40

(Linhares *et al.* 2004) or Connexin 30.2 (Munshi *et al.* 2009). *Connexin30.2* dysregulation has been linked to a shortened PR interval in the *Gata4-/+* mouse, implicating GATA4 in atrioventricular (AV) delay (Munshi *et al.* 2009). Yet, how this dysregulation might manifest in a cell model based platform is unclear. A better understanding of how the AV node functions and the role of GATA4 in this process would be necessary to elucidate this relationship.

GATA4 G296S/+ mutant CMs have a hypercontractile phenotype.

Intriguingly, other studies have shown a correlation of increased calcium transient amplitude with increases in force production (Haizlip *et al.* 2014; Monasky *et al.* 2008). To investigate this relationship of calcium transients with force generation, we performed contractility studies on our CMs. In brief, optimal force generation and sarcomeric alignment is achieved when cells are transferred to 10 kPa hydrogels patterned with the attachment matrix matrigel in 7:1 aspect ratios (pictured in **Fig 5A**). The hydrogels are filled with fluorescent beads such that when the cells contract, the beads are displaced and velocity, force, and power calculated from the movement of the beads. Cardiomyocytes attain mature appearing sarcomere alignment on these patterns and demonstrate the appropriate staining patterns of sarcomeric F-actin and the Z-line protein, alpha-actinin (**Fig 5A**). These analyses revealed that the GATA4 G296S/+ mutant cardiomyocytes have a hypercontractile phenotype. The contraction velocity, force generation, and power output are significantly higher than the

wildtype (**Fig 5B, C**). This phenotype was consistent across multiple wildtype and mutant lines and is reproducible. Although the increased calcium transients hinted that there might be a change in force generation of the CMs, this result was still surprising. For one, GATA4, although responsible for transcribing many sarcomeric genes, has not been directly linked to force production. However, there is a set of genes that are differentially upregulated in the G296S/+ CMs that are involved in function of the sarcomere (**Fig 3A**). Many sarcomeric genes are also dysregulated in the mouse model of *Gata4 G295S* (Misra *et al.* 2012) suggesting that this phenotype may be more directly related to the sarcomere and not to the calcium handling dynamics. It is possible that the loss of GATA4 leads to an imbalance of the sarcomeric genes such that the assembly of the sarcomere and its responsiveness to calcium signaling is altered to make the individual cell hypercontractile.

The Gata4 G295S/+ *knock-in mouse fails to respond appropriately to pressure-overload induced stress and develops a dilated cardiomyopathy.*

Previously the *Gata4 G295S/+* knock-in mouse has been published as having a congenital heart disease phenotype, namely ASDs and valvular stenosis. The KI mouse also displays dysregulated gene expression associated with GATA4 targets (Misra *et al.* 2012). We were curious if this mouse would

display a dilated cardiomyopathy similar to what has been reported for *Gata4-/+* mice in the literature (Oka *et al.* 2006; Bisping *et al.* 2006). It was important to test this because it is possible that the G296S mutation would not exhibit the same phenotype as *Gata4-/+*, as *Gata4-/+* is a deficiency model and the G296S mutation is not wholly proven to act in the same manner. This was a concern because many genes involved in dilated cardiomyopathy are also implicated in hypertrophic cardiomyopathy (Kimura 2010).

To test this hypothesis, we took the *Gata4 G295S* KI mouse and performed echocardiography under baseline conditions as well as in a pressure overload model of hypertrophy via trans-aortic constriction (TAC) (deAlmeida *et al.* 2009; Vedantham *et al.* 2012). These mice do not exhibit a phenotype under baseline conditions as assessed at 2 months (data not shown) and 6 months (**Fig 6**). This result contrasts with what has been shown before for the *Gata4-/+* mouse (Bisping *et al.* 2006; Oka *et al.* 2006). The *Gata4-/+* mouse demonstrated a baseline fractional shortening (FS) defect that worsened under TAC. Interestingly, the *Gata4 G295S/+* mouse did have a phenotype under stress induced by TAC (**Fig 6**). After one week of TAC, the mice exhibited a decline in the functional parameters FS (WT 28.98 vs mut 23.28, p=0.032) and ejection fraction (EF) (WT 56.51 vs mut 46.77, p=0.031) (**Fig 6A**) that mirrors what was observed previously (Bisping *et al.* 2006; Oka *et al.* 2006). The left ventricular (LV) volumes (diastole: WT 58.68uL vs mut 77.14uL, p=0.016 ; systole WT 25.55uL vs mut 41.48uL, p=0.016) (**Fig 6B**) and chamber diameters (diastole: WT 3.70mm vs mut 4.16mm, p=0.016 ; systole WT 2.63mm vs mut 3.2mm,

p=0.012) are significantly larger than wildtype. The posterior wall thickness also is thinner than the wildtype during systole (diastole: WT 1.1mm vs mut 0.98mm, p=0.181 ; systole WT 1.43mm vs mut 1.19mm, p=0.019) (**Fig 6B**). All of these observations indicate that the defect resembles a dilated cardiomyopathy and point to an inability of the *Gata4 G295S/+* mouse to respond appropriately to pressure-overload induced hypertrophy. This dilated cardiomyopathy mirrors what has been described in the human G296S/+ patients and also what was reported from two other families with *GATA4* mutation, albeit at different sites (Li *et al.* 2013; Zhao *et al.* 2014). Taken together, the evidence that the *Gata4 G295S* KI mouse also has dilated cardiomyopathy is concordant with both the patient phenotypes observed and with other mouse models of *Gata4-/+* deficiency.

Target validation with knockdown of GATA4

We wanted to make a prioritized list of genes dysregulated in GATA4 G296S/+ that were dysregulated in the same direction as with GATA4 depletion. To do this, we performed siRNA knockdown (KD) of *GATA4* mRNA in H7 differentiated cardiomyocytes. From this experiment we obtained 1333 differentially expressed genes between *GATA4* siRNA KD and scramble (**Fig 7A**). Of these genes 51% were downregulated and 49% were upregulated. GO analysis reveals that of the downregulated gene set, there was an abundance of genes involved in pathways associated with mitochondria (**Fig 7B**). Specific

genes of interest include *TBX20*, *HDAC2*, *TNNT2*, and *TNNI3*. In the GO analysis of the upregulated genes, there were many genes involved in the cytoskeleton and morphogenesis, but also in calcium ion binding, consistent with the G296S/+ dysregulated gene set (**Fig 7C**). Additionally, *NOTCH1*, *BCL2*, *CHD1*, *FGF2*, *MMP3*, and *Nodal* were all upregulated in the *GATA4* KD. Due to the small number of genes that were coordinately dysregulated across the different mutant lines, we were limited in our ability to compare that small number of genes with this relatively larger list. However, we were able to find three genes that were similarly dysregulated in both conditions: *PRDM16*, *TBX18*, and *LEFTY2* (**Fig 7A** in red).

In vivo *target-specific investigations into* PRDM16*, a gene dysregulated gene in* GATA4 G296S/+ *CMs*

PRDM16 is expressed at lower levels in both *GATA4* KD and in G296S/+ mutant cells (**Fig 8A**). PRDM16 was of interest to us because it is a transcription factor that serves as a coregulator of genes involved in mitochondrial biogenesis and energy regulation (Seale *et al.* 2007). Additionally, it was linked to 1p36 deletion syndrome, which is characterized by left ventricular non-compaction (LVNC) (Arndt *et al.* 2013). LVNC is characterized by thin walled myocardium and hypertrabeculations. The GATA4 G296S/+ patients have hypertrabeculation of the right ventricle that is similar.

In order to investigate the role of PRDM16 in GATA4 G296S/+ disease, we decided to cross *Prdm16-/+* mice with *Gata4 G295S/+* mice, as both of these mutations are embryonic lethal when homozygous. We then analyzed the pups, contrasting the double heterozygous offspring with the wildtype and single heterozygous mutant littermate controls. The birth ratios were equivalent between all genotypes indicating that there was no evidence of early prenatal lethality (**Fig 8B**). Baseline echocardiography at 2 and 6 months showed no difference between the genotypes (data not shown). We then decided to test if there was a difference between the *Gata4 G295S/+* and the *Prdm16-/+*; *Gata4 G295S/+* mice under conditions of pressure overload-induced hypertrophy. We tested all four genotypes using littermate controls. *Prdm16-/+* mice were virtually indistinguishable from wildtype in all conditions. The *Gata4 G295S* mutation showed the strongest effect in the mice. Significance for *Prdm16-/+*; *Gata4 G295S/+* over *Gata4 G295S/+* alone was only found for two measures during the 1 week post-TAC time point. Diastolic LV posterior (G 0.98 mm vs P&G 0.81 mm, p=0.046) and anterior (G 1.00 mm vs P&G 0.85 mm, p=0.035) wall thickness measurements showed a significant decrease in thickness in the *Prdm16-/+*; *Gata4 G295S/+ mice* as compared to *Gata4 G295S/+* alone (**Fig 8C**). The *Prdm16-/+* mouse is also significantly different from the *Prdm16-/+*; *Gata4 G295S/+* mouse at this measure. This finding implies that there is a decreased ability of the heart to respond to hypertrophic stimuli in the double heterozygous mice. However, this phenotype is subtle and disappears by the fourth week of TAC when the *Gata4 G295S/+* mouse loses some of its hypertrophic growth. Yet,

this observation is consistent in both the anterior and posterior wall. These data suggest that Prdm16 is a genetic interactor with GATA4, albeit weakly. Thus, it seems that using RNA-seq as a guide, interactors with GATA4 can be revealed.

DISCUSSION

The *GATA4 G296S* mutation has been associated with septal and valvular defects and now with cardiomyopathy in human patients. Previous work examining the homozygous knock-in of the orthologous allele in mice has shown that this mutation is not a true loss of function mutation, as it survives an additional two days embryonically (Misra *et al.* 2012) although it does have selective functional losses in DNA binding and in its interaction with TBX5 (Garg *et al.* 2003). It also appears that the Gata4 G295S mouse exhibits a dilated cardiomyopathy on pressure overload induced hypertrophy. This phenotype is similar to the one observed in the human patients and in two separate families with mutations in *GATA4* (Li *et al.* 2013; Zhao *et al.* 2014).

Presumably, the cardiomyopathy described with the *GATA4 G296S* mutation reflects an organ level response to the cellular processes dysregulated by the mutated transcription factor. A more detailed study of the GATA4 G296S/+ transcriptome is required for a comprehensive understanding of the functional consequences of this transcription factor mutation on the cardiomyocyte. Yet, we have already learned these cardiomyocytes have a cellular phenotype of

increased amplitude of calcium transients and hypercontractility. As these two processes are intricately linked and display a direct relationship *in vitro* (Haizlip *et al.* 2014; Monasky *et al.* 2008), these are mutually supportive observations. As gene expression profiles of genes involved in both calcium handling and the sarcomere are altered in G296S/+ CMs and are direct targets of GATA4, these could be phenomena coupled together by both function and transcriptional regulation.

Understanding the underlying causes of this cardiomyopathy phenotype is complicated. The literature is at times conflicting; there are many different theories for what the underlying cause of hypertrophic versus dilated cardiomyopathy (Kimura 2010 for a review). It is also possible that all are valid at some level and that the cause for each has to be determined on a case by case basis. However, a hypothesis that reflects a trend in the literature is that dilated cardiomyopathy may be more associated with decreased sensitivity of the sarcomere to calcium and hypertrophic cardiomyopathy with increased sensitivity (Morimoto *et al.* 2002; Rajan *et al.* 2007; Bottinelli *et al.* 1998). This hypothesis would also be in line with our results as presumably, the individual human G296S/+ mutant cardiomyocytes have the same phenotype as those in the mouse. Considering that the mouse and the human phenotypes have been amazingly concordant for both congenital structural disease and cardiomyopathy phenotype, this conclusion now appears more likely. Moreover, dilated cardiomyopathy represents a new phenotype associated with GATA4. Previously, the dilated cardiomyopathy was thought to be related a lower initial

cell number of cells in the heart and increased death due to previously published mechanisms of GATA4 in the heart (Bisping *et al.* 2006; Oka *et al.* 2006; Aries *et al.* 2004; Rojas *et al.* 2008). GATA4 is known to be involved in cell survival (Aries *et al.* 2004) and proliferation (Rojas *et al.* 2008). Both of these are important processes involved in the morphogenesis and remodeling in the heart (Maitra *et al.* 2009; James 1998; Zeisberg *et al.* 2005). However, the data presented here demonstrates that there is still another difference that could be implicated in causing the cardiomyopathy, and perhaps why none of the GATA4 mutations thus far have been associated with a hypertrophic cardiomyopathy.

We also presented an unbiased RNA-seq based profiling approach to uncover new mechanisms behind this GATAA4 mutation associated heart disease. Here, we performed assays based on the RNA-seq profiling of the dysregulated transcriptome and were able to find functional readouts and genetic interactors that were heretofore unknown. As these technologies and their feasibility become more accessible, opportunities for more complete profiling of the underlying mechanisms will become apparent.

ACKNOWLEDGEMENTS

We thank Bruce Spiegelman for providing the *Prdm16-/+* mice. We thank members of the Gladstone bioinformatics core, especially Alex Willams and

Ruben Oregon, for their assistance. We thank the Srivastava lab for their discussions and thoughtful comments.

AUTHOR CONTRIBUTIONS

Renee Rivas designed, performed, and supervised the work contained within this chapter and wrote it. Yen-Sin Ang designed, performed, and supervised the work and in particular did the ChIP-seq and RNA-seq experiments. Alex Ribeiro performed the contraction measurements. Huey Jiin “Jean” Liu and Janell Rivera performed experiments. C. Ian Spencer performed the calcium studies. Yu Huang performed the echocardiography and TAC experiments. Rohith Srivas and Molong Li assisted with bioinformatics analyses. Beth Pruitt and Michael Stryker assisted with design of experiments. Deepak Srivastava designed, provided funding, and supervised this work.

REFERENCES

Aronson B.E., Aronson S.R., Berkhout R.P., Chavoushi S.F., He A., Pu W.T., Verzi M.P., Krasinski S.D. (2014). GATA4 represses an ileal program of gene expression in the proximal small intestine by inhibiting the acetylation of histone H3, lysine 27. Biochimica et Biophysica Acta *1839*, 1273–1282.

Arndt, A., Schafer S., Drenckhahn J., Sabeh M.K., Plovie E.R., Caliebe A., Klopocki E., Musso G., Werdich A.A., Kalwa H., Heinig M., Padera R.F., Wassilew K., Bluhm J., Harnack C., Martitz J., Barton P.J., Greutmann M., Berger F., Hubner N., Siebert R., Kramer H., Cook S.A., MacRae C.A., Klaassen S. Fine Mapping of the 1p36 Deletion Syndrome Identifies Mutation of PRDM16 as a Cause of Cardiomyopathy. Amer. J. Human Genetics *93*, 67–77.

Azioune A., Carpi N., Tseng Q., Thery M., Piel M. (2010). Protein micropatterns: A direct printing protocol using deep UVs. Methods Cell Biol *97*,133-146.

Bisping E., Ikeda S., Kong S.W., Tarnavski O., Bodyak N., McMullen J.R., Rajagopal S., Son J.K., Ma Q., Springer Z., Kang P.M., Izumo S., Pu W.T. (2006). Gata4 is required for maintenance of postnatal cardiac function and protection from pressure overload-induced heart failure. PNAS *103*,14471-6.

Bottinelli R., Coviello D.A., Redwood C.S., Pellegrino M.A., Maron B.J., Spirito P., Watkins H., Reggiani C. (1998). A mutant tropomyosin that causes hypertrophic cardiomyopathy is expressed *in vivo* and associated with an increased calcium sensitivity. Circ Res. *82(1)*, 106-15.

Chen J., Bardes E.E., Aronow B.J., Jegga A.G. (2009). ToppGene Suite for gene list enrichment analysis and candidate gene prioritization. Nucleic Acids Res. *37*, W305–W311.

Cohen, P., Levy J.D., Zhang Y., Frontini A., Kolodin D.P., Svensson K.J., Lo J.C., Zeng X., Ye L., Khandekar M.J., Wu J., Gunawardana S.C., Banks A.S., Camporez J.P.G., Jurczak M.J., Kajimura S., Piston D.W., Mathis D., Cinti S., Shulman G.I., Seale P., Spiegelman B.M. Ablation of PRDM16 and Beige Adipose Causes Metabolic Dysfunction and a Subcutaneous to Visceral Fat Switch. Cell *156*, 304–316.

Crawford S.E., Qi C., Misra P., Stellmach V., Rao M.S., Engel J.D., Zhu Y., Reddy J.K. (2002). Defects of the Heart, Eye, and Megakaryocytes in Peroxisome Proliferator Activator Receptor-binding Protein (PBP) Null Embryos Implicate GATA Family of Transcription Factors. J. Bio. Chem. *277(5)*, 3585–3592.

deAlmeida A.C., van Oort R.J., Wehrens X.H.T. (2009). Transverse Aortic Constriction in Mice. JOVE *38*, 1729.

Flicek P., Amode M.R., Barrell D., Beal K., Billis K., Brent S., Carvalho-Silva D., Clapham P., Coates G., Fitzgerald S., Gil L., Girón C.G., Gordon L., Hourlier T., Hunt S., Johnson N., Juettemann T., Kähäri A.K., *et al.* (2014). Ensembl 2014. Nucleic Acids Res. *42*, D749–D755.

Garg V., Kathiriya I.S., Barnes R., Schluterman M.K., King I.N., Butler C.A., Rothrock C.R., Eapen R.S., Hirayama-Yamadak K., Joo K., Matsuokak R., Cohen J.C., Srivastava D. (2003). *GATA4* mutations cause human congenital heart defects and reveal an interaction with TBX5. Nature *424*, 443-447.

Haizlip K.M., Milani-Nejad N., Brunello L., Varian K.D., Slabaugh J.L., Walton S.D., Gyorke S., Davis J.P., Biesiadecki B.J., Janssen P.M. (2015). Dissociation of Calcium Transients and Force Development following a Change in Stimulation Frequency in Isolated Rabbit Myocardium. Biomed Res Int. *2015*, 468548.

He A., Gu F., Hu Y., Ma Q., Ye L.Y., Akiyama J.A., Visel A., Pennacchio L.A., Pu W.T. (2014). Dynamic GATA4 enhancers shape the chromatin landscape central to heart development and disease. Nat Comm *5*, 4907.

He A., Kong, S.W., Ma, Q., and Pu, W.T. (2011). Co-occupancy by multiple cardiac transcription factors identifies transcriptional enhancers active in heart. PNAS *108*, 5632–5637.

Ieda, M. Fu J.D., Delgado-Olguin P., Vedantham V., Hayashi Y., Bruneau B.G., Srivastava D. (2010). Direct Reprogramming of Fibroblasts into Functional Cardiomyocytes by Defined Factors. Cell *142*, 375–386.

James T.N. (1998). Normal and abnormal consequences of apoptosis in the human heart. Annu Rev Physiol. *60*, 309-25.

Kharchenko P.V., Tolstorukov M.Y., Park P.J. (2008). Design and analysis of ChIP-seq experiments for DNA-binding proteins. Nat. Biotechnol. *26*, 1351–1359.

Kim D., Pertea G., Trapnell C., Pimentel H., Kelley R., Salzberg S.L. (2013). TopHat2: accurate alignment of transcriptomes in the presence of insertions, deletions and gene fusions. Genome Biol. *14*, R36.

Kimura A. (2010). Molecular basis of hereditary cardiomyopathy: abnormalities in calcium sensitivity, stretch response, stress response and beyond. J. Human Genetics *55*, 81–90.

Kraning-Rush C.M., Carey S.P. , Califano J.P. , Reinhart-King C.A. (2012). Quantifying traction stresses in adherent cells. Methods Cell Biol *110*, 139-178.

Langmead B., Salzberg S.L. (2012). Fast gapped-read alignment with Bowtie 2. Nat. Methods *9*, 357–359.

Li H., Handsaker B., Wysoker A., Fennell T., Ruan J., Homer N., Marth G., Abecasis G., Durbin R., 1000 Genome Project Data Processing Subgroup. (2009). The Sequence Alignment/Map format and SAMtools. Bioinformatics *25*, 2078–2079.

Li Q.Y., Newbury-Ecob R.A., Terrett J.A., Wilson D.I., Curtis A.R.J., Yi C.H., Gebuhr T., Bullen P.J., Robson S.C., Strachan T., Bonnet D., Lyonnet S., Young I.D., Raeburn J.A., Buckler A.J., Law D.J., Brook J.D. (1997). Holt-Oram syndrome is caused by mutations in *TBX5*, a member of the Brachyury (T) gene family. Nat Genetics *15(1)*, 21-9.

Li R.G., Li L., Qiu X.B., Yuan F., Xu L., Li X., Xu Y., Jiang W., Jiang J., Liu X., Fang W., Zhang M., Peng L., Qu X., Yang Y. (2013) *GATA4* loss-of-function mutation underlies familial dilated cardiomyopathy. BiochemBiophys Res Commun *439*, 591–596.

Lian X., Hsiao C., Wilson G., Zhu K., Hazeltine L.B., Azarin S.M., Raval K.K., Zhang J., Kamp T.J., Palecek S.P. (2012). Robust cardiomyocyte differentiation from human pluripotent stem cells via temporal modulation of canonical Wnt signaling. PNAS *109(27)*, E1848-57.

Linhares V.L.F., Almeida N.A.S., Menezes D.C., Elliott D.A., Lai D., Beyer E.C., Campos de Carvalho A.C., Costa M.W. (2004). Transcriptional regulation of the murine *Connexin40* promoter by cardiac factors Nkx2-5, GATA4 and Tbx5. Cardiovasc Res. *64(3)*, 402–411.

Lopaschuk G.D., Jaswal J.S. (2010). Energy Metabolic Phenotype of the Cardiomyocyte During Development, Differentiation, and Postnatal Maturation. J Cardiovasc Pharmacol *56(2)*,130-140.

Maitra M., Schluterman M.K., Nichols H.A., Richardson J.A., Lo C.W., Srivastava D., Garg V. (2009). Interaction of Gata4 and Gata6 with Tbx5 is critical for normal cardiac development. Developmental Biology *326*, 368–377.

Misra, C., Sachan N., McNally C.R., Koenig S.N., Nichols H.A., Guggilam A., Lucchesi P.A., Pu W.T., Srivastava D., Garg V. (2012). Congenital Heart Disease–Causing *Gata4* Mutation Displays Functional Deficits *In Vivo*. PLOS Genetics *8*, e1002690.

Munshi N.V., McAnally J., Bezprozvannaya S., Berry J.M., Richardson J.A., Hill J.A., Olson E.N. (2009). *Cx30.2* enhancer analysis identifies Gata4 as a novel regulator of atrioventricular delay. Development *136*, 2665-2674.

Monasky M.M., Varian K.D., Davis J.P., Janssen P.M. (2008). Dissociation of force decline from calcium decline by preload in isolated rabbit myocardium. Pflugers Arch. *456(2)*, 267-76.

Nix D.A., Courdy S.J., Boucher K.M. (2008). Empirical methods for controlling false positives and estimating confidence in ChIP-Seq peaks. BMC Bioinformatics *9*, 523.

Oka T., Maillet M., Watt A.J., Schwartz R.J., Aronow B.J., Duncan S.A., Molkentin J.D. (2006). Cardiac-Specific Deletion of *Gata4* Reveals Its Requirement for Hypertrophy, Compensation, and Myocyte Viability. *Circ Res 9*, 837-845.

Okita, K., Matsumura Y., Sato Y., Okada A., Morizane A., Okamoto S., Hong H., Nakagawa M., Tanabe K., Tezuka K., Shibata T., Kunisada T., Takahashi M., Takahashi J., Saji H., Yamanaka S. (2011). A more efficient method to generate integration-free human iPS cells. Nature Methods *8*, 409–412.

Nakamura Y., Xing Y., Sasano H., Rainey W.E. (2009). The Mediator Complex Subunit 1 Enhances Transcription of Genes Needed for Adrenal Androgen Production. *150(9)*, 4145–4153.

Rajan S., Ahmed R.P., Jagatheesan G., Petrashevskaya N., Boivin G.P., Urboniene D., Arteaga G.M., Wolska B.M., Solaro R.J., Liggett S.B., Wieczorek D.F. (2007). Dilated cardiomyopathy mutant tropomyosin mice develop cardiac dysfunction with significantly decreased fractional shortening and myofilament calcium sensitivity. Circ Res. *101(2)*, 205-14.

Rojas A., Kong S.W., Agarwal P., Gilliss B., Pu W.T., Black B.L. (2008). GATA4 is a direct transcriptional activator of cyclin D2 and Cdk4 and is required for cardiomyocyte proliferation in anterior heart field-derived myocardium. Molecular and cellular biology *28*, 5420-31.

Sander J.D. and Joung J.K. (2014). CRISPR-Cas systems for editing, regulating and targeting genomes. Nature Biotechnology *32(4)*, 347-55.

Schlesinger J., Schueler M., Grunert M., Fischer J.J., Zhang Q., Krueger T., Lange M., Tönjes M., Dunkel I., Sperling S.R. (2011). The cardiac transcription network modulated by Gata4, Mef2a, Nkx2.5, Srf, histone modifications, and microRNAs. PLoS genetics *7*, e1001313.

Seale. P. Kajimura S., Yang W., Chin S., Rohas L. M., Uldry M., Tavernier G., Langin D., Spiegelman B.M. (2007). Transcriptional Control of Brown Fat Determination by PRDM16. Cell Metabolism *6*, 38–54.

Spencer C.I., Baba S., Nakamura K., Hua E.A., Sears M.A.F., Fu C.C., Zhang J., Balijepalli S., Tomoda K., Hayashi Y., Lizarraga P., Wojciak J., Scheinman M.M., Aalto-Setala K., Makielski J.C., January C.T., Healy K.E., Kamp T.J., Yamanaka S., Conklin B.R. (2014). Calcium Transients Closely Reflect Prolonged Action Potentials in iPSC Models of Inherited Cardiac Arrhythmia. Stem Cell Reports *3*, 269–281.

Stumpf M., Waskow C., Krotschel M., van Essen D., Rodriguez P., Zhang X., Guyot B., Roeder R.G., Borggrefe T. (2006). The mediator complex functions as a coactivator for GATA-1 in erythropoiesis via subunit Med1/TRAP220. PNAS 103(49), 18504–18509.

Theodoris C.V., Li M., White M.P., Liu L., He D., Pollard K.S., Bruneau B.G., Srivastava D. (2015). Human disease modeling reveals integrated transcriptional and epigenetic mechanisms of NOTCH1 haploinsufficiency. Cell *160(6)*, 1072-86.

Tohyama S., Hattori F., Sano M., Hishiki T., Nagahata Y., Matsuura T., Hashimoto H., Suzuki T., Yamashita H., Satoh Y., Egashira T., Seki T., Muraoka N., Yamakawa H., Ohgino Y., Tanaka T., Yoichi M., Yuasa S., Murata M., Suematsu M., Fukuda K. (2013). Distinct Metabolic Flow Enables Large-Scale Purification of Mouse and Human Pluripotent Stem Cell-Derived Cardiomyocytes. Cell Stem Cell *12*, 127–137.

Tseng Q., Duchemin-Pelletier E., Deshiere A., Balland M., Guillou H., Filhol O., Théry M. (2012). Spatial organization of the extracellular matrix regulates cell-cell junction positioning. Proc Natl Acad Sci *109(5)*,1506-1511.

van der Laan M.J., Pollard K.S. (2001). Hybrid clustering of gene expression data with visualization and the bootstrap. J. Stat. Plan. Inference *117*, 275–303.

Vedantham V., Evangelista M., Huang Y., Srivastava D. (2012). Spatiotemporal regulation of an Hcn4 enhancer defines a role for Mef2c and HDACs in cardiac electrical patterning. Developmental Biology *373*, 149–162.

Zambon A.C., Gaj S., Ho I., Hanspers K., Vranizan K., Evelo C.T., Conklin B.R., Pico A.R., Salomonis N. (2012). GO-Elite: a flexible solution for pathway and ontology over-representation. Bioinformatics *28*, 2209–2210.

Zang C., Schones D.E., Zeng C., Cui K., Zhao K., Peng W. (2009). A clustering approach for identification of enriched domains from histone modification ChIP-Seq data. Bioinformatics *25*, 1952–1958.

Zhou P., He A., Pu W.T. (2012). Regulation of GATA4 Transcriptional Activity in Cardiovascular Development and Disease. Current Topics in Developmental Biology *100*, 143-169.

FIGURES

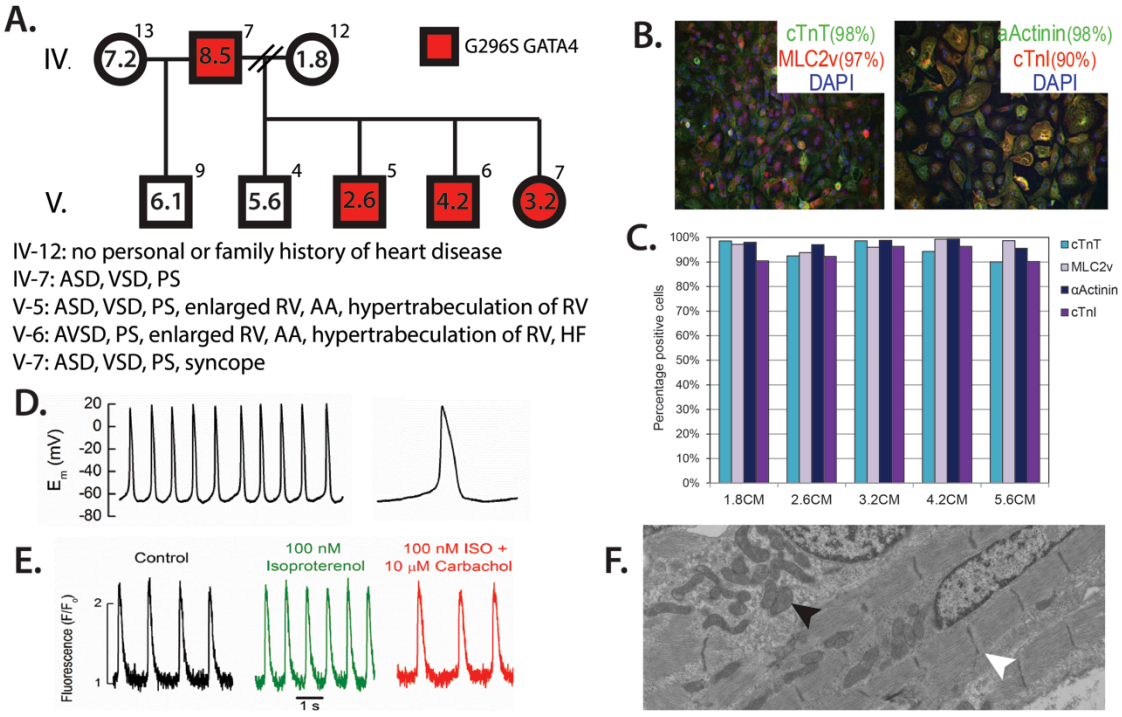

Fig. 1. Generation of functional iPS-derived cardiomyocytes from *GATA4* kindred A. Pedigree of kindred with *GATA4 G296S/+* mutation. The numbers inside the circles/squares represent the cell line derived from each patient. The Roman numerals to the left combined with the numbers to the top left of each circle/square represent the original location of this kindred in the greater pedigree published in (Garg *et al.* 2003). The phenotypes associated with each patient in addition to their originally published phenotypes are listed below. **B.** Immunocytochemistry of appropriate CM cell markers: cTnT, cTnI, MLC2v, and aActinin. **C.** Bar graph representing the percent staining of key cardiac markers demonstrating the high purity obtained by lactate purification. **D.** Action potentials of CMs measured by perforated patch clamping. **E.** Calcium flux assay with drug

treatment demonstrating CMs show apt responses to pharmacologic stimulation. **F.** Electron micrograph of iPSC-derived CMs showing well-formed sarcomeres (white arrow) and abundant mitochondria (black arrow).

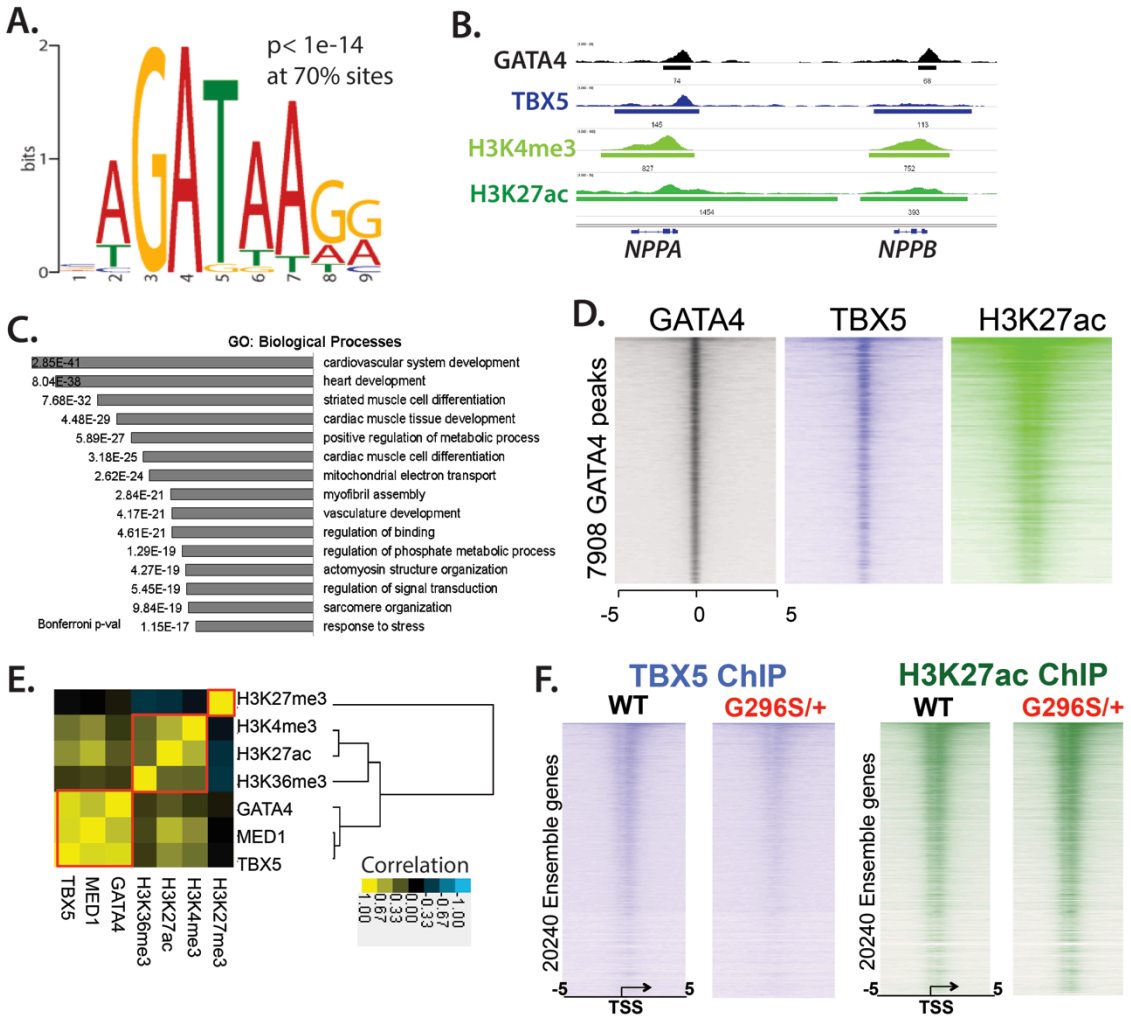

Fig. 2. Genome-wide localization profiling of GATA4 and modified histones in iPS-cardiomyocytes. A. Sequence logo from GATA4 ChIP-seq showing that about 70% of the peaks show at GATA4 consensus motif. **B.** Example genome

browser tracks of GATA4, TBX5 and histone marks H3K4me3 and H3K27ac localizations at known target genes *NPPA* and *NPPB*. **C.** Over-represented Gene Ontologies of all genes <10kb from GATA4 binding sites showing that peaks are overwhelmingly clustered near cardiac genes. **D.** Heatmap of GATA4 binding sites show strong correlation with TBX5 and H3K27ac binding genome-wide. **E**. Pearson correlation matrix scores of all ChIP-seq data. **F.** Heatmap showing reduced TBX5 binding but increased H3K27ac levels at gene promoters in G296S/+ CMs.

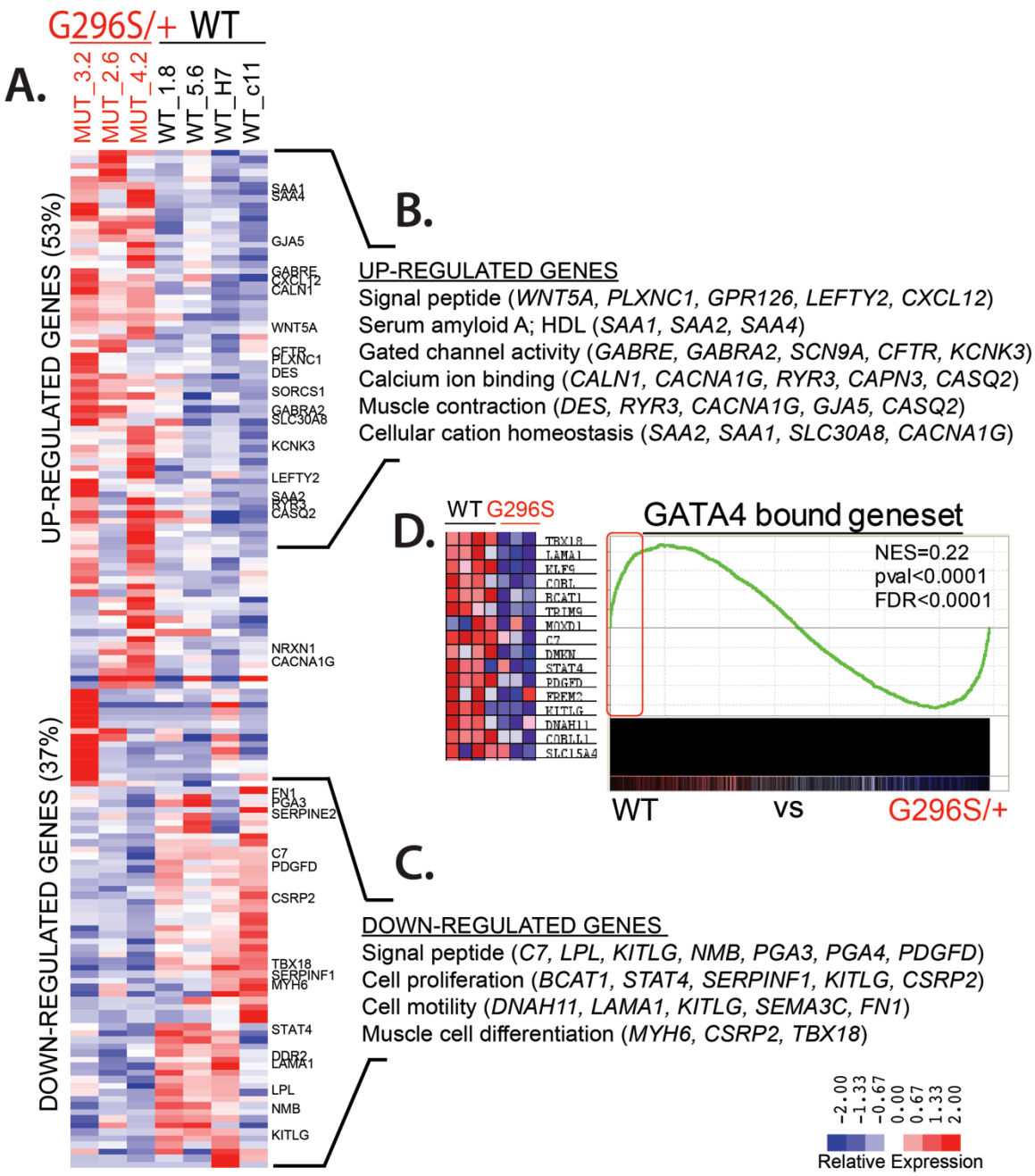

Fig. 3. Transcriptional perturbations in GATA4 G296S/+ CMs. A. Hierarchical clustering of 156 differentially expressed genes between WT (black) and G296S/+ (red) CMs. Genes were mean-centered to show their relative difference. Red, blue represents up- and down-regulation of genes, respectively. **B.** Examples of genes that are found in Up-, and **C.** down-regulated gene sets in

G296S/+ CMs. **D.** GSEA demonstrating that the differentially regulated genes are bound by GATA4.

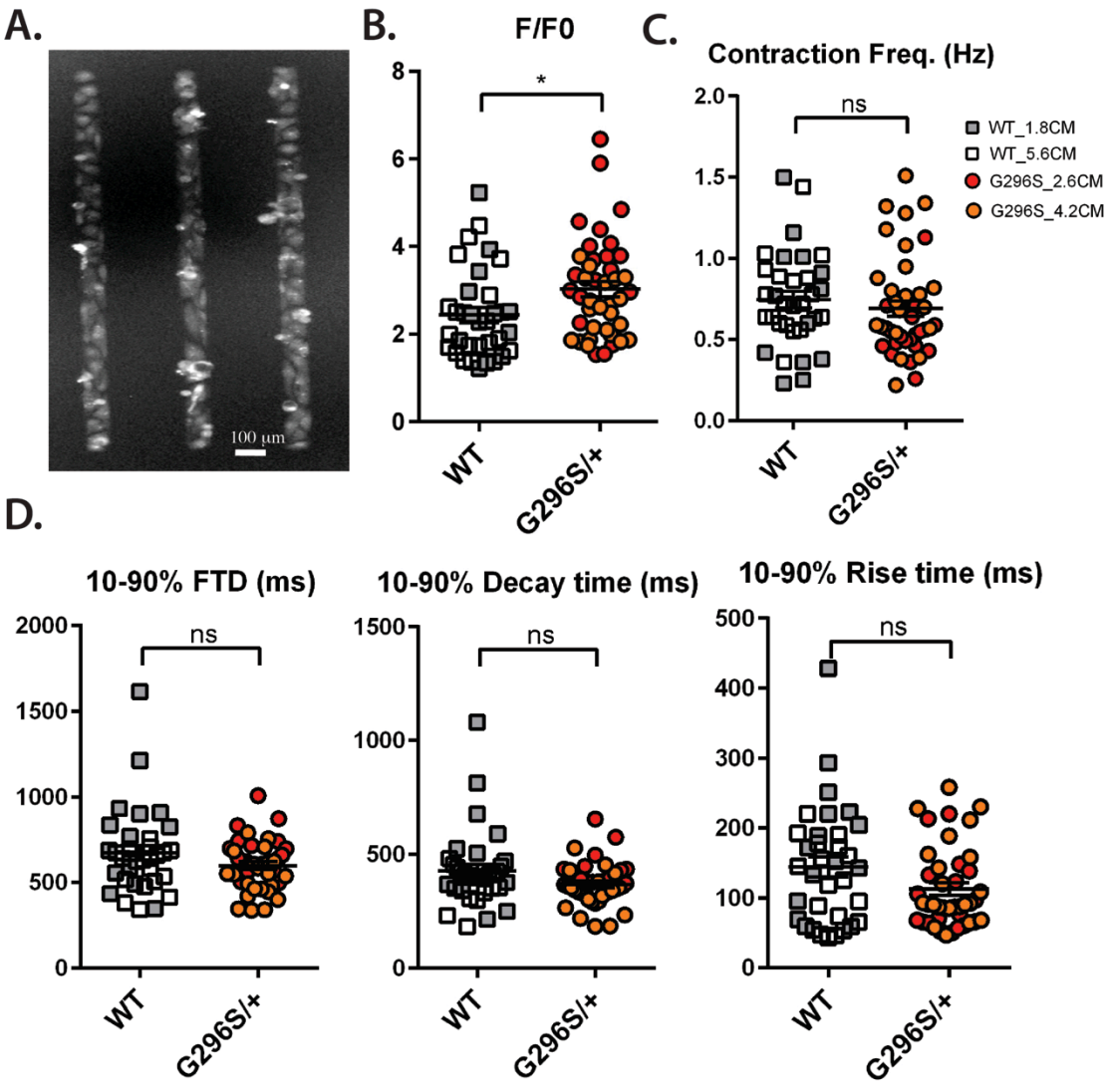

Fig. 4. GATA4 G296S/+ CMs have increased calcium transients. A. Micropatterns create 1mm cardiomyocyte microtissues and **B.** show increased amplitude of calcium transients in G296S/+ CMs (given in arbitrary units). **C.** There was no difference for the contraction frequency. **D.** Likewise there was not a difference for the fluorescent transient duration, rise time, or decay time. White

scale bar represents 100 microns. The legend to the right indicates the cell line recorded (Gray squares represent WT 1.8 CMs, white squares WT 5.6 CMs, red circles mutant 2.6 CMs, and orange circles are mutant 4.2 CMs.)

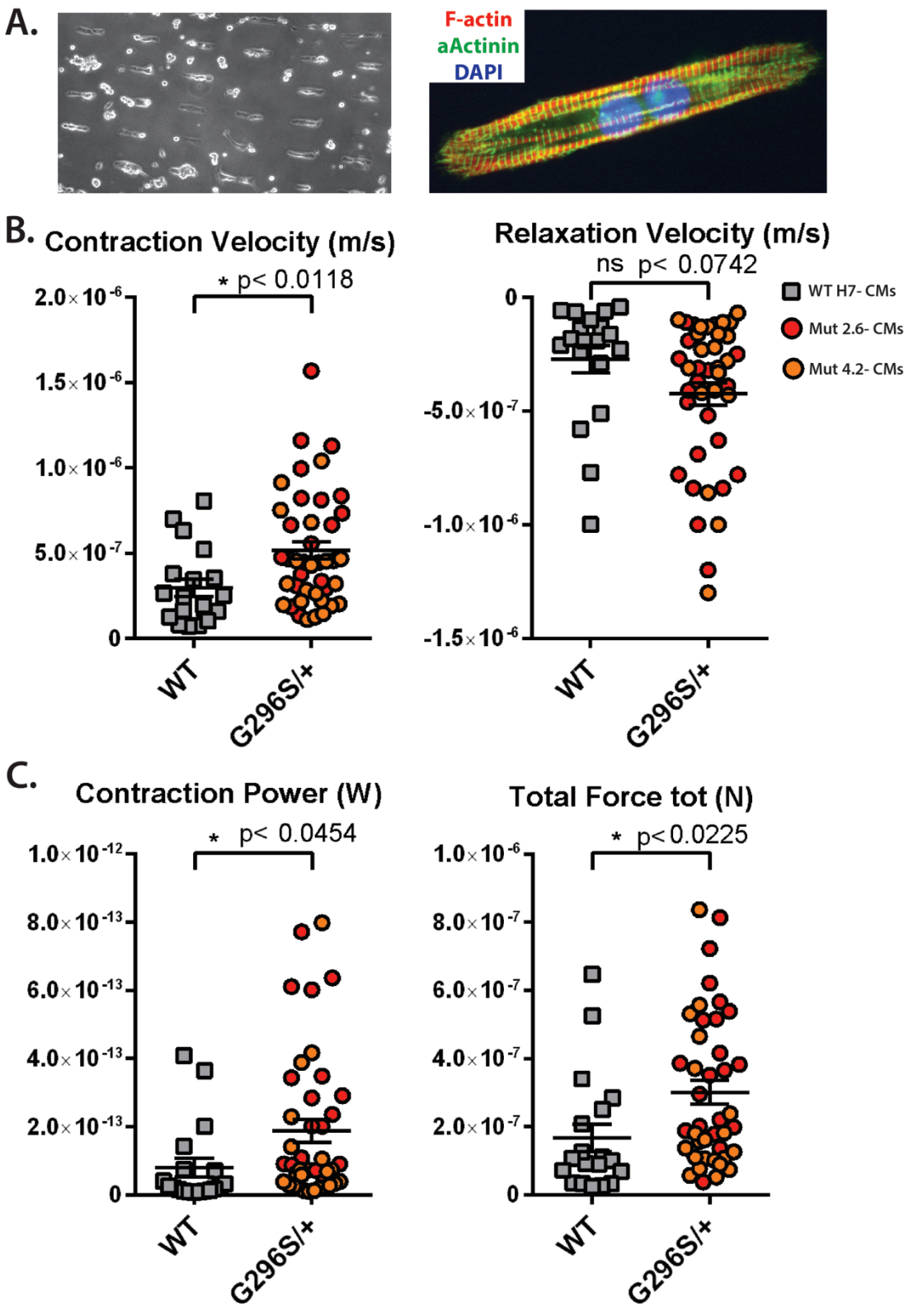
A.
F-actin
aActinin
DAPI
B.
Contraction Velocity (m/s)
* p< 0.0118
2.0×10-6
1.5×10-6
1.0×10-6
5.0×10-7
0
WT
G296S/+
Relaxation Velocity (m/s)
ns p< 0.0742
0
-5.0×10-7
-1.0×10-6
-1.5×10-6
WT H7- CMs
Mut 2.6- CMs
Mut 4.2- CMs
C.
Contraction Power (W)
* p< 0.0454
1.0×10-12
8.0×10-13
6.0×10-13
4.0×10-13
2.0×10-13
Total Force tot (N)
* p< 0.0225
1.0×10-6
8.0×10-7
6.0×10-7
4.0×10-7
2.0×10-7

Fig. 5. GATA4 G296S/+ CMs display a hypercontractile phenotype. A. (Left) Example of cells patterened on 10kPa hydrogels in 7:1 aspect ratio with matrigel. (Right) A patterned binucleated CM stained for F-actin (red), αActinin (green), and DAPI showing appropriate sarcomere assembly. **B.** Measurements from patterned CMs showing the contraction (left) and relaxation velocity (right). **C.** Contraction power (left) and total force (right) can be calculated from knowing the substrate stiffness and displacement of the fluorescent beads embedded in the gel. Gray squares are WT H7-CMs, red and orange circles are mutant lines 2.6 and 4.2 CMs, respectively. Statistics were calculated using Student's T-test and was considered significant if $p<0.05$.

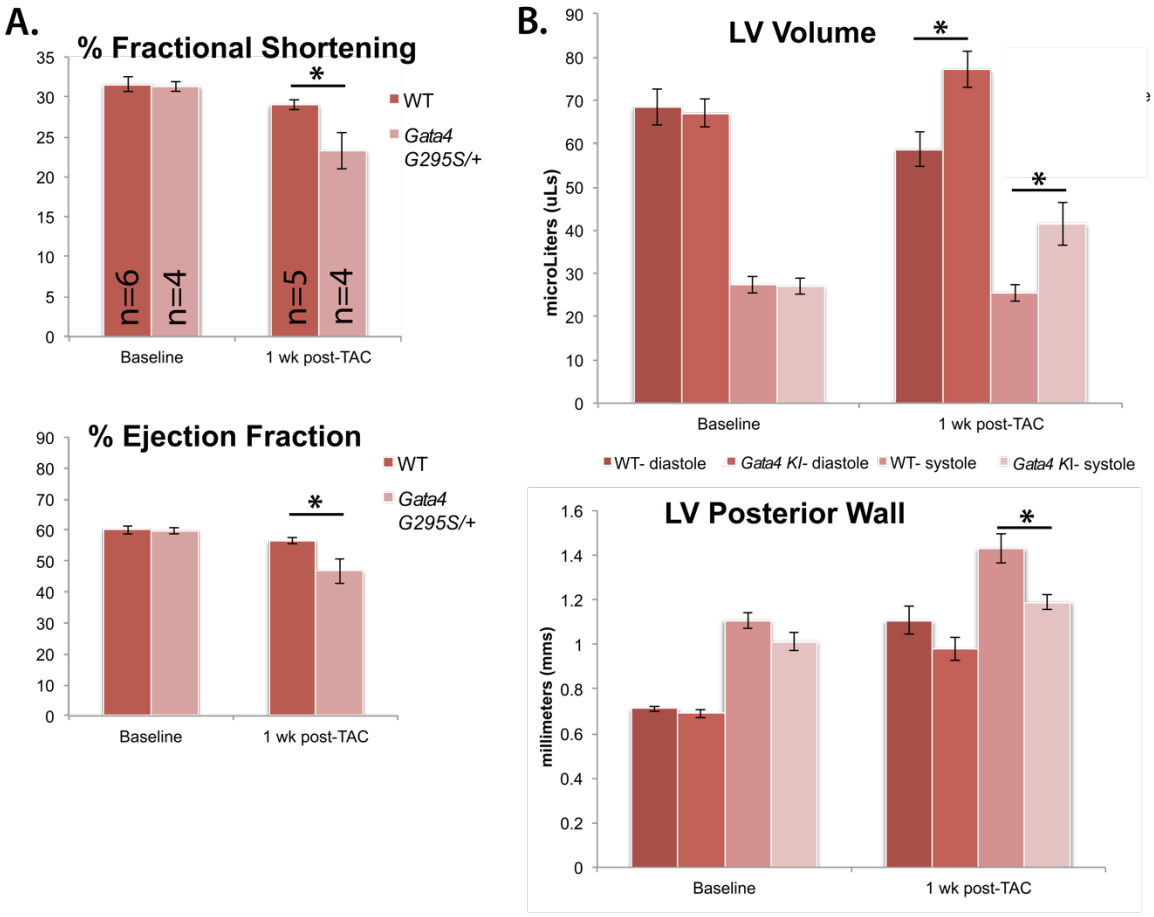

Fig. 6. *Gata4 G295S/+* knock-in mice exhibit an inability to respond appropriately to pressure-overload induced stress. A. Percent fractional shortening (%FS) (top) and percent ejection fraction (%EF) (bottom) in WT (dark red) and *Gata4 G295S/+* mice (light red) under baseline and stressed conditions (1 week after TAC). **B.** Left ventricle (LV) volume and posterior wall thickness measurements of WT and mutant mice in diastole (darker red bars on left) and systole (lighter red bars on right) under baseline and stressed conditions. Asterisk indicates $p<0.05$ by Student's T-test. Number of mice used in each experiment are printed on %FS graph bars.

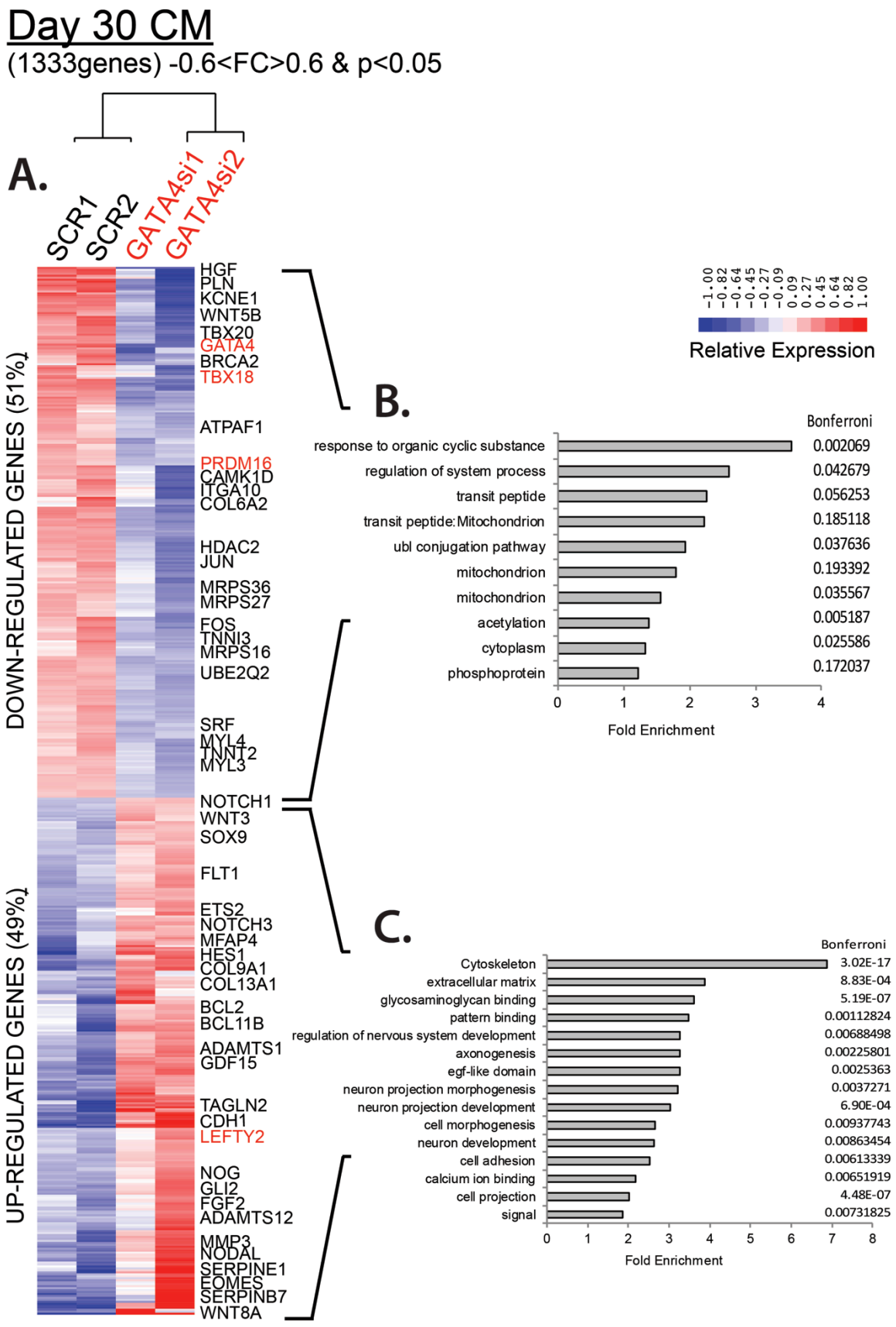
Day 30 CM
(1333genes) -0.6<FC>0.6 & p<0.05
A.
SCR1
SCR2
GATA4si1
GATA4si2
DOWN-REGULATED GENES (51%)
UP-REGULATED GENES (49%)
HGF
PLN
KCNE1
WNT5B
TBX20
GATA4
BRCA2
TBX18
ATPAF1
PRDM16
CAMK1D
ITGA10
COL6A2
HDAC2
JUN
MRPS36
MRPS27
FOS
TNNI3
MRPS16
UBE2Q2
SRF
MYL4
TNNT2
MYL3
NOTCH1
WNT3
SOX9
FLT1
ETS2
NOTCH3
MFAP4
HES1
COL9A1
COL13A1
BCL2
BCL11B
ADAMTS1
GDF15
TAGLN2
CDH1
LEFTY2
NOG
GLI2
FGF2
ADAMTS12
MMP3
NODAL
SERPINE1
EOMES
SERPINB7
WNT8A
−1.00
−0.82
−0.64
−0.45
−0.27
−0.09
0.09
0.27
0.45
0.64
0.82
1.00
Relative Expression
B.
Bonferroni
response to organic cyclic substance 0.002069
regulation of system process 0.042679
transit peptide 0.056253
transit peptide:Mitochondrion 0.185118
ubl conjugation pathway 0.037636
mitochondrion 0.193392
mitochondrion 0.035567
acetylation 0.005187
cytoplasm 0.025586
phosphoprotein 0.172037
0
1
2
3
4
Fold Enrichment
C.
Bonferroni
Cytoskeleton 3.02E-17
extracellular matrix 8.83E-04
glycosaminoglycan binding 5.19E-07
pattern binding 0.00112824
regulation of nervous system development 0.00688498
axonogenesis 0.00225801
egf-like domain 0.0025363
neuron projection morphogenesis 0.0037271
neuron projection development 6.90E-04
cell morphogenesis 0.00937743
neuron development 0.00863454
cell adhesion 0.00613339
calcium ion binding 0.00651919
cell projection 4.48E-07
signal 0.00731825
0
1
2
3
4
5
6
7
8
Fold Enrichment

Fig. 7. siRNA knockdown reveals direct targets of GATA4. A. Hierarchical clustering of 1333 differentially expressed genes between *GATA4* siRNA KD (red) and scramble (black) in CMs. Red, blue represents up- and down-regulation respectively. Gene Ontologies enriched in **B.** down-regulated and **C.** up-regulated genes.

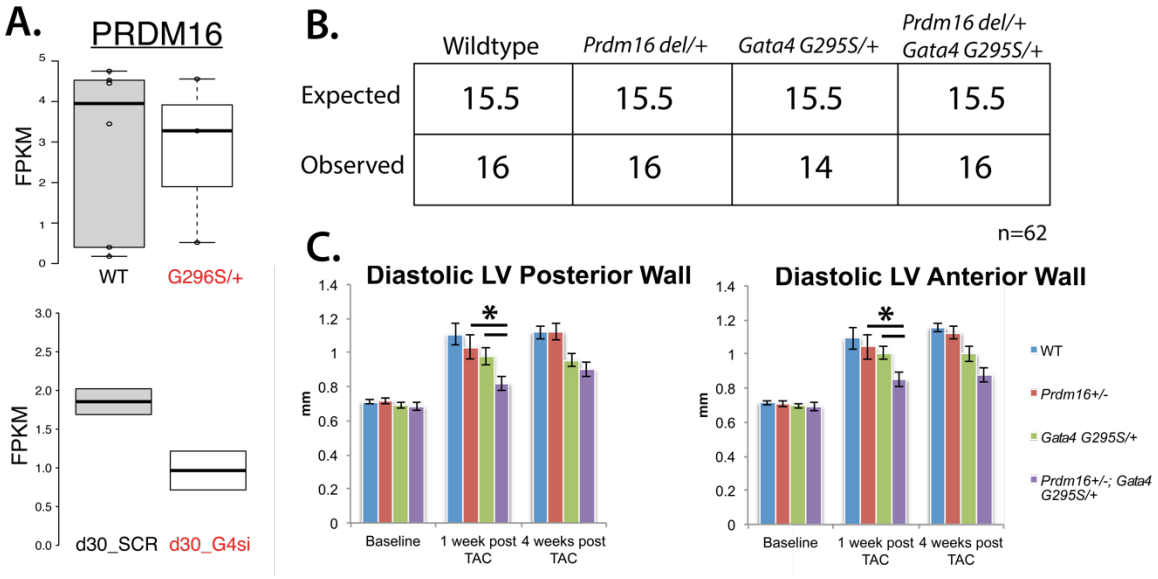

Fig. 8. *In vivo* target-specific investigations into *Prdm16*, a gene dysregulated in GATA4 G296S/+ CMs. A. RNA-seq demonstrates that *PRDM16* is more lowly expressed in the G296S/+ mutant CMs (top, red) as well as in the siRNA KD (bottom, red). **B.** Normal birth ratios for the *Prdm16-/+; Gata4 G295S/+* double heterozygous mice. A total of 62 mice were analyzed for this ratio. **C.** Diastolic left ventricular wall thickness (mm) at baseline of WT (blue, n=6), *Prdm16-/+* (red, n=6), *Gata4 G295S/+* (green, n=4), and *Prdm16-/+; Gata4 G295S/+* (purple, n=5). At both one week and 4 weeks after TAC the number of mice were n=5, n=4, n=4, n=4 for WT, *Prdm16-/+, Gata4 G295S/+,* and *Prdm16-/+; Gata4 G295S/+* respectively. Asterisks indicate $p<0.05$ by Student's T-test.

TABLES

Name of Primers for Genotyping	**Sequence 5' to 3'**
Human *GATA4 G296S* 5'	GGT GAA TGA TGG TTA GGA CTG
Human *GATA4 G296S* 3'	GGC ATC AGA AGG CAA GGA TGC
Mouse *Gata4 G295S* 5'	CAT CCA CTC ACC CCA TGG A
Mouse *Gata4 G295S* 3'	CAC GCT GTG GCG TCG TAA T
Prdm16 deletion 5'	GGG CAA TAA CCC TTA ATA TAA CTT CG
Prdm16 deletion 3'	CCA GTA TCA GAG AGG CAA GAA

Table 1. Table for the sequences of the human and mouse genotyping primers

Name of Taqman Probes for Genotyping	**Sequence**
Mutant specific probe = FAM	TGT AAT GCC TGC AGC C
Wildtype specific probe = VIC	AAT GCC TGC GGC CT

Table 2. Table for Taqman probe sequences used in mouse genotyping

Publishing Agreement

It is the policy of the University to encourage the distribution of all theses, dissertations, and manuscripts. Copies of all UCSF theses, dissertations, and manuscripts will be routed to the library via the Graduate Division. The library will make all theses, dissertations, and manuscripts accessible to the public and will preserve these to the best of their abilities, in perpetuity.

Please sign the following statement:

I hereby grant permission to the Graduate Division of the University of California, San Francisco to release copies of my thesis, dissertation, or manuscript to the Campus Library to provide access and preservation, in whole or in part, in perpetuity.

Renee Rivas
Author Signature

6/12/15
Date